NATIONAL TECHNICAL UNIVERSITY OF ATHENS
SCHOOL OF APPLIED MATHEMATICAL AND PHYSICAL SCIENCES
DEPARTMENT OF PHYSICS

EUROPEAN ORGANIZATION FOR NUCLEAR RESEARCH

Hadron Therapy:

Epidemiological Study of Cancer in Greece and Design of a Medical Synchrotron.

Bachelor Thesis

of

Marianna Kydonieos

Supervisor (N.T.U.A.): Evangelos N. Gazis

Professor

Supervisors (CERN): Manjit Dosanjh (DG/KTT)

Yannis Papaphilippou (CLIC)

Athens, March 2011

National Technical University Of Athens
School of Applied Mathematical and Physical Sciences
Department of Physics

European Organization For Nuclear Research

Αδρονική Θεραπεία: Επιδημιολογική Μελέτη για τον Καρκίνο στην Ελλάδα και Σχεδιασμός Ιατρικού Επιταχυντή για Αδρονική Θεραπεία.

Προπτυχιακή Διπλωματική Εργασία

της

Κυδωνιέως Μαριάννας

Επιβλέπων: Ευάγγελος Γαζής

Καθηγητής Ε.Μ.Π

Αθήνα, Μάρτιος 2011

Acknowledgments

I would like to express my sincere graditude to all the people who contributed in the realisation of the present Bachelor Thesis.
Specifically I would like to thank my supervisor at NTUA, Prof. Evangelos Gazis, for offering me this unique opportunity, as well as for his continous guidance and support. Moreover, I would like to thank my supervisors at CERN, Dr. Manjit Dosanjh and Dr. Yannis Papaphilippou for their constant guidance and help. Their patience and time helped me improve my way of working and enhance my knowledge in physics. I must say that without them, the effectuation of this thesis would not have been possible. Additionally, I want to thank Dr. Claudio Parinello, who provided the financial support for my stay at CERN all these months.
I also want to thank Dr. Fanouria Antoniou for her eagerness to help me and for the valuable assistance she offered any time I needed it. I would especially like to thank Mrs. Chrysoula Bekiari for her help and guidance on the layout of the final text. Moreover, I wish to thank Dr. Evangelia Dimovasili for her support and advice on the last version of my thesis.
I feel lucky that I was given the opportunity to effectuate my thesis at CERN, since it constitutes an ideal environment to work and enrich one's knowledge. All the people I met and worked with were always there for me and for this I want to express my graditude, especially to my officemates Glenn Vanbavinckhove and Guillermo Zamudio.
Last but not least, I want to thank my friends, Kyriakos Asvestas and especially my parents for their encouragment, patience and for believing in me throughout my studies and the duration of my thesis.

Abstract

Over the past decades, the constantly increasing mortality rates due to cancer are apposing cancer one of the leading causes of death worldwide. Despite the fact that over the years, there has been a significant improvement concerning the treatments applied, cancer continues to constitute an important, complex and unsolved medical issue. Tumor irradiation with protons or ions (Hadron Therapy) constitutes one of the most promising treatments available, using cyclotrons or synchrotrons to accelerate the particles. The present thesis, carried out at CERN, consists of two parts:
Part I, includes an epidemiologic study in the framework of descriptive epidemiology, concerning cancer in Greece and an analysis of cancer treatment with a focus on Hadron Therapy. Statistical data is acquired from cancer registries and information concerning the situation in Greece is obtained from meetings with oncologists and physicians from Greek hospitals specializing in cancer. Incidence and mortality rates for each type of cancer based on age and sex, as well as predictions for the next years are presented. Next, the basic types of treatment - chemotherapy, surgery and radiation therapy - are demonstrated along with the side-effects caused by each one. The physics of conventional radiation therapy is introduced, and more importantly, the physical and biological basis of Hadron Therapy is analyzed. Moreover, the benefits of Hadron therapy as well as the cases where it is preferably used are presented. Finally, the necessity for Hadron Therapy in Greece is discussed.
Part II, focuses on the design of a proton accelerator intended for cancer treatment. The objective is to design a very compact medical synchrotron with a 50 m circumference, smaller than most of the medical synchrotrons under construction or operating in Europe. To begin with, the accelerator optics, the particle motion and the beam circulation in a circular accelerator are examined while the concepts of phase advance, tune and emittance are introduced. Necessary parameters such as the strength, size and number of the different type of magnets used in the accelerator ring are defined. Moreover, the magnetic rigidity ($B\rho$) is calculated, based on the values mentioned above. Next, methods to eliminate the dispersion at the exit of the ring are demonstrated. In addition to this, the tunability of the lattice is examined while a summary of the lattice characteristics is presented. Finally, the stability of the lattice is studied, taking into account the strength of the magnets and the phase advance while a summary of the lattice characteristics is presented. The above study is based on linear beam optics, while the non-linear analysis exceeds the scope of this thesis.
This thesis has been performed in the context of a dissertation for a bachelor degree and as it may be easily understood, the time restrictions could not allow the nessecary investigations which might conclude in more realistic results. The reader should bear in mind that the current study aims at providing only the first steps of this very complex field of studies and of course a more thorough investigation is needed. Also, as it is well known worldwide, prestigious medical companies that design medical accelerators are working professionally on providing new and more practical technological solutions for a hadron therapy facility.

Περίληψη

Τα συνεχώς αυξανόμενα ποσοστά θνησιμότητας από καρκίνο τα τελευταία χρόνια, αναγνωρίζουν τον καρκίνο ως μια από τις κύριες αιτίες θανάτου παγκοσμίως. Παρά το γεγονός ότι με την πάροδο των χρόνων, έχει σημειωθεί σημαντική βελτίωση στους τρόπους θεραπείας, ο καρκίνος εξακολουθεί να αποτελεί ένα σημαντικό και πολύπλοκο πρόβλημα υγείας. Η ακτινοβόληση των καρκινικών όγκων με πρωτόνια ή ιόντα άνθρακα (*Αδρονική Θεραπεία*) με τη χρήση κύκλοτρων ή σύγχροτρων για την επιτάχυνση των σωματιδίων, αποτελεί μια από τις πλέον υποσχόμενες διαθέσιμες θεραπείες,. Η εκπόνηση της παρούσας διπλωματικής έγινε στο CERN και αποτελείται από δύο μέρη

Το πρώτο μέρος, περιλαμβάνει μια *επιδημιολογική μελέτη στα πλαίσια της περιγραφικής επιδημιολογίας*, που αφορά στον καρκίνο στην Ελλάδα, ενώ παράλληλα εστιάζει στην Αδρονική Θεραπεία, εξετάζοντας το ενδεχόμενο εφαρμογής αυτού του είδους θεραπείας στην Ελλάδα. Η συλλογή των στατιστικών δεδομένων έγινε από το διεθνή αρχεία νεοπλασιών (*cancer registries*) ενώ πληροφορίες σχετικά με την κατάσταση στην Ελλάδα αποκτήθηκαν από το Εθνικό Αρχείο Νεοπλασιών καθώς και από συναντήσεις με ογκολόγους και φυσικούς Ελληνικών νοσοκομείων που ειδικεύονται στον καρκίνο. Παρουσιάζονται τα ποσοστά εμφάνισης και θνησιμότητας για κάθε είδος καρκίνου, λαμβάνοντας υπ΄Α όψιν την ηλικία και το φύλλο, ενώ γίνονται προβλέψεις όσον αφορά στην εξέλιξη της κατάστασης τα επόμενα χρόνια. Εισάγονται οι φυσικές αρχές που διέπουν την συμβατική ακτινοθεραπεία, ενώ αναλύεται η φυσική και βιολογική βάση της Αδρονικής Θεραπείας. Επιπρόσθετα, παρουσιάζονται τα οφέλη της Αδρονικής Θεραπείας καθώς και οι περιπτώσεις καρκίνου για τις οποίες ενδείκνυται η χρήση της.

Το δεύτερο μέρος εστιάζει στη *σχεδίαση ενός επιταχυντή πρωτονίων για θεραπεία καρκίνου*. Ο στόχος είναι να σχεδιαστεί ένα πολύ μικρό ιατρικό σύγχροτρο, με περίμετρο 50 μέτρων, μικρότερο από την πλειοψηφία των ήδη υπαρχόντων ή υπό κατασκευή στην Ευρώπη. Αρχικά, γίνεται μια εισαγωγή στην οπτική των επιταχυντών ενώ εξετάζεται η κίνηση των σωματιδίων και η κυκλοφορία της δέσμης εντός κυκλικού επιταχυντή. Καθορίζονται απαραίτητες παράμετροι όπως η ισχύς, το μέγεθος και ο αριθμός των διαφόρων τύπων μαγνητών που χρησιμοποιούνται στον επιταχυντή. Επιπλέον, υπολογίζεται το μαγνητικό πεδίο και η ακτίνα καμπυλότητας του επιταχυντή για τα δεδομένα της συγκεκριμένης κατασκευής, με βάση τα χαρακτηριστικά που αναφέρθηκαν παραπάνω. Επίσης,επιλέγεται η πλέον κατάλληλη μέθοδος για την εξάλειψη της διασποράς των σωματιδίων στην έξοδο του επιταχυντή, ενώ μελετάται η σταθερότητα της δέσμης, λαμβάνοντας υπΆ όψιν την ισχύ των μαγνητών

. Τέλος, παρουσιάζεται μια σύνοψη των χαρακτηριστικών του επιταχυντή που προέκυψαν από την παραπάνω ανάλυση. Η παρούσα μελέτη έγινε με τη χρήση του προγράμματος MAD-X και βασίζεται στη γραμμική οπτική ενώ η μη-γραμμική ανάλυση υπερβαίνει το πλαίσιο της παρούσας διπλωματικής.

Contents

List of Figures

Part I

Chapter 1

Introduction

Over the past decades, mortality rates due to cancer have been increasing rapidly, and cancer is now one of the leading causes of death-in Europe and USA. Over the years, there has been a significant improvement in diagnosis and the methods of treatment. However, cancer continues to constitute an important, complex and difficult to cure health problem.
Cancer is a collective word which embraces more than 100 different diseases, each corresponding to therapy differently, characterized by an uncontrolable production of cells that penetrate healthy tissue and create malignant tumors. The prevalence, effects and causes of cancer are critical issues that must be studied. It is important to define what is meant by epidemiology and which factors should be considered in carrying out an epidemiological study. Epidemiology is a science based on population measurements and can be described as the study of distribution and determinants of diseases in human populations and the application of the results to their prevention or control. The two types of epidemiology are *descriptive* and *analytical*. Descriptive epidemiology examines differences in the distribution of disease occurrence with respect to population, place and time whereas analytical epidemiology compares risk factors [1]. In order to assess the distribution of cancer and any other disease, it is important to take into account parameters such as age, sex and time of cancer diagnosis. The most informative and reliable sources for the estimation of the frequency and distribution of cancer are *cancer registries* i.e. organizations which quantify *incidence* rates by recording all newly diagnosed cases of cancer occurring in a defined population. Another parameter recorded and quantified is the rate of *mortality*, indicated as the number of persons in a defined population certified as dying

from cancer. The relation between incidence and mortality varies by cancer site and is also influenced by early detection and the effectiveness and success of chosen treatment and the quality of health care provided for the patients. Incidence and mortality data are presented in the form of rates per 100.000 population per annum and represent the most useful form of cancer data for research and public health purposes. The rate used to measure the number of deaths is called *crude rate* and is calculated simply by dividing the number of cancer deaths observed during a given time period by the corresponding number of person years in the population at risk. For cancer, the result is usually expressed as an annual rate per 100,000 persons at risk [2], i.e the number of cancer deaths per year, per 100,000 people.

In the present study, an attempt has been made to investigate the status of cancer in Greece, mostly in the framework of descriptive epidemiological analysis. In addition, the various cancer treatment modalities available are examined, focusing on the possible need and use of Hadron Therapy. This study presented several challenges due to the vast bibliography and large dispersion and volume of data found, which leads to equivocal information. In addition to this, the scarcity of the data kept in the Cancer Registry in Greece [3], combined with the dependence of cancer on individual patient's medical history made reaching conclusions, based on the data obtained, even more difficult. Nevertheless, the analysis of reliable and established data was attempted, based on published information and official repository.
The structure of this part of the thesis is described as follows. In Chapter 2, World and European cancer statistics are presented, concerning the incidence and mortality rates by sex and by country. Next, in Chapter 3, cancer in Greece is being studied, examining the most common types of cancer as well as the mortality and survival rates. Moreover, future predictions are presented based on official data. In Chapter 4, the three usual treatments, chemotherapy, surgery and radiation therapy, are described, while the side effects of each type of treatment are also stated. Chapter 5, consists of a further analysis of Conventional Radiation Therapy, whereas in Chapter 6, the physical and biological basis of Heavy Particle Therapy is studied in depth. Furthermore, other issues such as the cases where it is preferably used, the available facilities and Hadron Therapy in Greece are examined. Finally, in Chapter 7, some basic conclusions concerning cancer and Hadron Therapy in Greece are presented.

Chapter 2

Cancer Statistics

2.1 Cancer Worldwide

Cancer is one of the leading causes of death worldwide. Specifically, it remains the second most common cause of death after cardiovascular disease in Europe and USA [4]. Incidence and mortality data are obtained from national cancer registry websites or annual reports issued by organizations such as the IARC-*International Agency for Research on Cancer*-, WHO-*World Health Organisation*-, and GLOBOCAN. The latest available data on cancer incidence and mortality worldwide, concerns the year 2008. Nearly 12.7 million new cancer cases and 7.6 million cancer deaths occurred in 2008 worldwide. The most common type of cancer worldwide is lung cancer, not only as the new number of cases, but also as the number of deaths per year. Fig. (2.1) demonstrates the percentages of cancer incidence and mortality worldwide [5]:

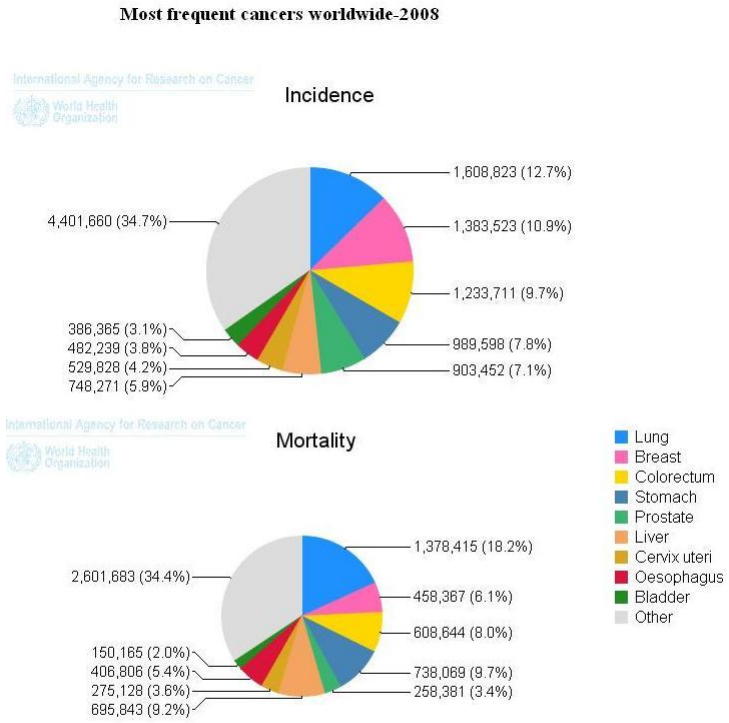

Figure 2.1: *Cancer Incidence and Mortality worldwide*

However, even though breast cancer is the second most common cancer worldwide, the mortality rate for breast cancer is not very high since early detection and effective treatment modalities have been developed. The three most common causes of death, with the highest mortality rates are: lung, stomach and colorectum cancer.

2.2 Cancer in Europe

For Europe, the epidemiological data presented are obtained from a European cancer registry, ECO-*European Cancer Observatory*. The latest data available are based on the year 2008 however, in addition, some data of ear-

lier years are presented as well, in order to examine the evolution of cancer. The total number of new cases of cancer diagnosed every year appears to have increased by 300,000 between 2004 and 2006. More recent studies have shown that in 2006 in Europe, there were an estimated 3.2 million cancer cases diagnosed up from 2.9 million in 2004 and 1.7 million deaths from cancer [5]. It is clear that cancer remains an important public health issue in Europe and the ageing of the European population will cause a further increase to these numbers [6]. Figures (2.2) and (2.3) demonstrate the incidence and mortality rates in Europe in men and women respectively in 2008.

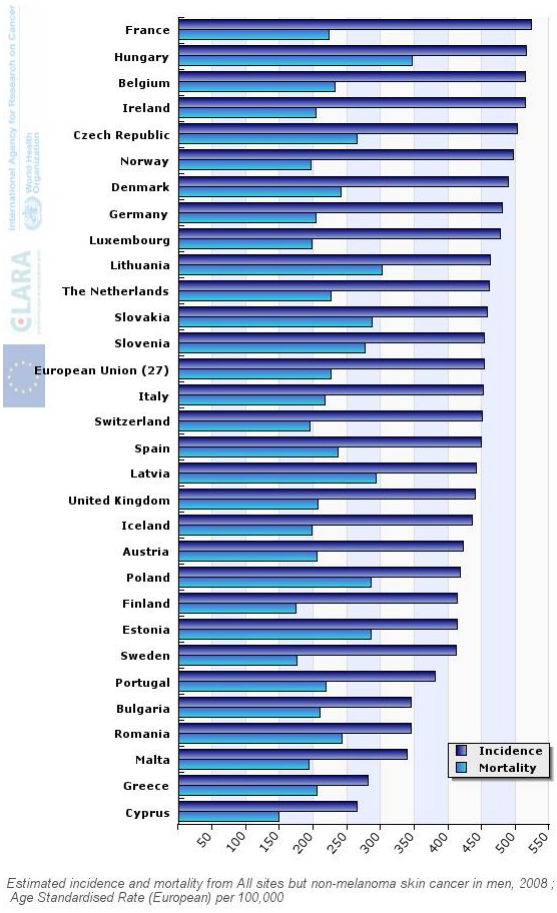

Figure 2.2: *Incidence and Mortality in Europe-Men.*

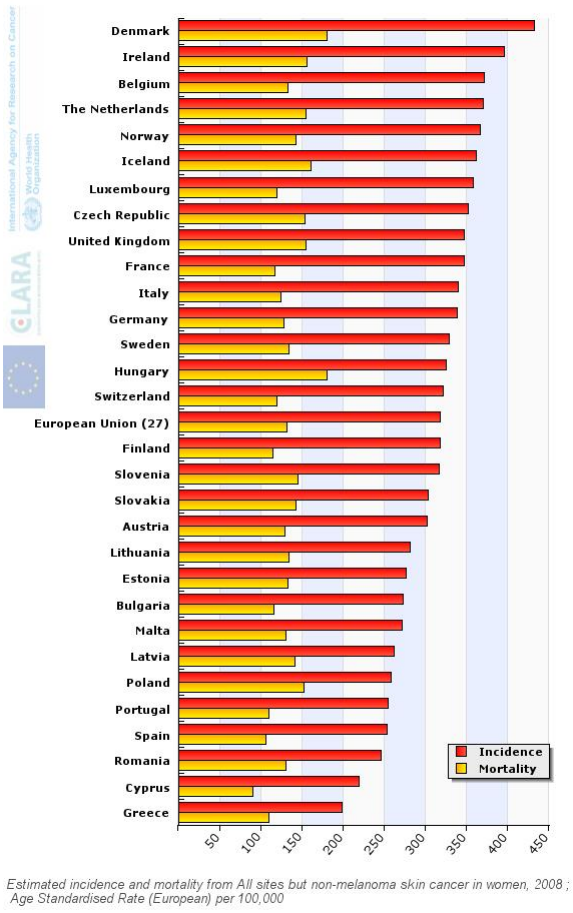

Figure 2.3: *Incidence and Mortality in Europe-Women.*

According to Fig. (2.2) and (2.3) , the lowest cancer incidence in men and in women are observed in Cyprus and Greece respectively, whereas the highest incidence rates are observed in France and Denmark for men and women respectively, possibly due to a more effective diagnosis than in other countries. Moreover, the lowest mortality rates are observed in Cyprus, whereas the highest rates are observed in Hungary. However, the highest mortality to incidence ratio is observed in Greece and Poland for men and women respectively. Thus, most cancer patients do not recover. This could mean that the treatment in these two countries may be inadequate.

The types of cancers are also extremely important when analysing the incidence and mortality rates. In Fig. (2.4), the incidence and mortality rates are presented for the most common cancers in Europe [6]:

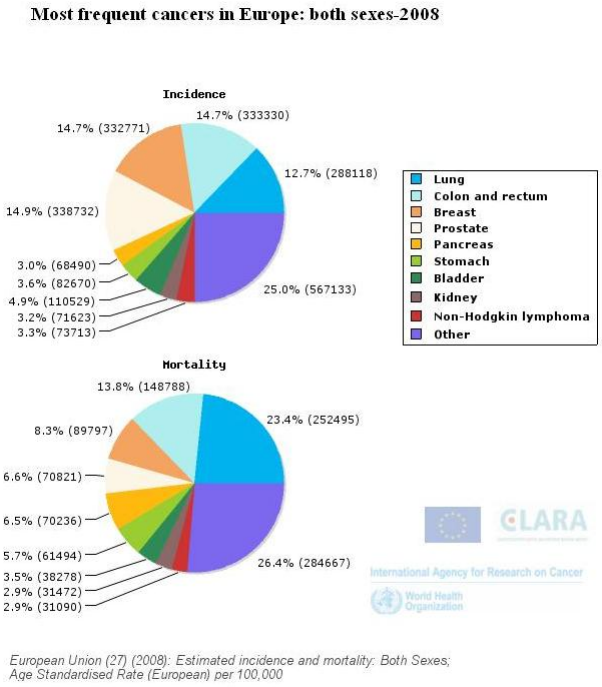

Figure 2.4: *European Cancer Incidence and Mortality rates*

The difference between Fig. (2.1) and (2.4) is obvious. Breast cancer in Europe, is one of the most common causes of death, along with lung and colon and rectum cancer, whereas stomach cancer does not have a very high

mortality rate.

Chapter 3

Cancer in Greece

3.1 Most common types of cancer

As already mentioned, during the assessment of the distribution of cancer, the population of the country of study must be taken into account. In Fig. (3.1) the evolution of the population of Greece is demonstrated [7]:

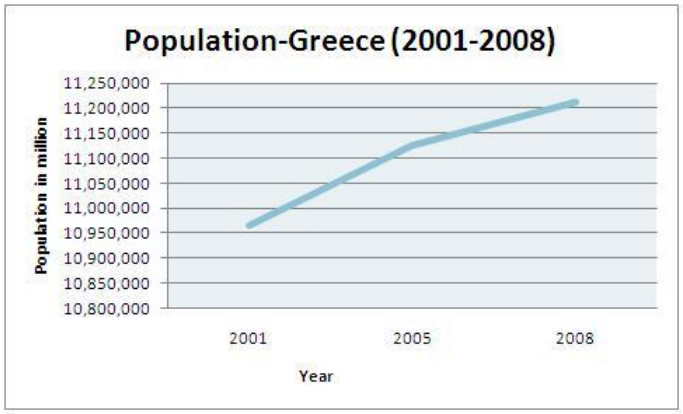

Figure 3.1: *Population Evolution in Greece*

The population of Greece at the end of 2009 was approximately 11.262.539. In Greece, like in all of Europe, cancer is the second most common cause of death after cardiovascular diseases as demonstrated in Fig. (3.2) [2]:

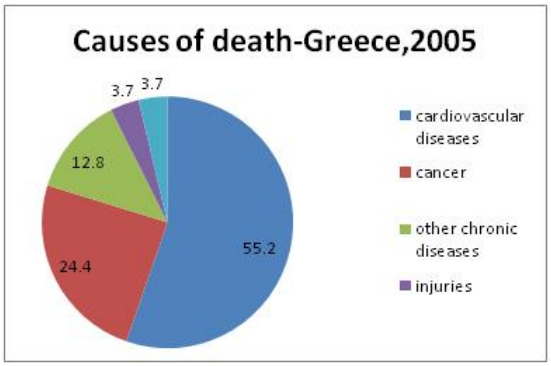

Figure 3.2: *Most common causes of death*

As far as cancer is concerned, Greece is a country with a significantly high mortality to incidence ratio [2]. This means that, a great percentage of cancer cases will result in death. Fig. (3.3), demonstrates the estimations for the main causes of death in Greece for 2005 as well as a projection for 2030 [2]:

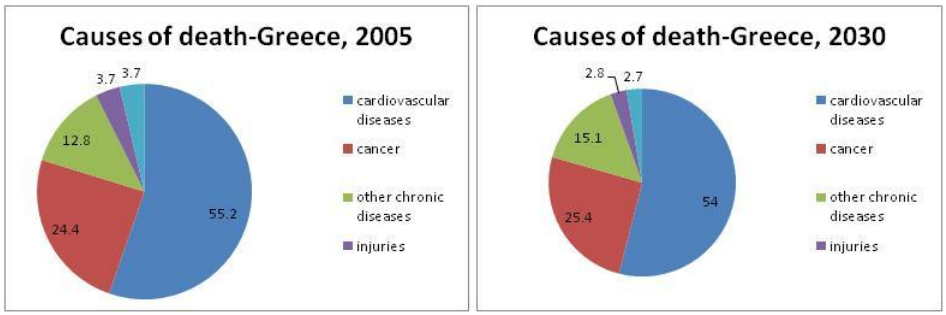

Figure 3.3: *Estimations for causes of death in Greece for 2005 and projections for 2030*

According to WHO-Global database, in 2005, there were approximately 29,000 cancer deaths, while 10,000 of those refer to patients under the age of 70. The evolution of cancer deaths in Greece, during the years 2000 to 2008 is demonstrated in Fig. (3.4) [2]:

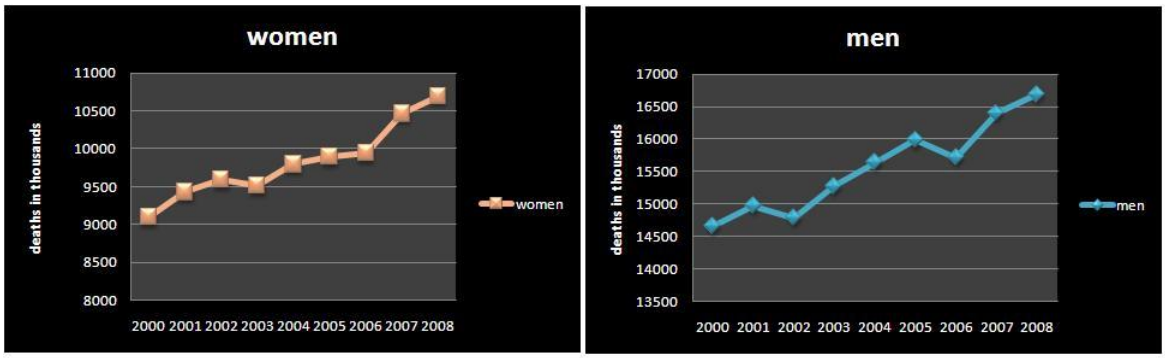

Figure 3.4: *The evolution of cancer deaths in Greece, during the years 2000 to 2008*

Taking into account the population and the number of deaths, Fig. (3.5) to (3.8) demonstrate the cancer incidence and mortality for both men and women for the years 2006 and 2008 [6]:

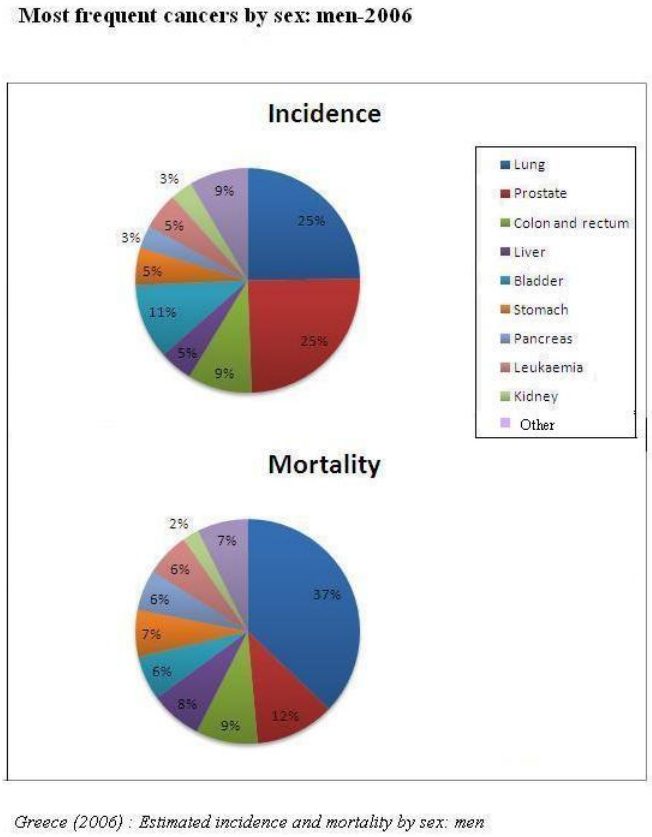

Figure 3.5: *Incidence and Mortality in men, in 2006, taking into account the population and the number of deaths.*

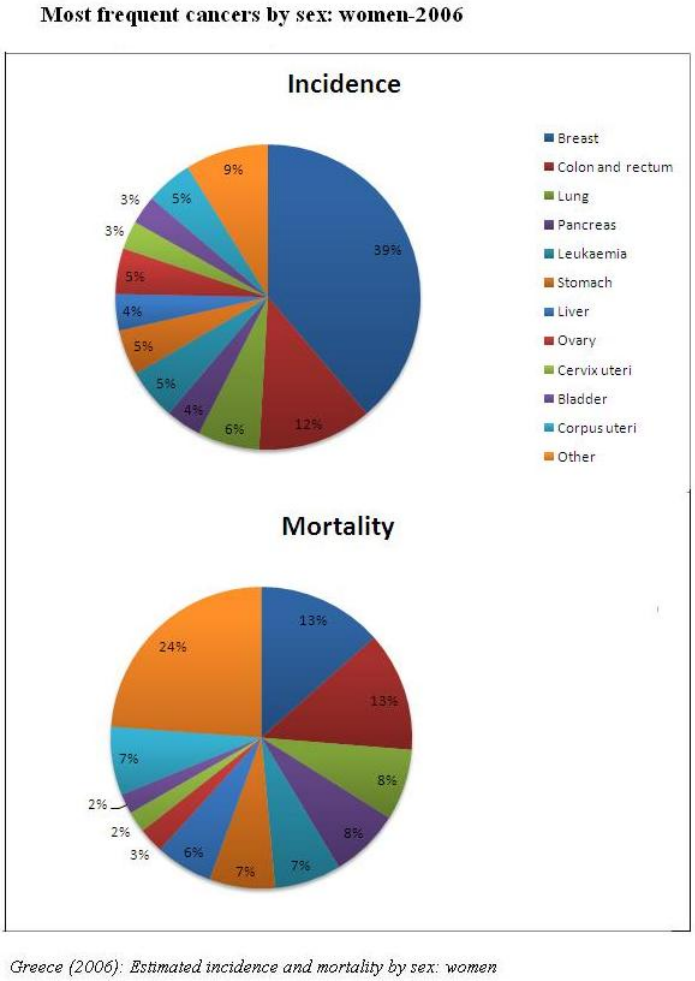

Figure 3.6: *Incidence and Mortality in women, in 2006, taking into account the population and the number of deaths.*

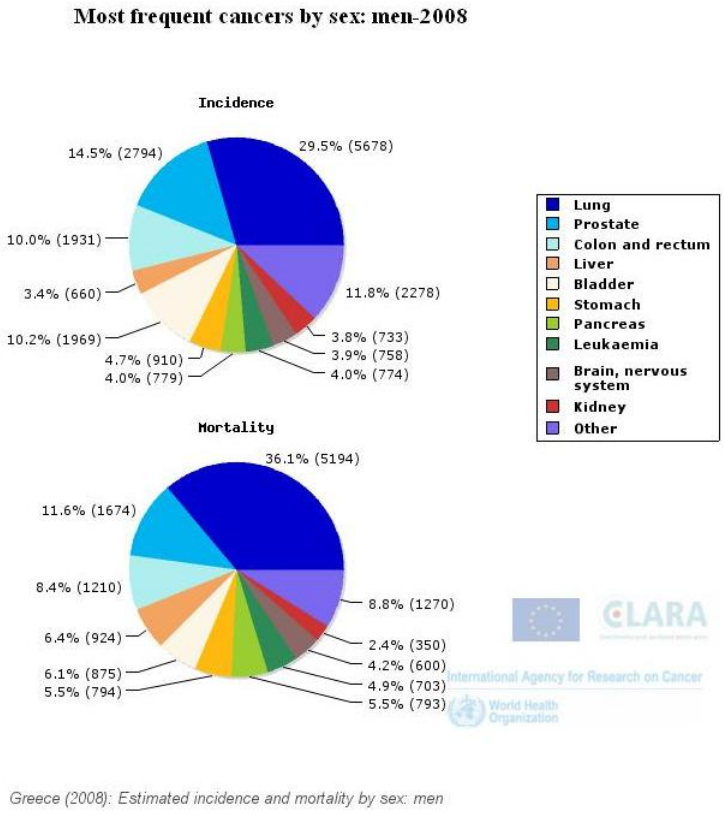

Figure 3.7: *Incidence and Mortality in men, in 2008, taking into account the population and the number of deaths.*

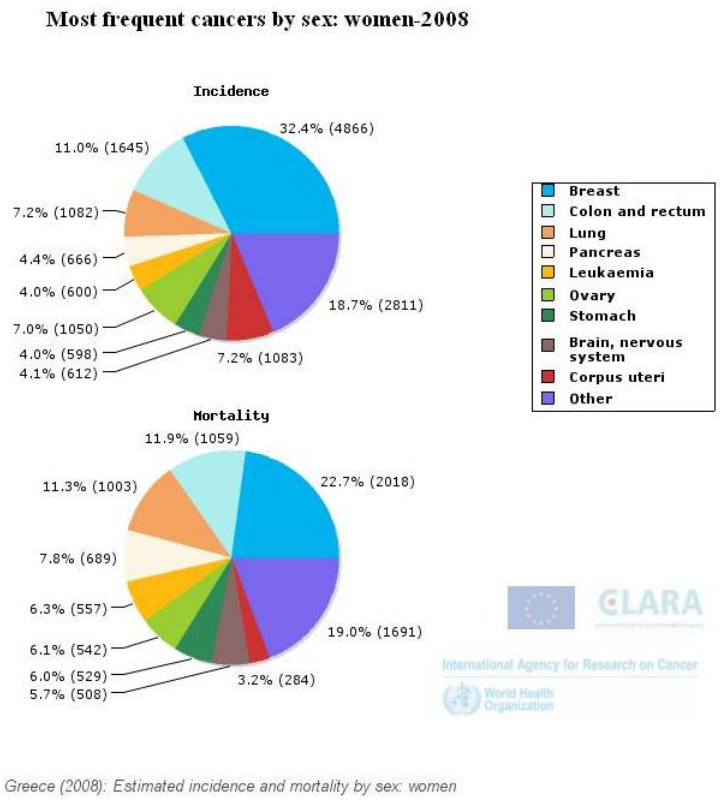

Figure 3.8: *Incidence and Mortality in women, in 2008, taking into account the population and the number of deaths.*

According to Fig. (3.5) to (3.8), the three most common cancers in men, remain lung, prostate and bladder cancer in both 2006 and 2008. The incidence of lung cancer increases from 24.8 to 29.5 percent and constitutes the first cause of death due to cancer, whereas for bladder cancer, it decreases from 10.8 to 10.2 percent. Moreover, prostate cancer presents a significant decrease of approximately 10 percent (from 24.7 to 14.5 percent). As far as mortality is concerned, lung cancer presents by far the highest mortality rates in both 2006 and 2008.
The three most common cancers in women, remain breast, colon and rectum and lung cancer in both 2006 and 2008. Breast cancer presents a quite important decrease of approximately 6 percent. Colon and rectum cancer also present a decrease of 1 percent, whereas the incidence rate of lung cancer increases by 1 percent approximately. The mortality rates for the three most

common cancers decrease around 1 percent as well, from 2006 to 2008. The same happens for most types of cancer.

3.2 Most common types of cancer by age

An important parameter while studying cancer epidemiology, is the age at which the cancers occur. On the basis of data obtained from the European cancer repository, the estimated incidence and mortality for the most frequent cancers are presented, for the year 2008, on an *Age Standardized Rate* for 10-age groups (Fig. (3.9) and (3.10))[6]. An age-standardised rate (ASR) is a summary measure of the rate that a population would have if it had a standard age structure. Standardization is necessary when comparing several populations that differ with respect to age because age has a powerful influence on the risk of cancer. The ASR is a weighted mean of the age-specific rates; the weights are taken from population distribution of the standard population [8].

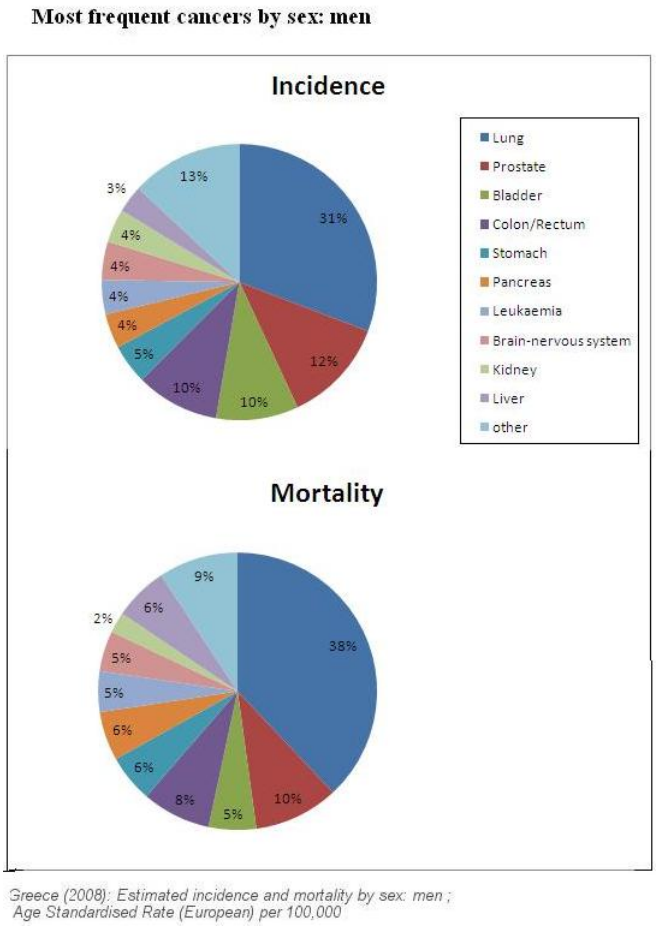

Figure 3.9: *Incidence and Mortality in men, in 2008, taking into account the Age Standarized Rate.*

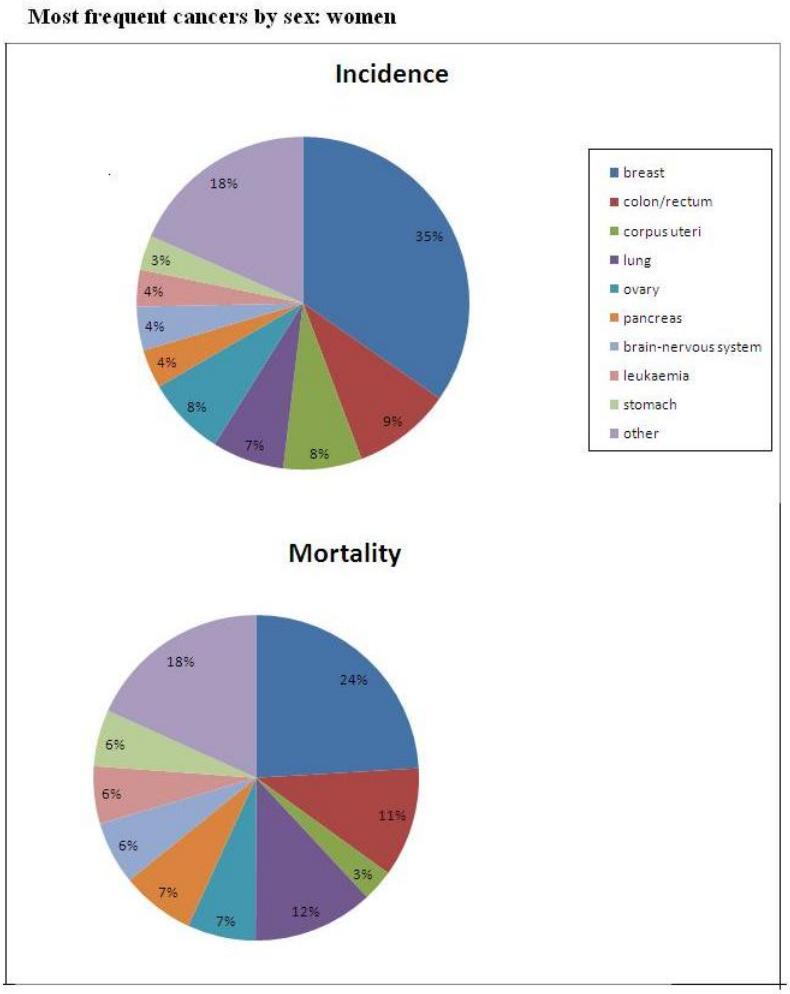

Figure 3.10: *Incidence and Mortality in women, in 2008, taking into account the Age Standarized Rate.*

Comparing Fig. (3.8) to (3.10), it is obvious that the incidence and mortality rates are different, even though they are referring to the same year. For example, the three cancer types in women, with the highest incidence rate, are now breast, colon and rectum and corpus uteri cancer instead of lung cancer. Hence, it is evident that age plays an important role.

Based on data acquired from the National Cancer Registry [3] concerning cancer incidence, Fig. (3.11a) to (3.11i) are obtained, where the most common cancers are presented, with respect to age and sex, for the year 2009:

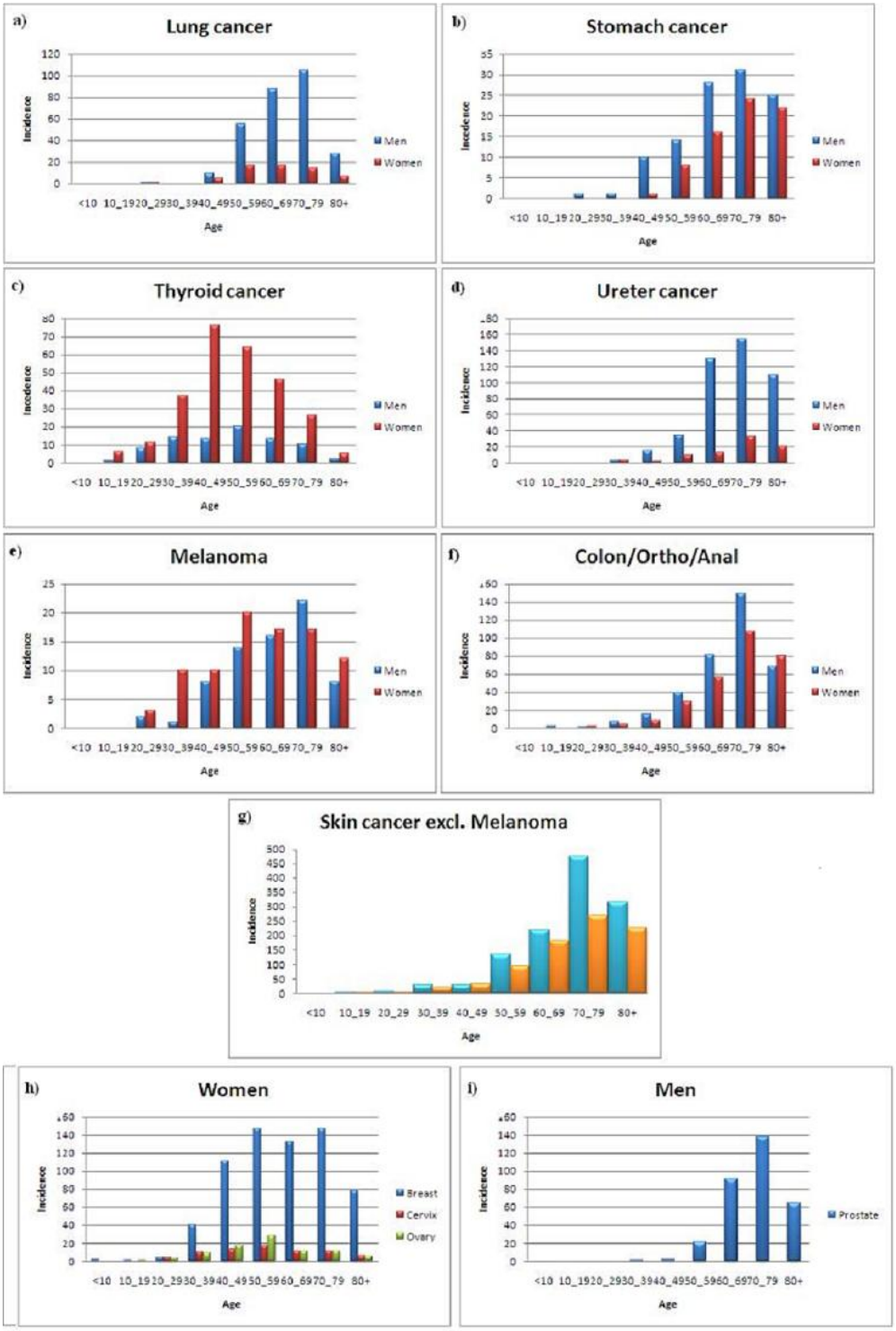

Figure 3.11: *Most common cancers with respect to age and sex.*

As can be seen from Fig. (3.11), skin cancer has extremely high incidence rate in both sexes from the age of 30-39 years. Until the age of ten, the percentages for all types of cancer are almost minimal or non-existent.
For the ages **10-19**, *colon* and *thyroid* cancer start to occur in men and women respectively.
At the ages of **20-29**, *thyroid* cancer is at high levels not only for women but for men as well. Moreover, the incidence rate of *testicular* cancer is very high and that is the age where it reaches it's maximum value. Cervix, ovary and breast cancer begin to appear as well.
At the ages of **30-39** *thyroid* cancer increases for both sexes, especially for women. Also, testicular cancer decreases but still holds a high percentage, whereas colon and rectum cancer begin to appear as well. As far as women are concerned, the incidence rate for *breast* cancer increases significantly, while the incidence rate for cervix, ovary and melanoma cancer increases as well, but remain in much lower levels.
At the ages of **40-49**, *thyroid* cancer remains at the same levels for men, whereas for women the incidence rate increases significantly and reaches a maximum value. As far as men are concerned, the percentages for *ureter, colon* and *stomach* cancer increase rapidly. *Breast* cancer in women increases to extremely high levels, while ovary cancer increases as well, though again in much lower levels.
At the ages of **50-59**, *lung* cancer reaches high levels especially in men. Moreover, colon, prostate and ureter cancer in men indicate also an important increase. In women, thyroid cancer still remains in very high levels but has decreased, whereas ovary cancer reaches it's maximum value along with *breast* cancer which reaches it's highest value and presents the highest incidence rate in all ages for women after skin cancer.
At the ages of **60-69**, *ureter* cancer in men increases significantly, along with *lung*, *prostate* cancer. *Colon* cancer presents an important increase in both men and women, while, as far as women are concerned, the percentage of cancers with the highest incidence rate decrease, but still remains at very high levels (breast, thyroid cancer).
At the ages **70-79**, almost all cancers present significant increase, with the percentage of *colon* and *skin* cancer reaching a maximum value.
For ages over **80** years, the incidence rates for almost all cancers decrease, as human cells do not multiply as fast as they do in younger ages.

Summarizing, in Fig. (3.12), the most common cancers are indicated, according to age for men and women respectively:

AGE	10-19	20-29	30-39	40-49	50-59	60-69	70-79	80+
CANCER	skin	thyroid	skin	skin	skin	skin	skin	skin
	colon/ othro	testicular	thyroid	colon/ ortho	lung	ureter	colon	ureter
			testicular	ureter	Colon/ ortho	Prostate + lung	Ureter- prostate- lung	

(a)

AGE	10-19	20-29	30-39	40-49	50-59	60-69	70-79	80+
CANCER	thyroid	thyroid	breast	breast	breast	skin	skin	skin
			thyroid	thyroid	skin	breast	breast	
							colon/ ortho	

(b)

Figure 3.12: *Most common cancers according to age for men and women respectively.*

3.3 Survival Rates

Taking into account data acquired from the European Cancer Observatory and from Charts (9) and (10), the *survival rates* can be obtained. The survival rate can be defined as indicated in equation (3.1):

$$SR = \frac{incidence - mortality}{incidence} \tag{3.1}$$

Thus, in Fig. (3.13) and (3.14), the survival rates are presented for men and women respectively:

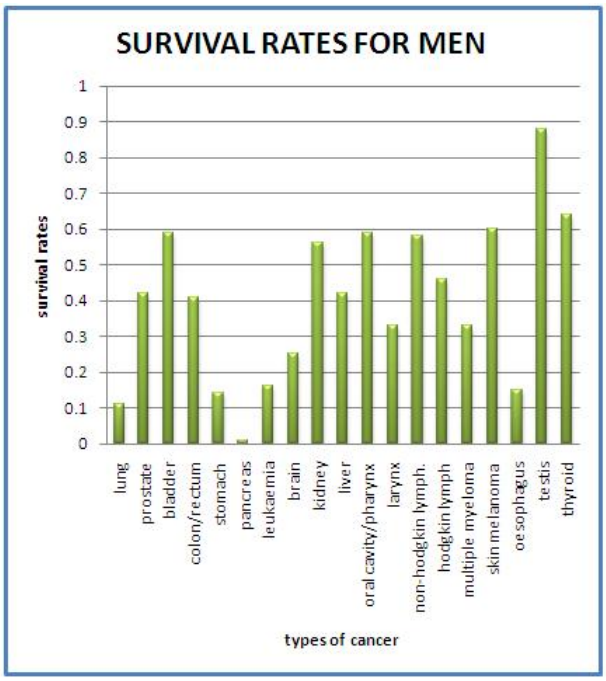

Figure 3.13: *Survival Rates for men.*

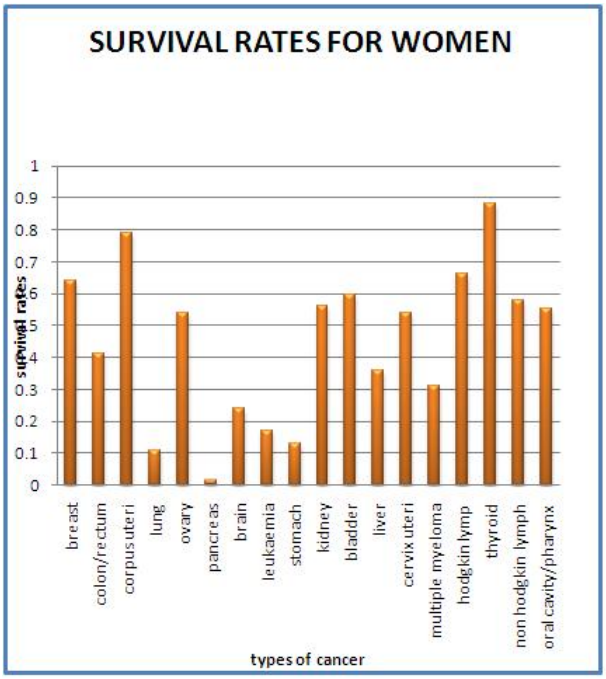

Figure 3.14: *Survival Rates for women.*

According to Fig. (3.12) and (3.13), pancreas cancer has the lowest survival rate for both sexes. Some common cancers such as breast and prostate cancer have a rather high survival rate, over 60 and 40 percent possibility of survival respectively. Almost 10 percent of all women will be affected by breast cancer in their life. Additionally, prostate cancer will affect almost 50 percent of all men, without being a cause of death. It is interesting that, common cancers such as breast, colon and rectum, prostate and bladder cancer, have a very high survival rate, despite their high incidence rate. However, lung cancer appears to be an exception, since the survival rate is one of the lowest.

It is a fact that, cure rates depend on type, location and stage of the cancer. Moreover, hormones, the type of therapy being used, the biological behavior as well as the reproduction phase of the patient, play an important role as well [9].

However, certain principles apply to the cure rates for specific types of cancer. As far as *breast* cancer is concerned, if it is diagnosed at an early stage,

the percentage for complete cure -considered to be 5 years disease free- is over 50. Additionally, after menopause, the cure rate increases and the prognosis improves. As for *prostate* cancer, in the case of an early stage diagnosis, there is a 95 percent possibility for 10 years survival, which, given the age of occurrence, is very satisfactory. *Lung* cancer has less than 40 percent possibility for 5 years survival, and is one of the most common causes of death from cancer. Cervix and uterus cancer have a 90-95 percent possibility for 5 year survival.
The lowest cure rates appear in the case of glioblastoma (brain cancer), pancreas and oesophagus cancer [10].

3.4 Outlook for 2015

Based on published information and official repository data from 2008, the evolution of cancer in Greece for the years 2010 and 2015 has been estimated as shown in Fig. (3.14) and (3.15). Incidence and mortality for the total number of cancer cases and deaths, as well as the four most common cancers-breast,lung,prostate and colorectum- are presented. Population forecasts were extracted from the United Nations, World Population prospects, the 2008 revision [8]. Numbers demonstrating the incidence and mortality rates by sex, are computed using age-specific rates and corresponding populations for 10 age-groups:

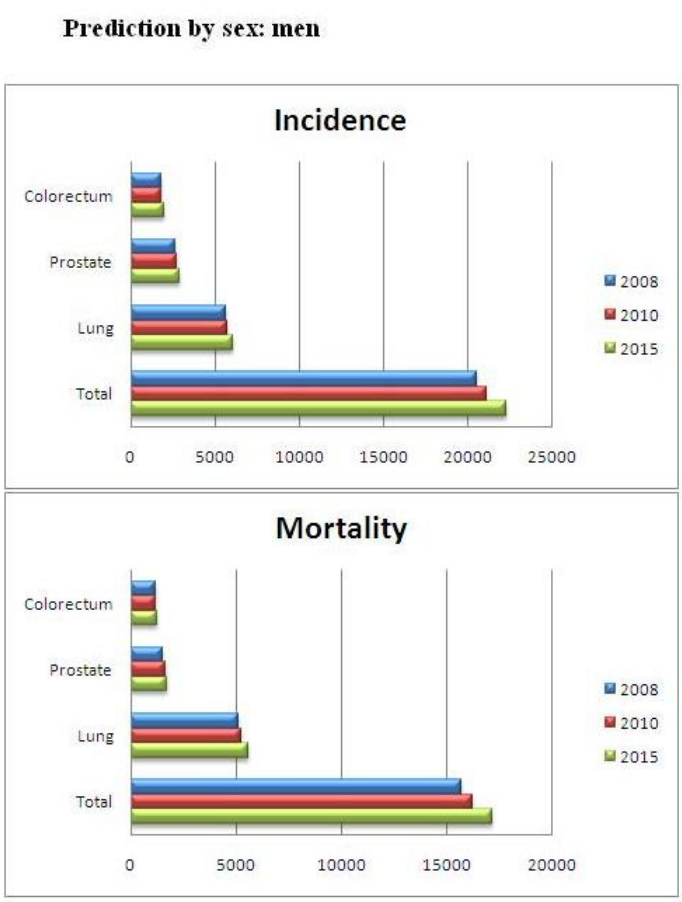

Figure 3.15: *Predictions for men.*

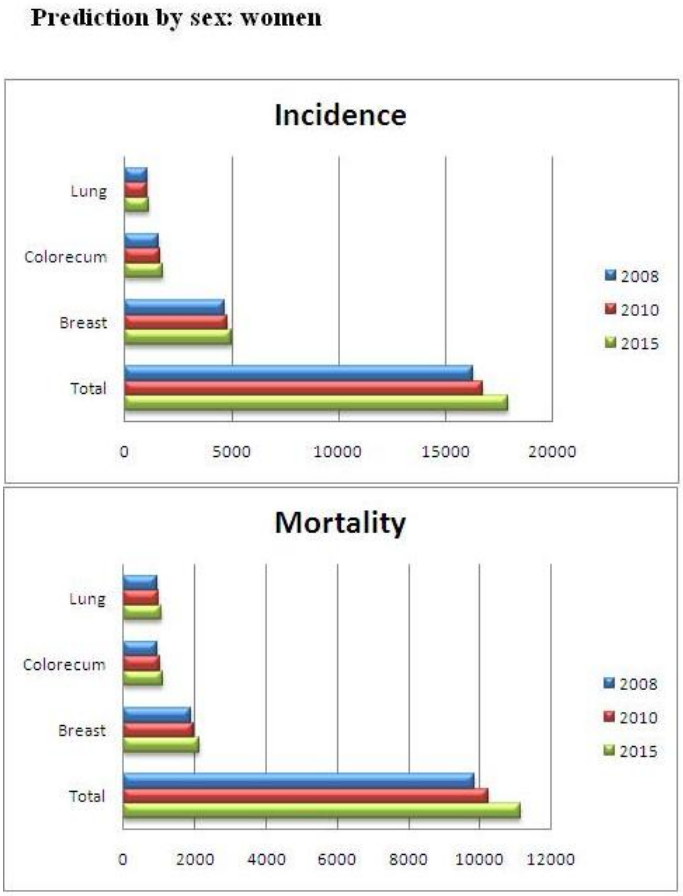

Figure 3.16: *Predictions for women.*

The high mortality of lung cancer in men and the extremely high incidence of breast cancer are evident. In general, the incidence as well as the mortality of all cancers are increasing steadily with time.

Chapter 4

Cancer Treatment

Cancer treatment is a major issue whose analysis exceeds the framework of this study. Therefore, a few aspects for each cancer treatment available will be presented, as well as some of the side effects which are caused by each treatment. Modern cancer management strategies recommend multimodality treatment that is assessed and delivered in an integrated multidisciplinary setting. Current methods to treat cancer are the *surgical removal* of the tumour tissue, *radiotherapy, chemotherapy*, and *immunotherapy* [1]. Radiotherapy destroys cancer cells through local or regional radiation. Chemotherapy involves the administration of a prescribed course of medication through the bloodstream that aims to kill or inhibit the growth of such cancerous cells. The combination of several cancer treatments is called combined modality treatment. Palliation treatment involves the alleviation of symptoms due to cancer. The extent in wich each treatment is used is illustrated in Fig. (4.1) [13].

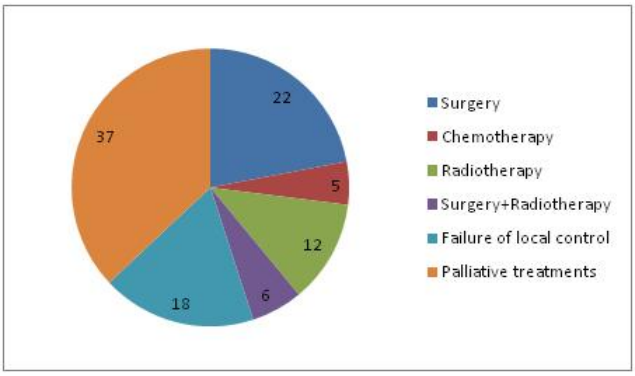

Figure 4.1: *Cancer treatment.*

Published literature and data gathered from Greek hospitals for surgery, chemotherapy and radiotherapy as modalities of treatment are analysed in the following sections.
However, during the choice of the treatment, many factors such as: the patient's co-morbidities and medical history, age etc should be taken into account. Cancer can be treated in different ways depending on the histological form of the tumor, the physical course of the cancer, the location, extent and the type of the tumor, how 'aggressive' it is, the stage of detection (there are different stages for cancer progression).
For example, if the cancer is diagnosed in an early stage, local treatment can be performed: For lymph node cancer, stages 1,2 and 3 can be treated with surgery, whereas stage 4 can only be treated with chemotherapy [9, 10].
Prostate cancer in an early stage, should be treated with radiation therapy or surgery.
According to the NCR, currently half of the diagnosed cancers are curable. In fact, for many kinds of cancer cases, complete cure can be achieved without the possibility of recurrence. In order for this to happen certain conditions must be fulfilled. However, even for cancers which are considered non curable, the appropriate treatment can offer significant advantages such as life extension and improved quality of life, setting to a minimum the effects of the disease. A treatment is considered successful if the patient survives for over than 5 years after the diagnosis for adults and over than 2 years for children.

4.1 Chemotherapy

Chemotherapy indicates the treatment of infections by compounds, of known chemical constitution, which effect cure by leading to destruction of the pathogenic organisms or their products. Thus, a contrast is implied between chemotherapeutic substances and the class of antibodies, which represent highly complex products of the biological reactions to infecting organisms [14]. In the case of cancer, medication is used, aiming to kill the cancer cells. The treatment of cancer by drugs is essentially pharmacodynamic because both, economic (healthy cells) and uneconomic (cancer cells) cells are part of the same organism. Chemotherapy aims to exterminate the uneconomic cell completely [14]. The goal is either to kill the cancer cells or stop them from dividing. The drugs used, reach the cancer cells though the blood stream and destroy them when they are in the dividing phase. However, not all cells are in the dividing phase at the same time and thus cannot be destroyed at once. For this reason, chemotherapy is repeated several times, while each time the chemotherapy drug is administered is called *cycle*. One cycle involves the administration of the drug and takes place once every month or approximately twenty days. The number of cycles depends on the type and stage of the cancer as well as the medical history of the patient. However, an average number of cycles is six to eight. The dose administered, depends on the body surface and is modified during the treatment, depending on the toxicity and the side effects induced. In some cases, combination chemotherapy is used. Several anti-cancer drugs, instead of only one, are administered (known as choemotherapy *cocktail*), which have different mechanisms of cytotoxic action on cancer cells. As a result, different classes of drugs may be more effective in destroying cancer cells which would have acquired some drug resistance. The principle of combination chemotherapy is most frequently applied to cancers potentially curable with chemotherapy such as lymphoma, leukaemia, germ cell tumors and childhood malignancies.

However, the drugs usually affect the economic cells as well. Among the healthy cells, the more prone to be affected are cells with low reproduction time, such as the cells on the bone marrow, the enteric mucous membrane, the reproductive system and the hair enclaves. After the termination of treatment, those cells usually recover.

Drugs are often used as part of multi-modality therapy, that is, along with surgery and/or radiotherapy, to achieve and maintain remission. The process is likely to be long term, where single agents or combination chemotherapy

are given at intervals in cycles and is highly dependent upon the tumor type and characteristics.
As far as the cost is concerned, it depends on the type of cancer and the drugs administered, but an average cost in a public hospital is approximately 12,000 euros.

4.1.1 Types of Chemotherapy and Side Effects

The aim of chemotherapy is to induce remission [15], that is, subsiding the symptoms of the disease for at least 1 month. The challenge of anticancer treatment, though, is to prevent recurrence, which may occur locally or at a distance (metastasis) of the primary tumor site. Chemotherapy can be administered before (*neoadjuvant*) or after (*adjuvant*) a localized treatment is applied. Sometimes, chemotherapy is administered with the aim of achieving significant cytoreduction, and, ideally, complete remission of the disease (*induction chemotherapy*) or to control the disease or provide palliation (*salvage chemotherapy*) [15].
All cancer treatments can result in side effects such as oral mucositis, peripheral neuropathy, nausea/vomiting, and fatigue but also greater and long term side effects as well. However, side effects may vary depending on each type of treatment. The most common side effects caused by chemotherapy are presented in Fig. (4.2):

Side effects caused by Chemotherapy
Hair loss
Oral wounds
Swallowing difficulty
Hyposalivation
Nausea
Vomit
Diarrhea
Bleeding
Infections

Figure 4.2: *Chemotherapy induced side-effects.*

Moreover, heart, liver, lung, kidney and nerve damage may be caused by

chemotherapy. Nerve damage usually causes hand and feet numbness. In most cases, the side effects disappear as soon as the treatment is completed [16].

4.2 Surgery

For many years, surgery has been considered fundamental for cancer treatment. It can be carried out in order to remove the primary tumor along with a margin of surrounding normal tissue to prevent local recurrence (*surgical resection*), to alleviate symptoms and improve the quality of life (*palliative surgery*) or in certain inherited conditions (*prophylactic surgery* [15]).
The likelihood of a surgical cure is dependent on the size, location, and stage of the disease. Surgery can be more effective if the tumor is localized. However, in case of cancer metastasis where cancer cells spread, travel through the blood or the lymphatic system and form secondary tumors, surgery is less likely to succeed. Sometimes, after the removal of the primary cancer, only one metastatic tumor is created, the removal of which can lead to complete cure. This usually happens to patients with colon or testicle cancer. The metastatic tumors in this case are found in the lungs, the liver or the brain.

4.2.1 Surgery induced side effects

According to the NCR, many people do not have long-term complications after cancer surgery. However, not all patients experience the same short or long term side effects. The type of long-term problem and how likely it is to happen will largely depend on the type of operation and on each patient's medical history.

Problems caused during as well as after surgery are presented in Fig. (4.3):

Side effects caused during surgery
Damage to organs in the body
Blood loss
Adverse reactions to medication
Side effects caused after surgery
Pain or discomfort
Infections
Other illnesses, such as pneumonia
Blood loss or clots

Figure 4.3: *Surgery induced side-effects.*

4.3 Radiotherapy

Radiotherapy is the first non-invasive treatment. It is considered to constitute the most widely applied cancer therapy, using Cobalt units, accelerators and radioisotopes. The purpose of radiotherapy is the administration of a perfectly computable and precisely directed dose of ionizing radiation to a specified geometrical volume of tissue. The aim of radiotherapy is the delivery of a high dose to the malignant tumors. The main difficulty is to deliver both a precise and accurate large dose of radiation to destroy cancer cells in a diseased organ but at the same time, cause as little damage as possible to the surrounding tissue. Thus, since the delivered doses are highly above the lethal level, they must be delivered with extreme caution.
The principle on which radiation therapy is based on, is damaging the DNA of cells. Ionizing radiation (electron, photon, proton or neutron) causes the formation of free radicals within the cell, leading to its destruction. However, cells have a DNA-repairing mechanism. Despite the fact that normal cells have greater repair capacity than cancer cells, damaging both strands of the DNA proves to be the only effective technique to modify cell characteristics. Cancer cells reproduce faster and as already mentioned, appear to have a limited ability to repair damage, compared to healthy cells. However, cancer cells are characterized by a low-oxygen state known as *hypoxia* when tumors outgrow their blood supply. Hypoxic cells are resistant to radiation and thus, difficult to destroy. The fractionation of the total dose delivered

provides healthy cells the necessary time to recover, while tumor cells are as already mentioned, less efficient in repair between fractions.
The *cell-cycle* plays an important role in the extermination of cancer cells. The cell cycle, is the series of events that takes place in a cell leading to its division and duplication (replication). It consist of four phases: G1 phase, S phase (synthesis), G2 phase (collectively known as interphase) and M phase (mitosis). The most radiosensitive phases are M and G2, while the most radioresistant is the S phase. Since not all cells are in the same phase during each schedule, one schedule will selectively kill sensitive cells. Fo this reason, radiation treatment is repeated several times and this procedure is called *fractionation*. Fractionation allows tumor cells that were in a relatively radio-resistant phase of the cell cycle during one treatment to enter a sensitive phase of the cycle before the next fraction is given. Moreover, tumor cells that were hypoxic during the former schedule (and therefore more radioresistant) may reoxygenate between fractions and thus, be vulnerable to the dose delivered. By decreasing the time between schedules, the effectiveness is increased, since there is no time for the cancer cells to repair. This, however, increases the side-effects since healthy cells do not have a chance for damage repair either.
In all malignant tumors, the tissues that should be irradiated are the protopathic origins and the possible spread region of cancer cells. Usually, the radiation dose is delivered in daily schedules and the amount of dose delivered depends on various factors such as: the type and the radio-sensitivity of the tumor and the resistance of the surrounding tissue [9]. Radio-sensitivity is demonstrated by the lethal dose of a tumor or the cure dose of radiation by which 95 percent local tumor control is accomplished [4].
The number of schedules also depend upon the type of cancer. The delivered dose is measured in *(cGy)* and depends not only on the type of cancer and the number of schedules. For example, for lung cancer treatment, the total dose delivered is 6000 cGy with 200 cGy per schedule. In the case of larynx cancer, the total dose delivered is 7000 cGy. Prostate cancer requires a higher total dose of 10000 cGy, but since it is located between two very sensitive organs (bladder and rectum), the delivery of such a high dose, will destroy the surrounding tissue. Thus, a total dose of 7000-8000 cGy may be delivered, while the use of brachytherapy -which will be analysed in the following section- is a preferred form of radiation treatment in the case of prostate cancer. However, an average dose is 180 cGy-200 cGy per day. If the dose per schedule decreases, then the number of schedules must increase

in order to deliver the necessary total dose [9].
In Greece, 20,000 patients require radiation therapy every year and the equipment in public hospitals is barely able to cover their needs. There are only 24 linear accelerators in public health centres while only half of them are high-energy, whereas only one public hospital is capable of providing modern techniques (IMRT). As a result, patients turn to private hospitals and clinics, where the cost for conventional radiation therapy varies from 8,000 to 20,000 euros. The total number of linear accelerators in both public and private health centres is 35, whereas, based on the population and the number of patients requiring radiation therapy, the number of linacs needed is 56. Moreover, the machines being used are rather old (up to 26 years) in public hospitals [10, 11]. According to [9], radiotherapy alone is used to treat 18 percent of the patients, whereas only 4 percent of the patients require chemotherapy and the remaining 78 percent requires combination treatment. As for particle therapy, it is not yet available in Greece.
Radiation therapy may be used to treat almost every type of solid tumor, including cancers of the brain, breast, cervix, larynx, lung, pancreas, prostate, skin, spine, stomach, uterus, or soft tissue sarcomas. Radiation can also be used to treat leukaemia and lymphoma (cancers of the blood-forming cells and lymphatic system, respectively). Radiation dose to each site depends on a number of factors, including the type of cancer and whether there are tissues and organs nearby that may be damaged by radiation [3, 14].
For some types of cancer, radiation may be applied to areas that do not have evidence of cancer. This is done to prevent cancer cells from growing in the area receiving the radiation. This technique is called **prophylactic radiation therapy**. Radiation therapy also can be applied to eliminate symptoms such as pain from cancer that has spread to the bones or other parts of the body. This is called **palliative radiation therapy**. In this case, the dose delivered is approximately 500 cGy per schedule.

4.3.1 Types of Radiation Therapy

Radiation therapy consists of three main types: Brachytherapy, Radioisotope Therapy and External Radiation Therapy.
Brachytherapy
Brachytherapy is delivered by placing radiation sources directly at the site of the cancerous tumour. As a result, very high doses are delivered to the area

requiring treatment. Thus, the affect of the irradiation is localized, reducing the exposure of healthy tissues. This type of treatment is usually administrated for cervical, prostate, breast and skin cancer [14, 17].

Radioisotope Therapy

Radioisotope Therapy is a form of targeted therapy. Radioisotopes are delivered through infusion into the bloodstream or ingestion. Chemical properties of the isotope result in its absorption by specific organs, different for each isotope. For example, radioiodine, used to treat thyrotoxicosis, is specifically absorbed by the thyroid gland. Moreover, radioisotopes can be attached to a molecule or antibody and guided to the target tissue. Radioisotope Therapy is usually used in the treatment of bone metastasis from cancer. The radioisotopes subside selectively to areas of damaged bone, and spare normal undamaged bone [18].

External Radiation Therapy

External Radiation Therapy procedures involve the delivery of a high energy beam to the area that requires treatment and fall into two categories: Conventional Radiation Therapy and Heavy Particle Radiation Therapy.

Conventional Radiation Therapy

Conventional external beam radiotherapy is carried out with photon or electron beams, delivered to the target with linear accelerators or, formerly, Cobalt units. The linear accelerator is a device that uses high-frequency electromagnetic waves to accelerate charged particles such as electrons to high energies through a linear tube. The high energy electron beam, can be used for treating superficial tumors, or it can be made to strike a target to produce x-rays to treat deeper-seated tumors [18, 17]. Medical linear accelerators produce X-rays and electrons with an energy range from 4 MeV up to around 25 MeV, while cobalt units produce beams of average energy equal to 1.25 MeV.Even though cobalt untis have generally been replaced by linear accelerators. However, cobalt treatment is still in use due to the reliability and simple maintenance of it's machinery compared to linear accelerators.

Other forms of radiation therapy are **IMRT** and **SBRT** radiotherapy: *Intensity-modulated radiation therapy* (IMRT) is an advanced mode of high-precision radiotherapy that utilizes computer-controlled linear accelerators to deliver precise radiation doses to a malignant tumor or specific areas within the tumor. A *stereotactic radiation treatment* (SBRT)is a treatment procedure that involves the use of a specially designed coordinate-system for the exact localization of the tumors in the body in order to treat it with limited but highly precise fields.

Particle Radiation Therapy

Particles currently used in radiation oncology are neutrons, protons and heavier ions such as carbon, known as heavy charged particles, are of interest in radiation

therapy due to several distinct physical properties which will be discussed in the following chapter. The rationale for charged-particle radiotherapy lies in either a physical dose distribution advantage (protons) or a combination of physical and biological advantages (heavy ions and pions). A characteristic of heavy particles is that as they pass through a medium -and in the case of cancer treatment, human tissue- their rate of energy loss or specific ionization increases with decreasing particle velocity, giving rise to a sharp maximum in ionization near the end of the range. Therefore, such particles deposit most of their energy in greater depth than electron and photons, and at a much more localized area. As a result, the local tumor control can be increased without increasing normal tissue complications, which provides them with an advantage over electrons and photons[19].
In external radiation therapy, the area that requires treatment, is irradiated in many different angles-fields due to the fact that the target is usually covered by other tissues. This way, the dose delivered is absorbed mostly from the tumor.

4.4 Radiotherapy induced side effects

Fig. (4.4) demonstrates some of the long-term side effects that can occur, but they depend upon the part of the body that has been treated. The long-term side effects can take months and sometimes years to develop.

Radiotherapy induced side effects
Hair loss
Alteration in skin color
Infertility – if the ovaries or testicles are within the treatment area.
Swelling in a limb or on the body (lymphoedema)
Red skin marks (telangectasia) may appear due to damage of small blood vessels
Shortness of breath
Difficulty swallowing due to a narrowing of the gullet (oesophagus) or reduced amounts of saliva.
Frequency passing urine
Narrowing of the vagina.-if that is the treatment area

Figure 4.4: *Radiotherapy induced side-effects.*

Modern ways of giving radiotherapy are designed to limit the chance of permanent side effects as much as possible and very few people develop long-term effects nowadays.

Development of new cancers

Radiotherapy can cause cancer and a small number of people will develop a second cancer because of the treatment they have had. However, the chance of a second cancer developing is so small that the risks of having radiotherapy are far out-weighed by the benefits.

Particle therapy appears to have minimal to non- existent side effects according to research done by the Loma Linda University [20]. However, in case side effects do appear, they would be similar to radiotherapy side effects but of course they are not as frequent and severe due to the fact that the amount of healthy tissue injured is much less in the case of ions than in the case of photons. Nevertheless, like in conventional radiotherapy, the side effects differ for each patient and depend not only on the patients medical history, but also on the dose delivered and whether the patient is receiving any other treatment such as chemotherapy.

particle therapy, like conventional radiation therapy, is dominated by certain principles and the particles used have distinct physical properties which are important in order to understand its mechanism of action. In the following chapters, both conventional and heavy particle radiation therapy will be analysed.

Chapter 5

Conventional Radiation Therapy

5.1 Conventional Radiation Therapy

It was previously indicated that the purpose of radiotherapy is the delivery of a specified dose to a cancerous tumor in order to exterminate it. The distribution of the dosed absorbed within the body depends on: 1. The energy and 2. The kind of radiation (photons, electrons). During the use of photons an interaction is observed (photoelectric effect, Compton Effect) with the atoms of the target (e.g. tissue). The electrons released due to the photoelectric effect or due to the Compton Effect cause ionization and have a biological impact to the tissue. This impact depends on the dose absorbed from the tissue. For a certain depth, the dose has an initial maximum energy which subsequently diminishes. The higher the particle energy, the larger the maximum effective depth of the dose. This maximum effect does not happen in the surface due to the straight trajectory of the secondary electrons produced.

For X photons emanating from an X-ray tube (200 kV) the electron trajectories are very short and the maximum dose appears in the surface of the skin. Thus, the photon X-ray radiotherapy is more suitable for surface tumors. The point where the maximum dose is deposited is called *electronic equilibrium*. In case of an electron beam the dose initially increases. But when the depth exceeds the half of the electron path, the dose diminishes very fast. Figure (5.1) demonstrates dose distribution in the tissue for both, photons and electrons:

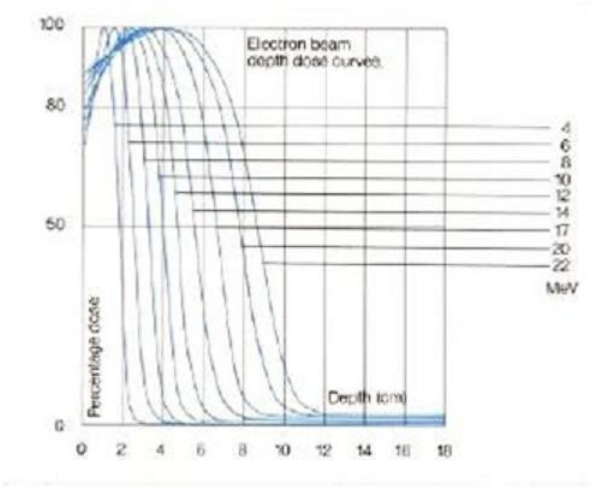

Figure 5.1: *Dose distribution in the tissue for electrons.*

The dose distribution within the X-rayed body is depicted by the isodose curves. In any point of those curves the dose has a constant value. The treatment planning is accomplished through the appropriate design of these curves.

Chapter 6

Particle therapy

6.1 Physical and Biological Basis of Protons and of Carbon Ions

particle therapy or otherwise known as *Hadron therapy* is a form of radiation therapy with proton or ion beams. Due to the favorable physical and biological properties of the particle beams being used, Hadron Therapy constitutes an improved treatment technique [13]. The finite range of the particle beam is the basic physical advantage for the clinical use of proton or carbon-ion beams in radiation therapy. The range is dependent on the beam's initial energy, as well as the density and atomic composition of tissues along the beam path. The particle energy required for Hadron Therapy is up to 250-300 MeV for protons and up to 400 MeV for carbon-ions. Beams can be designed in order to penetrate to the required depth and deliver a uniform biologically effective dose across the depth of interest. The loss of particle energy along their path is indicated by what is known as *Stopping Power*. The Stopping Power is expressed by the *Bethe Bloch* formula, presented in equation (6.1):

$$\frac{dE}{dx} = -\frac{4\pi}{m_e c^2}\frac{nz^2}{\beta^2}(\frac{e^2}{4\pi\epsilon_0})^2[ln(\frac{2m_e c^2\beta^2}{I(1-\beta^2)}) - \beta^2] \tag{6.1}$$

where c is the speed of light, $\beta = v/c$ (v being the particle velocity), E is the particle energy, x is the distance travelled by the particle, z is the particle charge, e is the electron charge, m_e is the rest mass of the electron, n is the electron density of the target, I is the mean excitation potential of the target and ϵ_0 is the vaccum permittivity [21].

The biologically effective dose (BED) is the amount of radiation absorbed by the region of interest, that has an effect on the irradiated organ or tissue of interest.

The result in dose distribution is superior to that achieved by photon beams. The main advantage of this radiation treatment method is the precision of the beam delivery. As a result, the possibility of eradication of the tumor alone increases while a minimal dose is delivered to the surrounding healthy tissue. Secondary malignances caused by radiation therapy may be observed. However, in the case of Hadron Therpay, no increase or a lesser risk of treatment related morbidity is achieved [13, 22].

Protons and C-ions used in Hardon Therapy, present several significant, physical characteristics which establish Hadron Therapy as the treatment of choice for many cases:

Higher physical selectivity

During conventional radiotherapy, the interaction of radiation with matter results in a dose profile according to which the amount of dose delivered reaches a maximum at the surface of the body while it decreases with depth, making irradiation of deep-seated tumors difficult. On the contrary, according to the ion beam dose profile, a large amount of dose is delivered to a narrow region close to the end of the particle tracks. This is the so-called Bragg Peak and is presented in Fig.(6.1). This constitutes ions ideal for the treatment of deep-seated tumors, while the narrowness of the irradiated region prevents the eradication of healthy tissue. The position of the peak is controlled by the energy of the incoming beam according to where the tumor is located [13]. For proton and carbon ion beams, the Bragg Peak decreases in height with beam energy, i.e. the depth of penetration, as shown in Fig. (6.2) for carbon ion beams of 135 MeV, 270 MeV and 330 MeV [22].

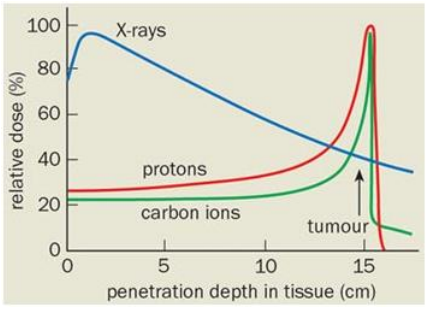

Figure 6.1: *A large amount of dose is delivered to a narrow region close to the end of the particle track. This is a characteristic of ion beams and is called Bragg Peak.*

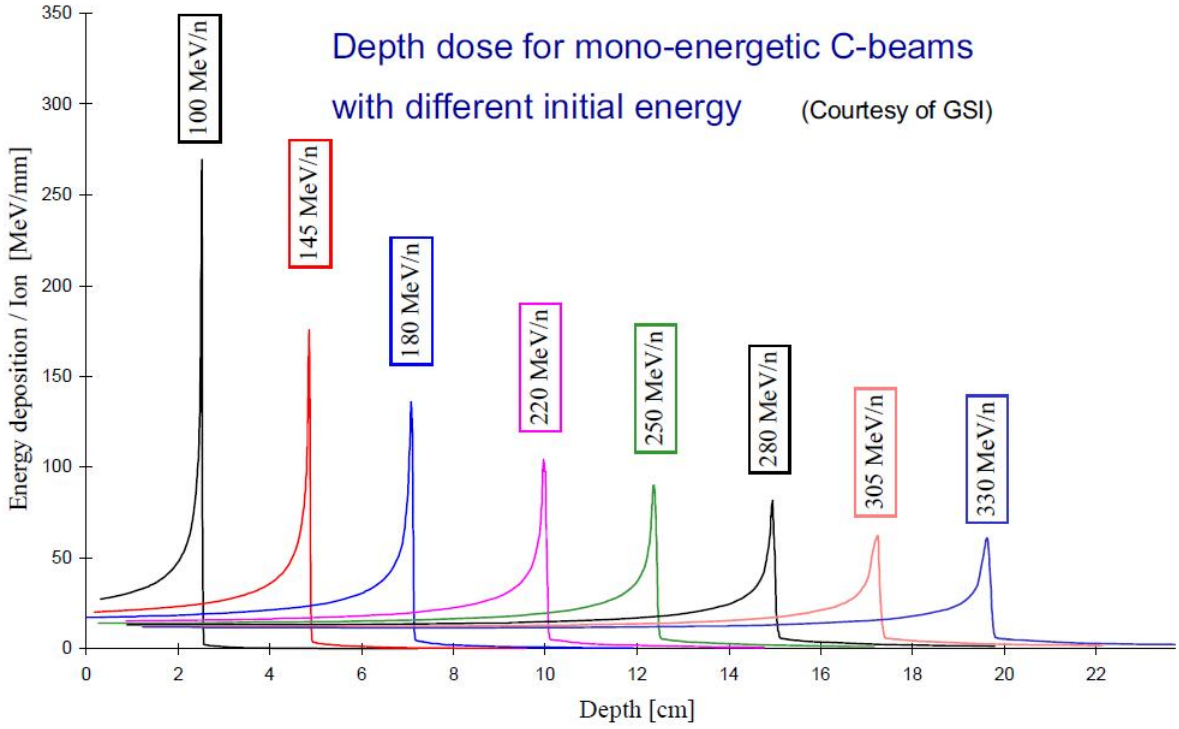

Figure 6.2: *The Bragg Peak decreases in height and thus, in depth of penetration, with beam energy.*

Higher biological effectiveness of ion beams

Use of these beams makes the planning and delivery of *biologically effective dose* (BED) distributions feasible which are superior to those by the highest technology x-ray therapy for most kinds of tumors. This means that for a defined dose and dose distribution to the target, there is a lesser dose to uninvolved normal tissues [22]. A clinical beam is designed to provide a nearly uniform BED over the range in depth that covers the whole tumor, despite the fact that Bragg Peaks are not usually wide enough to cover most treatment volumes. This is achieved by superimposing a set of beams with decreasing energies along the depth of interest in order to generate a flat dose for the majority of tumors despite the difference in anatomy and shape(Fig.(6.3))[23, 24]. This flat region is known as the spread-out Bragg peak (SOBP). To appreciate the large and clear advantage of a particle beam in radiation therapy, examine the depth-dose curves for a clinical proton beam (with its SOBP) and a high energy x-ray beam, in Fig.(6.4)[23]. The x-ray dose is not fully delivered to the target, since it decreases exponentially with the depth and exits the body. On the contrary, the proton beam, delivers the maxi-

mum dose in the target region. Additionally, the dose close to the target is lower for the proton beam except for the initial few mm, leaving the healthy surrounding tissue unaffected.

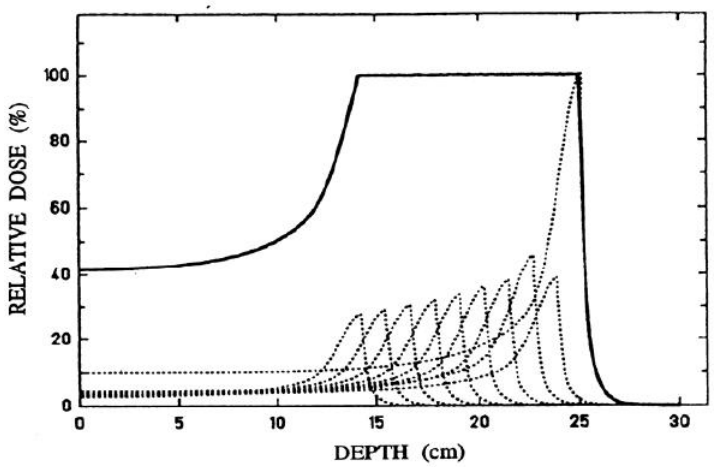

Figure 6.3: *The Spread Out Bragg Peak is achieved by superimposing a set of beam with decreasing energies, in order to adapt to the anatomy of each tumor.*

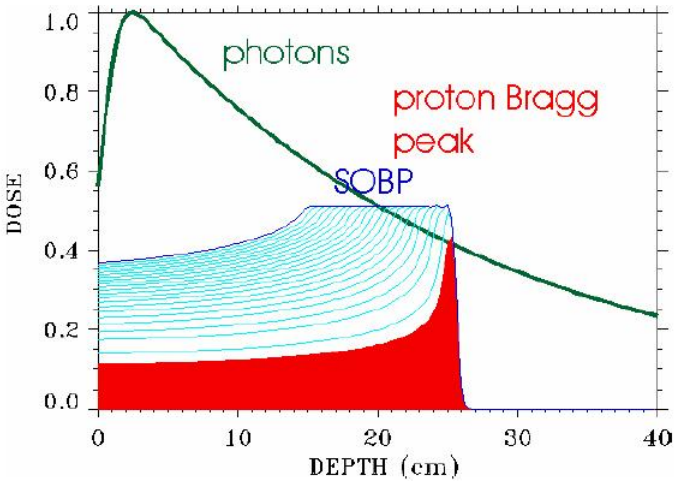

Figure 6.4: *Depth-Dose curves for both a clinical proton beam and a high energy x-ray beam.*

Enhanced Oxygen Enhancement Ratio

Heavy ions may overcome the relative radioresistance of some tumors which may be conferred by hypoxia as contrasted with the comparative radiosesetivity of normal tissues which results from their good oxygenation. However, inter-fractionation and re-oxygenation within the tumor may, in some sites reduce the problem potentially posed by tumor hypoxia. [24].

Linear Energy Transfer

Another determinant factor is the *Linear Energy Transfer* (LET) which is defined as the energy transferred to material, in this case tissue, as an ionizing particle travels through it. Protons have a low LET whereas carbon ions have a high LET and consequently have a high RBE relative to proton beams. Higher LET indicates lower cell survival and thus a greater effect on tumor cells [22]. In heavy ion radiotherapy the high-LET region can be conformed to the tumor. However, there will always be a small volume of normal tissue surrounding the tumor which is included in the irradiated (high-LET) volume.

However, proton and ion beams have certain disadvantages as well:

A lesser dependence of radiosensitivity on position in the cell-cycle

Normal cells tend to spend less time in the X-radiosensitive phases of the cell-cycle than malignant cells do. This may result in a relative protection when irradiated using X-rays. However, this protection would be partially lost with heavy ions since the high LET radiosensitivity is much less variable over the cell-cycle [24].

A loss of repair capacity in exposed cells

This constitutes a disadvantage for heavy ions since only one possible reason for the efficacy of X-rays is that they tend to allow normal tissue to repair damage-possibly more than malignant cells can do [24].

Factors that differentiate hadron therapy from conventional radiation therapy are the *dynamic scanning beam delivery* and the *verification of irradiation by PET*:

Dynamic scanning beam delivery

Another difference between conventional radiotherapy and hadron therapy is the fact that it is possible to steer the charged particles using magnetic fields. This way, well-focused, pencil-like charged particle beams with an adjustable spot size can be formed and scanned over the treatment field. This way the beam will follow precisely the tumor contours and by adjusting the intensity and scanning speed it is possible to attain any desired dose distribution within the target volume.

Verification of irradiation by PET

Another important advantage of the use of ions is the fact that when the beam penetrates through the tissue, positron emitting isotopes are generated by the fragmentation of primary ions. Those isotopes stop nearly at the region where the primary particles deliver the maximum dose. Thus, the region where the radiation dose is delivered can be identified by a positron emitting tomography. Moreover,

this can be done even during irradiation and thus it is possible to monitor and verify the correctness of the irradiation procedure [22].

In Figures (6.5),(6.6) and (6.7) comparative treatment plannings are demonstrated for three different tumors:

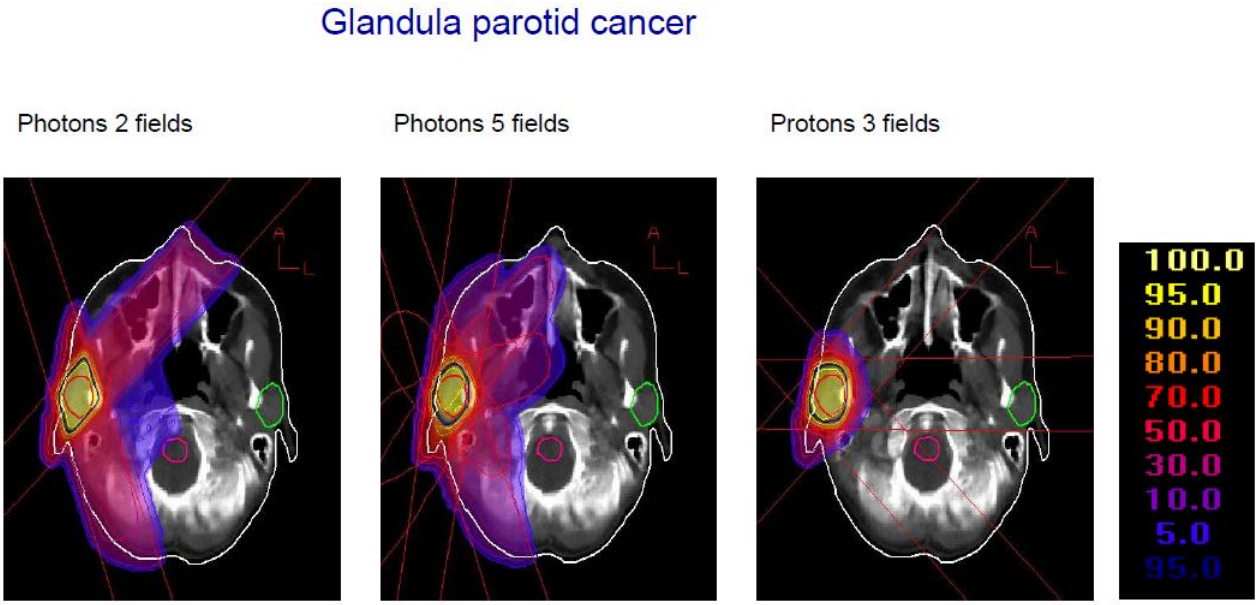

Figure 6.5: *Treatment planning for parotid cancer.*

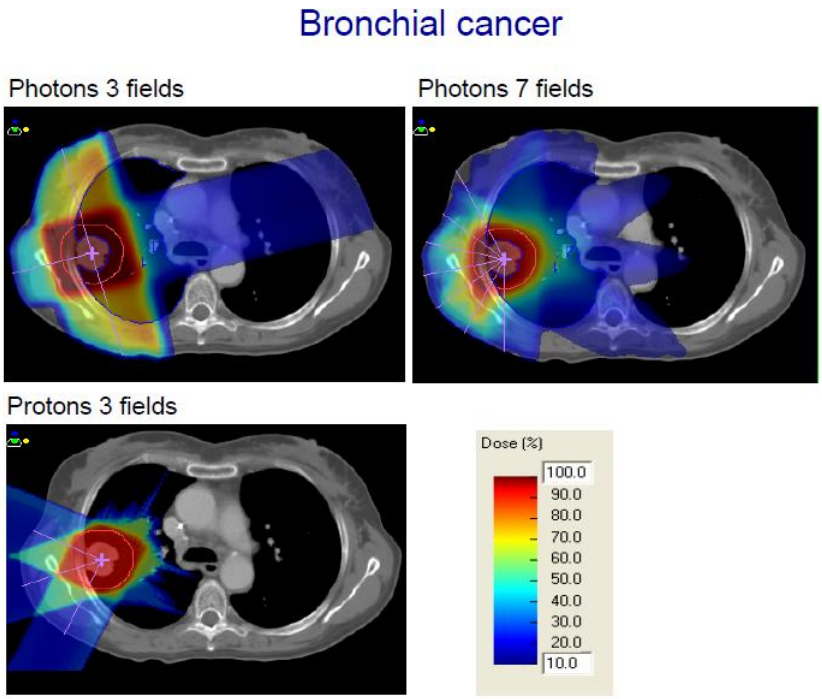

Figure 6.6: *Treatment planning for bronchial cancer.*

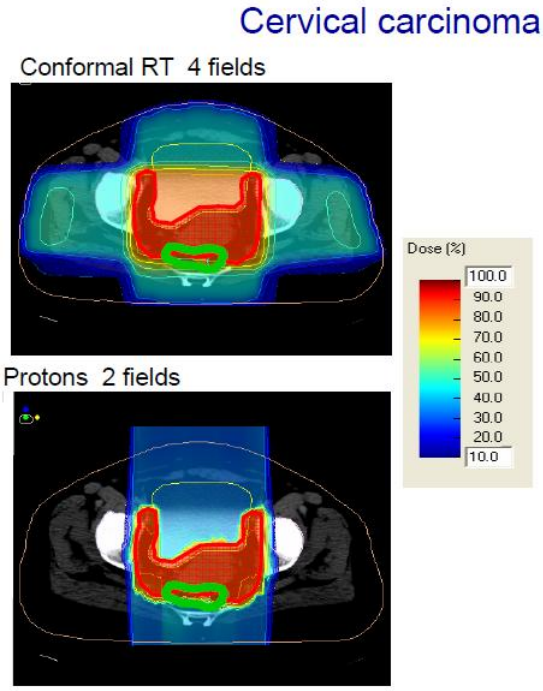

Figure 6.7: *Treatment planning for cervical carcinoma.*

As it can be observed from the figures above, the irradiated area surrounding the tumor, is much less in the case of protons. Therefore, the amount of healthy tissue being damaged by radiation is clearly less when Hadron Therapy is used.

6.2 Cases where Hadron Therapy is used

Theoretically, hadron therapy offers the potential of both physical and biological advantages in the treatment of *localized* tumors. This type of treatment is characterized by radiation-induced side effects including the risk of secondary malignancies, especially pronounced in comparison to conventional radiation therapy, where the normal tissue outside the target volume receives much larger doses. The treatment in pediatric tumors is one of the most important indications for proton therapy because a clear benefit by means of reduced toxicity is assumed. Based on research and data from clinical trials, the use of hadron therapy for treating certain types of cancer will be presented.

6.2.1 Prostate cancer

Prostate cancer needs relatively high doses in order to be controlled and thus prostate cancer cells are assumed to be radioresistant to conventional photon RT. Therefore, the delivery of higher single doses is currently under discussion and high-LET beams such as carbon ions provide a physical and biological advantage. From clinical trials preformed in Chiba, Japan within a total of 201 patients, Fig. (6.8) was obtained [25, 26]:

PROSTATE CANCER	5-year Local Control	5-year Overall Survival	Gastrointestinal Toxicity	Genitourinary Toxicity
Protons	74%	89%	15%	7%
Carbon Ions	100%	89%	6%	<5%
Photons	83%	66%	29%	28%

Figure 6.8: *Hadron Therapy in prostate cancer.*

The results for 5-year local control are very similar for all three types of treatment. However, toxicity rates are much higher in high dose photon therapy.

6.2.2 Lung cancer

Early stages
Surgery continues to provide the best chance for cure in early-stage patients with 60 percent 5-year survival rate. Conventional radiotherapy with X-rays (XRT) is inadequate for a large fraction of patients providing 5-year survival rates up to 30 percent, due to the lack of local control. Treating early stage non small cell lung cancer (NSCLC) with SBRT is considered effective and safe with high rates of local control at two years (67-95 percent). On the other hand, the use of carbon ions has presented encouraging results, the limited number of patients treated is unable to lead to a conclusion. Proton therapy in the treatment of early stage lung cancer offers very encouraging results, with local control rates at two years of 80-95 percent and overall survival at 60-70 percent, obtained with very few acute and late toxicity [27].
Advanced stages
The treatment of patients with tumors in advanced stages appears to be very challenging since local control constitutes a major problem. The role of surgery, combined radiotherapy and chemotherapy and SBRT is very limited due to extremely low rates in overall survival, significant and excessive toxicity respectively

[27]. Proton therapy could be a possible solution for technical difficulties in irradiating advanced cases enabling high-dose delivery to the tumor, while minimizing the irradiated volume and dose given to normal tissues. However, the clinical data available in the literature are very limited (33 patients). Short term results were very promising, with 70-100 percent 2-year survival. Unfortunately, the long term causing specific survival were very disappointing for stage III and IV patients (0 percent) and more favorable for patients suffering from recurrence (50) percent [27].
Proton therapy is a promising modality of irradiation in the treatment of early-stage disease producing favorable results and low toxicity, whereas indications for PT in advanced stages are based mainly on planning studies and further clinical investigations are needed. However, while treating lung tumors, there is a need for compensating for breathing motion and for the changes in lung density due to respiration, which must be balanced against unnecessary irradiation of the healthy lung.

6.2.3 Skull-Base tumors

Conventional photon RT offers poor results, with local control rates at 5 years at 17-23 percent. With stereostatic photon techniques 50 percent local control rate at 5-years is obtained while increasing the dose from 50 Gy to 65 Gy offers favorable results. However, proton therapy, with the delivery of a higher dose (up to 83 CGE) achieves better results where the 5 and 10-year control rates reach 73 and 54 percent respectively for 375 patients treated at Massachusetts General Hospital[25]. Carbon ion therapy has been shown to yield similar results. Between 1997 and 2001 a clinical trial was performed at GSI for treatment of chordomas and chondrosarcomas of the skull-base with carbon ions. For a total dose of 60 CGE, Fig. (6.9) is obtained [25]:

Skull Base Tumors	4-year Local Control	4-year Overall Survival
Chordomas	74%	86%
Low-grade chondrosarcomas	87%	100%

Figure 6.9: *Hadron Therapy in skull-base tumors.*

As it is obvious, hadron therapy is the treatment of choice for skull-base tumors.

6.2.4 Head and Neck cancer

For 62 patients with head and neck cancer treated with PT, the local control rates varied between 74 and 84 percent, where the 5-year survival varied between 44 and 65 percent. As far as carbon ion therapy is concerned, the local control and survival rates are higher than 75 percent! For squamous cell carcinomas, the results of photon therapy seem to be similar to proton and carbon ion therapy, whereas for adenoid cystic carcinomas, local control rates achieved with C-ions are much higher than the ones achieved with photon (75 and 50 percent respectively) [26].

6.2.5 Bladder cancer

In clinical trials on proton therapy with 55 patients with bladder cancer a 59 percent for both 5-year survival and local tumor control was achieved and in approximately 16 percent of the patients higher than grade 2 toxicity occurred. The results are similar to combined modality therapy using photon RT. However, higher bladder preservation rate was reported with proton therapy (63 vs 80 percent) [26].

6.2.6 Ocular tumors

Eye preservation rates are generally over 90 percent, with useful vision in approximately 50 percent after 5 years were reported with protons, while in larger tumors and in some specific anatomical localizations in the eye, protons also present the best results. Clinical trials performed at Chiba, showed that proton and SRT therapy have similar results. However, most series with SRT photon therapy only show 2-3 years results, whereas proton therapy studies show 5 year results. [26].

For cancers such as cervix, pancreatic, hepatocellular and gastrointestinal tumors, the role of protons or C-ions either remains unclear or has similar results to photon RT.

6.3 Hadron therapy facilities and Cost Analysis

Based on studies concerning the cost efficiency of hadron therapy [28, 26], radiotherapy costs are determined for three different facilities (carbon ion and proton, protons and photon facilities) and considerations that must be taken into account

about hadron therapy facilities are presented. There is a considerable public, scientific, clinical and commercial interest in the further development of hadron therapy. Since the number of new treatment facilities is increasing, it is important to assess the evidence available on the clinical efficacy of particle therapy as well as construction costs and costs for running such a facility [26]. Other than construction costs, specific treatment costs for four cancer types (prostate, lung, head and neck and skull-base chordoma) are determined [28].
The calculated cost per fraction for all three facilities is demonstrated in Fig. (6.10):

Facilities	Combined	Proton only	Photon
Cost	1128 euros	743 euros	233 euros

Figure 6.10: *Calculated cost per fraction for p/C, C and p facilities.*

However, other factors should be taken into account such as the number of fractions needed for each type of therapy, the lifetime of the facility, the number of patients being treated as well as the treatment time. The construction and operation of a radiotherapy facility depends on many local factors since the financial plan, budgetary conditions, construction/vendor market providing the facility may differ internationally and even within a country [28].
Based on the data presented in previous sections concerning the effect of heavy particles in treating certain types of cancer, it is clear that there are specified sites that can undoubtedly benefit from hadron therapy. However, firm conclusions cannot be drawn on the efficacy of charged particles on other sites, probably due to the lack of facilities required for clinical research. According to [26], if only four tumor sites are considered (left-sided breast cancer, childhood medulloblastoma, prostate and head and neck cancer), when proton therapy is compared to conventional RT, the cost per quality-adjusted life year gained is 10,130 euros. Moreover, 15 percent of patients currently treated with conventional RT would benefit from PT [26]. **Hadron Therapy Facilities**
There are currently 35 Hadron Therapy facilities in operation worldwide, most of them using protons, a few using C-ions and only 2 providing both. In Fig. (6.11) the increase in the construction of such facilities throughout the years is shown:

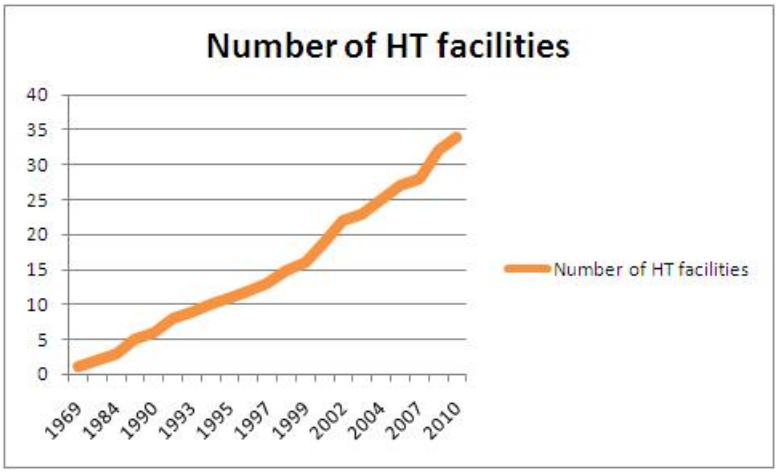

Figure 6.11: *Rapid increase in construstion of Hadron Therapy Facilities.*

In Russia, there are 3 Hadron therapy facilities, all using protons. In the rest of Europe, there are 12 facilities, 9 of which are using protons, 1 is using C-ions (GSI, Darmstadt, Germany) and 1 using both (HIT, Heidelberg, Germany). In the USA, there are 8 facilities in operation, all using exclusively protons. In Asia, there are 10 facilities out of which 1 provides therapy with both protons and C-ions, 2 are using only C-ions and the rest are using protons. Last, there is one facility in Canada using protons.
A few more HT centers are under construction in Europe: The CNAO facility in Pavia, Italy, Med-Austron in Austria and PTC in Marburg, Germany, all providing both proton and C-ion therapy.

6.4 Hadron Therapy in Greece

The data presented in previous chapters, indicate that Hadron Therapy, can provide great benefits for certain types of cancer. In summary, higher local tumor control and overall survival rates are achieved with proton or C-ion therapy for head and neck tumors, early stage lung cancer and central nervous system tumors (skull-base). For ocular and bladder cancer, the results of hadron therapy are similar to SRT (Stereostatic Radiotherapy) and combined modality photon RT respectively, but the preservation of the tissue is higher in the case of proton therapy. Head and neck, as well as skull-base tumors benefit significantly from hadron therapy. Last, as far as prostate cancer is concerned, the local tumor control rates are similar for hadrons and photons. However, 5-year survival rates are higher when prostate cancer is treated with protons or C-ions with a much lower toxicity

rate.
Lung and prostate cancer are two of the most common cancers in Greece. More specifically, Greece has the second highest crude rate in lung cancer for men. Moreover, central nervous system cancer, represents a significant percentage in incidence and mortality rates for both men and women (4.1, 5.7 percent and 3.9, 4.2 percent respectively). According to latest information obtained from the database of the World Health Organization [2] for the year 2008, Greece is the third country in the world regarding mortality (645 deaths in 2008) from skull-base tumors and has the highest crude rate for both, men and women (11.7 and 9.5 respectively). Bladder cancer, according to Fig. (3.7), is the fourth most common cancer for men and the fifth most common cause of death from cancer, while according to data acquired from [2], Greece has the highest crude rate for men in bladder cancer. This can be observed in Fig. (6.12) and (6.13), where the crude rate for the types of cancer that require HT is demonstrated based on data concerning the year 2008. Taking this into account, it is clear that Greece, can benefit from having access Hadron Therapy.

Country	Lung	Brain	Bladder	Prostate
Greece	2(96.4)	1(11.7)	1(16.1)	9(28.3)
Croatia	1(100.4)	2(13)	2(10.2)	6(30.1)
Slovenia	4(81.6)	5(8.4)	3(12.1)	2(34.3)
Lithuania	9(74.5)	8(7.4)	4(12)	3(34)
Serbia	8(77.7)	7(7.6)	10(8.3)	11(19.2)
Romania	10(72.5)	9(7.4)	6(10.7)	12(16.7)
Czech Republic	7(77.7)	6(7.7)	7(10.1)	10(25.5)
The Netherlands	6(78)	10(7.2)	8(9.8)	7(29.6)
Austria	11(58.7)	12(6)	9(8.4)	8(29.1)
Estonia	3(90.4)	3(8.7)	5(10.8)	1(40.4)
Japan	5(78.4)	15(1.6)	11(7.2)	13(16.1)
Finland	12(53.3)	11(6.5)	12(6.9)	5(31.2)
Republic of Moldova	13(41.9)	13(4.7)	13(6)	15(7.8)
Iceland	14(38.6)	4(8.7)	14(5)	4(33.6)
Kazakhstan	15(34.9)	14(3.6)	15(3.8)	16(4.9)
Mauritius	16(16.7)	16(1.6)	16(1.6)	14(9.1)

Crude and Age-Standardised Rates per 100,000

Figure 6.12: *Crude Rates for Men- Types of cancer for which Hadron Therapy is most effective.*

Country	Lung	Brain	Bladder
Greece	11(19.2)	1(9.5)	8(3.6)
Croatia	7(26.7)	4(7.4)	7(3.5)
Slovenia	4(28.4)	9(5.3)	1(5.6)
Lithuania	13(12.9)	3(8.4)	12(2.7)
Serbia	8(23.6)	8(6.1)	11(2.8)
Romania	12(16.5)	7(6.2)	13(2.4)
Czech Republic	5(28.2)	6(6.4)	3(4.1)
The Netherlands	2(42.3)	12(4.9)	2(4.4)
Austria	3(28.6)	11(5)	6(3.6)
Estonia	10(20.1)	5(7.3)	5(3.9)
Japan	6(27.9)	15(1.2)	10(3.1)
Finland	9(22.6)	10(5.2)	9(3.2)
Republic of Moldova	14(9.2)	13(3.1)	14(1.8)
Iceland	1(46.5)	2(8.4)	4(3.9)
Kazakhstan	15(7.5)	14(2.5)	15(0.8)
Mauritius	16(5.7)	16(0.8)	16(0.8)

Crude and Age-Standardised Rates per 100,000

Figure 6.13: *Crude Rates for Women- Types of cancer for which Hadron Therapy is most effective.*

Chapter 7

Conclusion

Hadron Therapy is an important form of cancer treatment and provides significant advantages to a considerable number of patients. Valuable clinical experience has been gained over the last years, but further research is needed in order to overcome the difficulties and take full advantage of what a therapy like this can offer. It is not to replace conventional radiation therapy but to provide another modality of treating certain types of tumours which cannot easily be treated using conventional radiation therapy. Both types of treatment offer advantages. However, particle therapy constitutes the treatment of choice for many types of cancer while it provides benefits in terms of treatment and quality of life that must not be neglected.

As far as Greece is concerned, several aspects should be evaluated. Greece is a country with the lowest incidence rate for women and the second lowest for men when at the same time, presents the highest mortality to incidence ratio for both sexes [6]. Taking into account that it is a relatively small country, the fact that the mortality to incidence ratio is so high, should be taken under serious consideration. Aspects such as the reasons for such low survival rates and most importantly the access to, the availability and the quality of treatment should be examined. According to data from the epidemiological analysis, as already mentioned, Greece presents some of the highest crude rates for most types of cancer that require Hadron Therapy, while in the case of bladder cancer and skull-base tumors, the crude rate is the highest in the world for men and for both sexes respectively. From Tables (6.5) and (6.6), it is clear that in most of the Balkan countries, the crude rates are also high, especially for men. Thus, it is obvious that not only Greece but other Balkan countries can benefit from Hadron Therapy, potentially increasing the survival rates significantly.

Bibliography

[1] J. Higginson, C.S Muir and N. Munoz *Human Cancer, Epidemiology and Environmental Causes*. Cambridge University Press, 1992.

[2] World Health Organization, *http://www.who.int/en/*.

[3] National Cancer Registry.

[4] Hellenic Union of Medical Oncology, *http://www.onco.gr/eepoe-oncology-book.html*.

[5] International Agency of Research on Cancer, *http://www.iarc.fr/*.

[6] European Cancer Observatory, *http://eu-cancer.iarc.fr/*.

[7] *Hellenic Statistical Department* http://www.statistics.gr/portal/page/portal/ESYE.

[8] GLOBOCAN, *http://globocan.iarc.fr/*.

[9] *Onclogy Hospital-'Agios Savvas'*.

[10] *Attikon Hospital*.

[11] *Athens Navy Hospital*.

[12] G. Cuttone, *Applications of Particle Accelerators in Medical Physics*. https://espace.cern.ch/partnersite/Bibliography

[13] J. Debus et al., *Proposal for a dedicated ion beam facility for cancer therapy*. 1998.

[14] J. Cameron, J. Skofronick, *Medical Physics*. John Wiley and Sons, Inc, 1978.

[15] Rachel Airely, *Cancer Chemotherapy: Basic Science to the Clinic*. Wiley-Blackwell, 2009.

[16] Edward L. Alpen, *Radiation Biophysics*. Prentice-Hall International Editions, 1990.

[17] faiz M. Khan , *The Physics of Radiation Therapy*. Lippincott Williams and Wilkins 4th Edition, 2009.

[18] C. K. Bomford and I.H Kunkler, *The Textbook of Radiotherapy and Radiation Physics and Oncology*. Elsevier Science-Churchill Livingstone, 6th edition 2003.

[19] *Protocol for Heavy Charged-Particle Therapy beam dosimetry*. AAPM Report No. 16 American Institute of Physics, April 1986.

[20] http://www.protons.com/

[21] E.Gazis *Ionizing Radiation: Applications is Biology and Medicine* Papasotiriou,2002

[22] Alexander W. Chao, *Reviews of Accelerator Science and Technology, Vol. 2: Medical Applications of Accelerators*. World Scientific Publishing Co. Pte. Ltd, 2009.

[23] Michael Benedikt, *Small Synchrotrons*. CAS, Cern Accelerator School 2005.

[24] Michael Goitein, Journal of Radiotherapy and Oncology-95, *Trials ans tribulations in charged particle radiotherapy* Elsevier Ireland Ltd., 2009.

[25] Mark Lodge, Madelon Pijls-Johannesma, Lisa Strik, Alastair J. Munro, Dirk De Ruyssecher, Tom Jefferson, Journal of Radiotherapy and Oncology-83, *A systematic literature review of the clinical and cost-effectiveness of hadron therpay* Elsevier Ireland Ltd, 2007.

[26] Daniela Schulz-Ertner, Oliver Jakel, Wolfgang Schlegel Journal of Radiotherapy and Oncology, *Radiation therapy with Charged Particles* Elsevier Ireland Ltd., 2006.

[27] Lamberto Widesott, Maurizio Amichetti, Marco Shwarz, Journal of Radiotherapy and Oncology-86, *Proton therapy in lung cancer: Clinical outcomes and technical issues. A systematic review* Elsevier Ireland Ltd., 2008.

[28] Andrea Peeters, Janneke P.C. Grutters, Madelon Pijls-Johannesma, Stefan Reimoser, Dirk De Ruysscher, johan L. severens, Manuela A. Joore, Philipe Lambin, Journal of Radiotherapy and Oncology, *How costly is particle therapy? Cost analysis of external beam radiotherapy with carbon ions, protons and photons* Elsevier Ireland Ltd, 2009.

[29] Michael Benedikt, *Introduction to Hadron Therapy and the Medaustron Project*. CAS, Cern Accelerator School 2004.

Part II

Chapter 8

Introduction

8.1 Particle Accelerators

The 50 percent of particle accelerator installations, worldwide, is mainly devoted to medical applications such as radiotherapy, medical radioisotopes production, and biomedical research [1]. Also they contribute in the improvement of the technical features of medical diagnostics.
Particle accelerators are structures used to accelerate charged particles such as protons and ions to very high speeds, using electromagnetic fields, and to maintain them in a well-defined beam. An accelerator consists of the particle source, the injection section, a copper tube where the beam circulates, powerful electromagnets used to steer the beam, radiofrequency(RF) accelerating cavities, drift and extraction sections etc. Particle accelerators may be linear or circular.
In *linear accelerators* (LINACs), charged particles are accelerated in a straight line, in one single pass, with a target of interest at one end, using a RF electric field.
In *circular accelerators* however, the particles preaccelerated and then injected with an initial energy into the accelerator where they move in a circular path until they reach a sufficient energy. The particle track is typically bent into a circle using electromagnets [2].
Circular accelerators have an advantage over linear accelerators (linacs) due to the fact that the ring topology allows continuous acceleration, as the particle can transit indefinitely. On the contrary, in linear accelerators, the particles perform only one pass from the accelerating structure. Another advantage is that, a circular accelerator is extremely compact compared to a linear accelerator of comparable power.
In medical applications, when circular accelerators are used, these are cyclotrons

and synchrotrons. A *cyclotron* consists of two hollow semicircular electrodes, called dees. In each dee there is a magnetic field, constant and perpendicular to the beam direction. In the gap separating the dees, there is an alternating electric field pointing from one dee to the other. This way, the particles injected near the center of the magnetic field, in the gap, are accelerated continuously from one dee to the other and the magnetic field guides them in a circular path. As the particles gain speed, the radius of the particle track increases and they spiral outward, as presented in Fig. (8.1). A cyclotron operates at a fixed radiofrequency and all the settings of the beam are predetermined.

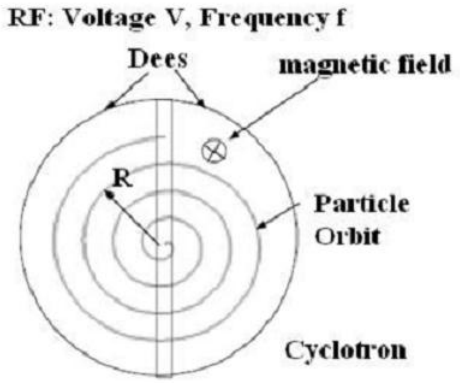

Figure 8.1: *In a cyclotron the particles are injected near the center of the magnetic field. As they are accelerated from one dee to another, the gain speed and they follow a spiral outward path [3].*

A *synchrotron*, consists of a ring of constant radius where magnets are placed to bend, focus and steer the beam. The magnetic and electric field are varied and synchronized with the travelling particle beam and the particles are accelerated in one or more RF cavities. By increasing the magnetic and electric field appropriately as the particles gain energy, their trajectory can be held constant as they are accelerated.Particles are often pre-accelerated in a linear accelerator before injected into a synchotron. In the case of relativistic particles, particles which move with a speed of light ($|\vec{u}| = c$), the orbit radius increases with energy according to equation (8.1):

$$R = \frac{\vec{E}}{ec\vec{B}} \tag{8.1}$$

where R is the orbit radius, $\vec{E}$ is the particle energy, e is the particle charge, c is the particle velocity which is equal to the speed of light in the case of relativistic

particles and $\vec{B}$ is the magnetic field. Since the radius is constant, according to the equation above, it follows that the ratio E/B must also be constant. This means that the magnetic field increases as the energy increases. However, there is a technical limit to the maximum magnetic field that can be produced with conventional magnets- currently it is around $—\vec{B}—$=1.7 Tesla, whereas with superconducting magnets it is $—\vec{B}\bar{5}$ Tesla.

Since the accelerator is circular, magnets are used to bend the particle beam into a circular orbit. The particles experience a divergence caused by the bending magnets, hence, focusing of the beam is required which is handled independently by specialized quadrupole magnets (Fig. (8.2)[3]).

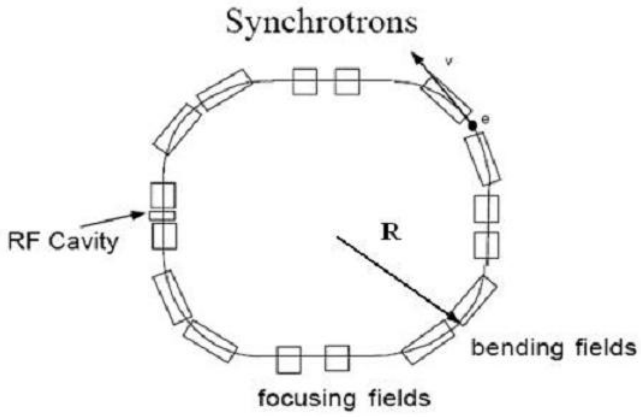

Figure 8.2: *A synchrotron consists of bending and focusing magnets.*

However, there is no necessity for a synchrotron to be completely circular but rather the beam pipe may have straight sections (sections where no bending of the beam takes place) between magnets as shown in Fig. (8.3)[4].

In medical applications, the particles used in linear accelerators are usually electrons which can be used for treatment directly or they can be collided with a target to produce X-rays. The particles used in circular medical accelerators (cyclotrons as well as synchrotrons) are usually Protons or Carbon ions (Hadrons) since they are the most suitable for treatment of deep-seated tumors (see Part I, Chapter 6).

There are many Hadron Therapy facilities in Europe. The following table includes some of the under construction or operating European facilities, along with the accelerator's circumference and particles' kinetic energy.

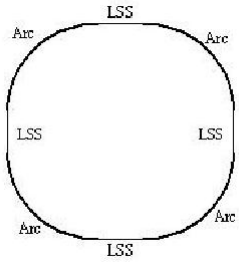

Figure 8.3: *A synchrotron that consists of straight sections and arcs instead of being completely circular [3].*

Facility	**Country**	**Circumference (m)**	**Energy(MeV)**
Medaustron	Austria	78	250 p
HIT	Germany	65	250 p
CNAO	Italy	78	250 p
GSI	Germany	65	250 p
TSL	Sweden	93	200 p

Table 8.1: Hadron Therapy Facilities in Europe

8.2 The present study

The present study concentrates on the design of an accelerator for medical applications, specifically designed for the treatment of deep-seated cancer tumors, focusing on the linear beam dynamics. This accelerator should be very compact and have low production cost. Considering the above requirements, the designed accelerator will be a compact synchrotron with a small circumference. In addition to that, the magnets which will be used should be regular instead of superconducting. Superconducting magnets are electromagnets constructed from superconducting wire and cooled to cryogenic tempratures during operation. These magnets achieve greater magnetic fields than conventional magnets which reach a field of 1.7 Tesla, but the construction and operation costs are significantly higher.
Concluding, the specifications, which are followed in the design of the compact synchrotron, are:

- The circumference of the synchrotron is 50m.
- The particle kinetic energy is 300 MeV.

- The accelerated particles are protons.

Furthermore, in the framework of this study, issues such as beam circulation and linear beam optics are discussed. Parameters, such as the strength, the number and the size of the magnets used in the synchrotron, the drift spaces between each magnet and the produced magnetic field, are defined. Program code has been written on specific simulation tools for the definition and optimization of these parameters. This study has the following structure.
In *Chapter 9*, the basic principles of accelerator optics are described and particle motion in circular accelerators are presented. Additionally, the type of structure of the synchrotron is examined and the necessary parameters (magnet length, size etc.) are discussed.
In *Chapter 10* a parameterization process is presented for determining the characteristics of the lattice, for a medical synchrotron of 50 m circumference and maximum kinetic energy of the particles equal to 300 MeV.
Chapter 11, consists of an analysis of the modifications required in order to acquire a proton beam with zero dispersion. The code for the dispersion suppression is written in MADX.
In *Chapter 12*, the effect of weak focusing on accelerators functioning in the MeV range is discussed. Moreover, the determination of transfer matrices of the magnets taking into account the weak focusing is presented and the stability of the lattice is examined. Computational software programs, Matlab and Mathematica are used, in order to preform the nessecary calculations and plots creation, while program code is written in MADX to examine the stability of the lattice.
In *Chapter 13* the conclusions drawn as a result of the study are presented.
The Appendix which follows in the end of this study contains the program code written in MADX.

Chapter 9

Accelerator Optics

As previously defined, a synchrotron is a type of circular accelerator in which electromagnetic fields are used to accelerate and bend the particle beam in order for the particles to move in a circular orbit until they reach sufficient energy, thus they follow a closed path over and over again and as a result, cover an extremely large total path [2]. The general concept in circular accelerators is that the particles of the beam are accelerated constantly and brought back to the same accelerating structures time after time. Magnets are used to control the direction of a beam. Magnetic fields exert a force on charged, moving particles. The magnetic force produced increases with the particle velocity and always focuses and steers the beam while it brings the particles back to the desired orbit. Particle motion is determined by the electric and magnetic forces that they encounter as they circulate through the ring. Circular accelerators have magnets distributed all around the circumference-sometimes reffered to as the *lattice* [5]; these produce the magnetic force responsible for focusing and steering the beam. Thus, when designing a circular accelerator, accelerator magnets, particle motion and particle trajectories should be examined.

9.1 Linear beam optics

In any kind of accelerator there is exactly one curve - the design or nominal orbit or trajectory - on which ideally all particles should move. However, the trajectories of individual particles have a certain angular divergence which causes them to slightly deviate from the design orbit as shown in Fig. (9.1) [7].

Without controlling these trajectories, the particles will eventually hit the wall of the vacuum chamber and will be lost. In order to minimize these deviations,

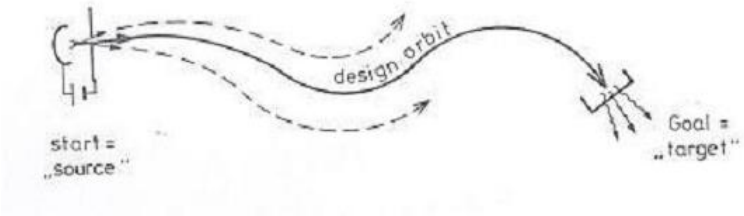

Figure 9.1: *Particle trajectory and ideal orbit.*

focusing forces are required.
Focusing can be accomplished by defining, first, the particle trajectory in a general arbitrary curve and then by steering the diverging particles back to the nominal trajectory each time. This is done by using electromagnetic fields in which particles of charge e and velocity $\vec{v}$ experience the Lorentz Force, defined by equation (9.1)[6]:

$$\vec{F} = e(\vec{J} + \vec{v} \times \vec{B}) = \dot{\vec{p}} \tag{9.1}$$

where $\vec{F}$ is the Lorentz force, $\vec{J}$ is the electric field, $\vec{B}$ is the magnetic field and $\dot{\vec{p}}$ is the first derivative of the momentum $\vec{p}$.

At relativistic velocities the electric field $\vec{J}$ is related to the magnetic field with equation:

$$\vec{J} = c\vec{B} \tag{9.2}$$

This means that a magnetic field of 1 Tesla corresponds to an electric field of $3 \times 10^8 V/m$. However, although it is relatively easy to have a magnetic field of 1 Tesla, it is not so easy to have an electric field of $3 \times 10^8 V/m$. This is the reason why, magnets are almost always used in accelerating structures to steer the beams whereas electrical fields are only used at very low energies or to seperate particles according to their charge [6].
Based on linear algebra, $\vec{v}$ is perpendicular to the cartesian product $\vec{v} \times \vec{B}$. In order to represent the particle acceleration ($\dot{\vec{p}}$), it is necessary to substitute $\vec{p}$ with ($m\dot{\vec{p}}$). Considering the above substitutions and the fact that magnetic fields are used more, instead of electrical fields, equation (9.1) becomes:

$$\dot{\vec{v}} = \frac{e\vec{v} \times \vec{B}}{m} \tag{9.3}$$

The principals used for the focusing and steering procedures are called *beam optics* [2].

9.2 Accelerator Magnets

As mentioned earlier, nowadays separated-function, electromagnets are used in accelerators for bending and focusing the beam. Dipoles are used for bending, whereas quadrupoles are used for focusing (Fig. (9.2) [5]).Higher multipoles (sextupoles, octupoles etc) either cause unwanted field errors or are usually used for compensation or field correction [2]. For linear beam optics, higher multipoles are not used and thus and will not be discussed in this analysis.

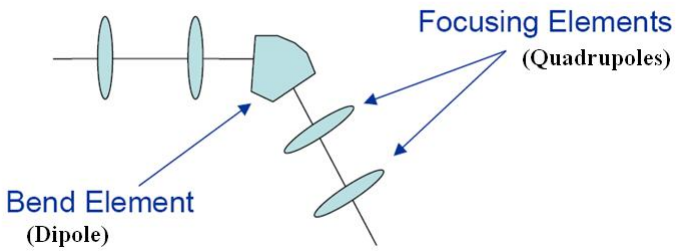

Figure 9.2: *Dipoles are used for bending while quadrupoles are used to focus the particle beam.*

9.2.1 Dipole Magnets

A dipole magnet consists of two parallel iron poles, with coils wrapped around them, as shown in Fig. (9.3) [2] and is used to bend the beam into a circular trajectory.

It generates a homogeneous field $|\vec{B}| = B_0$ (Fig. (9.4)) [5] within the gap which is constant along the $x-$axis and is defined by equation (9.4)[2]:

$$B_0 = \mu_0 \frac{nI}{h} = const \tag{9.4}$$

where h is the space between the two poles, n is the number of coils, I is the current passing through the coils and μ_0 is the magnetic permeability in the gap (μ_0=1). Since the magnetic field is constant along the $x-$axis, the first derivative of the

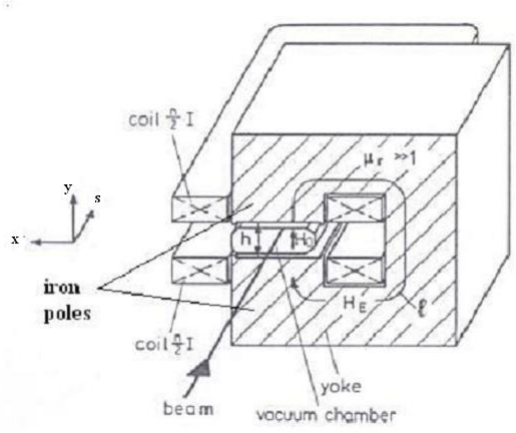

Figure 9.3: *A dipole magnet consists of two parallel iron poles. The space between the two poles is demonstrated by (h), (n) is the number of coils, (I) is the current passing through the coils and (μ) is the magnetic permeability.*

magnetic field with respect to the $x-$axis is zero:
$|\vec{B_x}| = 0$.
On the contrary, the magnetic field along the $y-$axis varies. Thus, the first derivative is expressed by the following formula: $B_y = B_0$

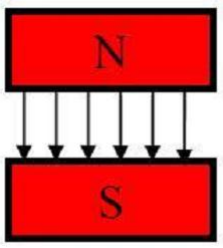

Figure 9.4: *A dipole magnet generates a homogenous magnetic field B_0.*

The radius by which the trajectory of a moving particle beam is bent due to the magnetic field produced by the dipoles is expressed by ρ. It is known as *bending radius* and determines the curvature of the beam. The factor$(1/\rho)$ represents the 'strength' of the magnetic field produced by a dipole magnet. It is expressed by equation (9.5):

$$\frac{1}{\rho} = \frac{0.2298 B_0[T]}{p[GeV/c]} \tag{9.5}$$

where B_0 is the homogeneous magnetic field generated by the dipole and p is the particle momentum. Substituting equation (9.4) in equation (9.5), the dipole strength can also be expressed by equation (9.6):

$$\frac{1}{\rho} = \frac{0.2298\mu_0}{p}\frac{nI}{h} \tag{9.6}$$

However, in reality, there are deviations from this ideal field, B_0. Only a magnet with infinitely long poles is able to produce such a homogeneous magnetic field. After a certain distance from the central axis, the field starts to fall away, as shown in Fig. (9.5), which limits the useful region of the magnet[2]. In order to compensate for this,iron strips,the so-called *shims*, are fitted at the end of the magnet in both poles, increasing the useful region.

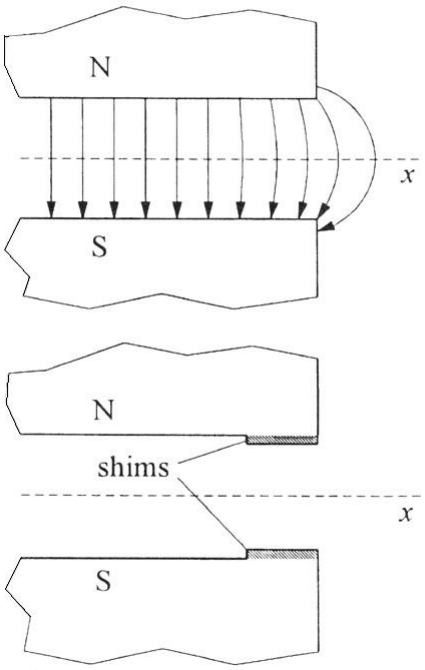

Figure 9.5: *In a dipole magnet, iron shimps increase the usefull field region.*

The angle in which a dipole magnet bends the beam is called *bending angle*, while the radius of curvature of the orbit is called *bending radius*.

Considering a ring with a N_b dipoles (N_b is the number of dipoles), of length L_b, equation (9.7) determines the bending angle θ of the dipoles:

$$\theta = \frac{2\pi}{N_b} \tag{9.7}$$

The bending radius of the dipoles is expressed by equation (9.8) :

$$\rho = \frac{L_b}{\theta} \tag{9.8}$$

It can be inferred from equation (9.8) that, the bending radius increases in analogy with the dipole length. The bending radius ρ and the magnetic field B produced by the dipoles are related through equation (9.9):

$$B\rho = \frac{\beta E}{0.2998} \tag{9.9}$$

where E is the desired output energy of the synchrotron and β is a multiplication factor expressed by equation (9.10), while the product $B\rho$ is the *magnetic rigidity*. Magnetic rigidity determines the resistance of charged particles to change their direction of motion caused by the magnetic field.

$$\beta = \sqrt{1 - \frac{E_0^2}{E^2}} \tag{9.10}$$

where E_0 is the inertia energy [1].

The energy of a moving particle is defined as the sum of the particle's kinetic energy(T) plus it's inertia energy (E_0):

$$E = E_0 + T \tag{9.11}$$

Since the particles' mass is constant and the desired output energy is predetermined, according to equation (9.9), $B\rho$ is constant for a certain output energy of a specific particle beam. However, the magnetic rigidity changes in analogy with the desired output energy. Moreover, in order to keep the desired energy constant, a variation in the magnetic field B demands a variation in the bending radius ρ as well. For example, if the magnetic field increases, the bending radius must decrease and consequently, from equation (9.8), the dipole length must decrease as well (smaller dipoles).

[1] The energy of the particle due to it's mass alone

9.2.2 Quadrupole Magnets

Quadrupoles, as mentioned before, are electromagnets used for focusing the beam. They consist of four iron poles, with hyperbolic contour, with coils wraped around them as shown in Fig. (9.6)[7].

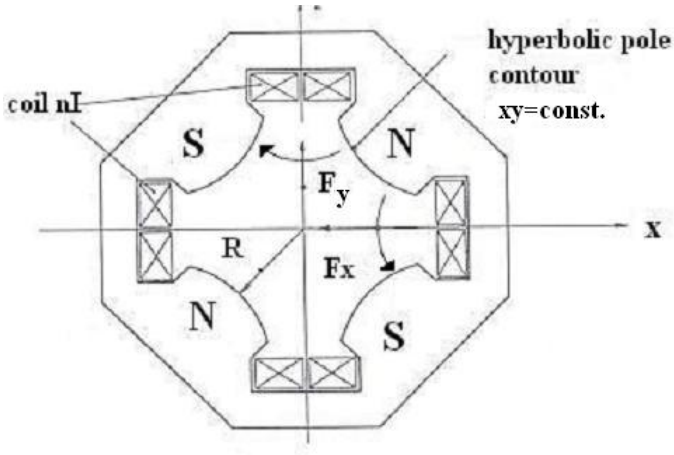

Figure 9.6: *Quadrupole Magnet.*

According to Fig. (9.6), F_x (horizontal component of the Lorentz force on a positively charged particle) is directed towards the axis, whereas the vertical F_y is moving away from it [2]. Thus, this magnet focuses the beam in the horizontal plane and defocuses the beam in the vertical. If any of the following: current direction, particle charge or its direction of motion changes, then the quadrupole has the opposite effect (defocusing of the beam in the horizontal plane and focusing in the vertical) In order to have this opposite effect, without changing the beam characteristics, the polarity of the quadrupole can be reversed. Therefore, in circular accelerators quadrupole magnets with alternating polarity are used.

The field is linear in the deviation from the x-axis and z-axis as the following formulas indicate:
$\vec{B_x} = -g\hat{y}$
$\vec{B_y} = -g\hat{x}$

where $\vec{B_x}$ and $\vec{B_y}$ are the derivative of the magnetic field B produced by the quadrupole, with respect to x and y respectively. Moreover, g is the field gradient, which describes the change in the magnetic field:

$$g = \frac{\partial B_z}{\partial x} \tag{9.12}$$

Figure (9.7) demonstrates the field lines in a quadrupole magnet[5].

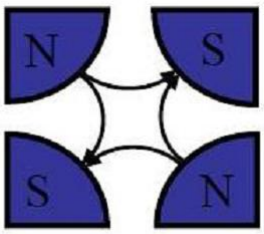

Figure 9.7: *Magnetic field generated by a quadrupole magnet.*

The quadrupole strength, is defined according to the bending strength of a dipole magnet:

$$k = \frac{eg}{p} \tag{9.13}$$

where p is the particle momentum and e is the particle charge.
The strength k for a focusing quadrupole is positive ($k \geq 0$) whereas for a defocusing quadrupole, the strength k is negative ($k \leq 0$). In equation (9.13) g is the field gradient as already mentioned and is also expressed by equation (9.14):

$$g = \frac{2\mu_0 nI}{R^2} \tag{9.14}$$

with μ_0 being the magnetic permeability, n being the number of coils, I being the current in the coil and R being the average radius of the accelerator.
Also the quadrupole strength can be expressed by equation (9.15):

$$k[m^{-2}] = \frac{0.2998 \times g[T/m]}{p[GeV/c]} \tag{9.15}$$

Moreover, according to equation (9.9) and assuming for simplicity that $c = 1$ the quadrupole strength is also expressed by equation (9.16):

$$k = \frac{0.2998 \times g[T/m]}{\beta E[GeV]} = \frac{0.2298 \times g[T/m]}{B\rho} \tag{9.16}$$

Quadrupole magnets function like glass lenses, while they focus or defocus the beam in the same way a glass length works when light passes through them. The effect of a focusing and a defocusing quadrupole on the beam is demonstrated in Fig. (9.8) [8]:

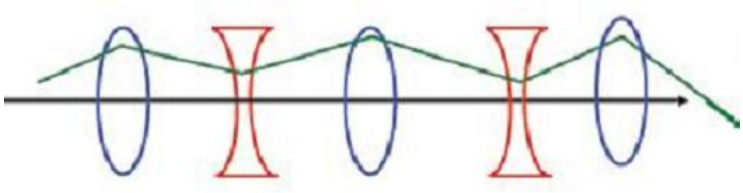

Figure 9.8: *The beam is focused by the focusing quadrupoles and defocused by the defocusing quadrupoles, which have the effect of a focusing and defocusing lens.*

If l is the length of the quadrupole, the focal length f is given from equation (9.17):

$$\frac{1}{f} = kl \tag{9.17}$$

Therefore, since the strength of a focusing quadrupole is positive ($f \geq 0$), the focal length f is also positive, according to equation (2.17). On the contrary, the focal length of a defocusing quadrupole is negative ($f \leq 0$). As mentioned before, the quadrupole field can focus the beam on one axis and defocus it on the other. However, if quadrupoles with strengths of equal absolute value are used at some distance from one another, the beam will be focused in both planes as shown in Fig. (9.9)[6]:

Figure 9.9: *Quadrupole magnets with strengths of equal absolute value, result in overall focusing of the beam in both planes.*

9.3 Particle Motion and Trajectory Equations in a Circular Accelerator

In this section, the trajectory equations used in particle motion in circular accelerators are discussed. The particle motion is described by *trajectory equations* which demonstrate the particle trajectory and are expressed by the following second-degree differential equations ((9.18) and (9.19)):

$$x''(s) + (\frac{1}{\rho^2(s)} - k(s))x(s) = \frac{1}{\rho(s)}\frac{\Delta p}{p} \tag{9.18}$$

$$y''(s) + k(s)y(s) = 0 \tag{9.19}$$

where k is the strength of the quadrupole, p is the particle momentum, ρ is the bending radius and the s coordinate refers to the nominal orbit. Both, dipoles and quadrupoles have an affect on the particle orbit. As previously defined, the factor factor $\frac{1}{\rho(s)}$ indicates the dipole strength whereas the factor $\frac{1}{\rho^2(s)}$ represents a focusing effect caused by the dipole, known as *weak focusing*. Moreover, the factor $k(s)$ indicates the quadrupole strength. Both x and y define the particle trajectory in the horizontal and vertical plane respectively. It can be observed that both, ρ and k, are functions of s. This is due to the fact that, based on the position (s) of the particles in the lattice, they encounter different elements (dipoles, quadrupoles etc.) and thus their motion is affected accordingly. For example, when a particle passes through a quadrupole, it is not affected by bending forces and as a result, the factors $\frac{1}{\rho^2(s)}$ and $\frac{1}{\rho(s)}$ are considered zero.
The horizontal and the vertical plane in normal dipole and quadrupole magnets are independent of one another, hence, it is sufficient to consider only one plane. There are certain assumptions made for simplicity, in order to proceed with the analysis of the particle motion:

- The design orbit is thus assumed to be in the horizontal plane.
- The magnetic field ends abruptly at the beginning and at the end of the magnets, whereas within the magnets, the field is constant. This means that the quadrupole and dipole strength are independent of the s coordinate (nominal orbit) Fig. (9.10)[2].
- Last, it is assumed that all the particles of the beam have the same energy and thus the same momentum p ($\frac{\Delta p}{p} = 0$).

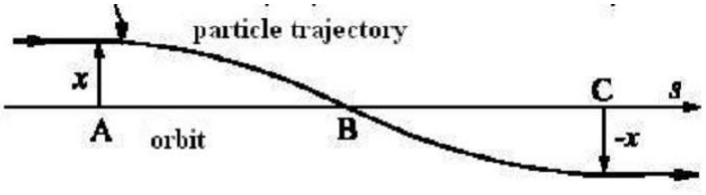

Figure 9.10: *Particle orbit and trajectory.*

In order to obtain the solution to the trajectory equation in the horizontal plane when the particle pass through a quadrupole, equation (9.15) is used. Since the aim is to define the trajectory of the particle based only on the effect of a quadrupole, the dipole strength $\frac{1}{\rho}$ is considered zero since no bending of the beam caused by the quadrupole. Thus, equation (9.18) becomes:

$$x''(s) - kx(s) = 0 \tag{9.20}$$

where k is the strength of the quadrupole. In case of a defocusing quadrupole, $k \leq 0$ and the solution of equation (9.20) above is:

$$x(s) = A\cosh\sqrt{|k|}s + B\sinh\sqrt{|k|}s \tag{9.21}$$

$$x'(s) = \sqrt{|k|}A\sinh\sqrt{|k|}s + \sqrt{|k|}B\cosh\sqrt{|k|}s \tag{9.22}$$

The constants of integration A and B are determined by the initial conditions. The point where the beam enters the magnet is considered to be at $s = 0$, where the point trajectory is defined by the following vector:

$$\begin{pmatrix} x_0 \\ x_0' \end{pmatrix} = \begin{pmatrix} x(0) \\ x'(0) \end{pmatrix}$$

Thus, equations (9.21) and (9.22) can be written as follows:

$$x(s) = x_0\cosh\sqrt{|k|}s + \frac{x_0}{\sqrt{|k|}}\sinh\sqrt{|k|}s \tag{9.23}$$

$$x'(s) = x_0\sqrt{|k|}\sinh\sqrt{|k|}s + x_0'\cosh\sqrt{|k|}s \tag{9.24}$$

Equations (9.21) and (9.22) can be written in a matrix form as well:

$$\begin{pmatrix} x(s) \\ x'(s) \end{pmatrix} = \begin{pmatrix} \cosh\Omega & \frac{\sinh\Omega}{\sqrt{k}} \\ \sqrt{k}\sinh\Omega & \cosh\Omega \end{pmatrix} \begin{pmatrix} x_0 \\ x_0' \end{pmatrix}$$

where $\Omega = sqrtks$.

So for the quadrupole, depending on the strength k, there are 2 matrices-one for a focusing quadrupole and one for a defocusing:

$$M_{foc} = \begin{pmatrix} \cos\Omega & \frac{1}{\sqrt{|k|}}\sin\Omega \\ -\sqrt{|k|}\sin\Omega & \cos\Omega \end{pmatrix}$$

with $k \geq 0$

$$M_{defoc} = \begin{pmatrix} \cosh\Omega & \frac{1}{\sqrt{|k|}}\sinh\Omega \\ \sqrt{|k|}\sinh\Omega & \cosh\Omega \end{pmatrix}$$

with $k \leq 0$

By replacing the quadrupole strength k with the dipole strength $1/\rho$, the dipole matrix is obtained:

$$M_{dipole} = \begin{pmatrix} \cosh\frac{s}{\rho} & \rho\sinh\frac{s}{\rho} \\ -\frac{1}{\rho}\sinh\frac{s}{\rho} & \cosh\frac{s}{\rho} \end{pmatrix}$$

It may seem that, like the quadrupole matrix, the matrix above describes beam focusing, but in this case with a strength of $1/\rho^2$. This focusing effect, caused be the dipoles, is relatively small, compared to the focusing caused by the quadrupoles and as already mentioned, is called *weak focusing* [7].
There are two types of dipole magnets, depending on their shape: *sector* and *rectangle* magnets. The assumption that the field ends abruptly at the end of the magnet and starts sharply at the beginning, leads to the fact that the faces of the bending magnets are perpendicular to the nominal trajectory. This is exactly what happens in the case of *sector* magnets as demonstrated in Fig. (9.11) [2].

However, due to the fact that *rectangular* magnets are easier to manufacture, many of them are nowadays used. In this case, the trajectory of the beam is not perpendicular to the magnet at the entrace nor at the exit of the beam, results in an extra focusing effect which is known as *edge focusing* [2]. This is caused by the fact that the particles cross the face of the magnet at an angle ψ as it can be seen in Fig. (9.11). Comparing the particle trajectories for both, sector and rectangular bending magnets, it is clear that the particles, travelling through a rectangular magnet, cover a shorter path, by a distance:

$$\Delta l = x_0 \tan\psi \tag{9.25}$$

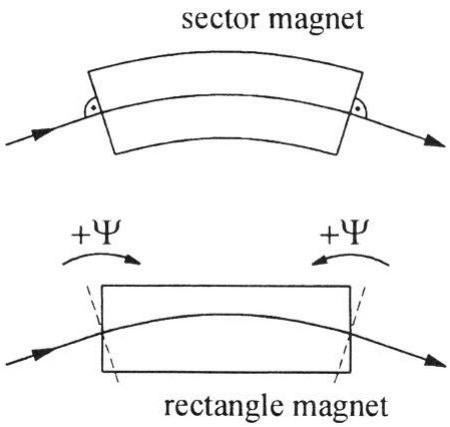

Figure 9.11: *Dipoles: Sector and Rectangle magnets.*

where Δl is the difference in the travelling distance, x_0 is the travelling distance within a sector magnet and ψ is the angle in which the particle cross the face of the magnet. This causes the particles to be bent in a smaller angle ($\Delta\omega = \frac{\Delta l}{\rho}$)

The matrix form for the trajectory transformation is :

$$M_{edge} = \begin{pmatrix} 1 & 0 \\ \frac{\tan\psi}{\rho} & 1 \end{pmatrix}$$

It is possible to observe the circulation of the particle beam through the magnet structure, with the use of matices that represent each magnet element. These matrices are known as *transfer matrices*. The transfer matrices for the quadrupole and the dipole magnets:

$$M_{quad} = \begin{pmatrix} \cosh\theta & \frac{1}{\sqrt{|k|}}\sinh\theta \\ \pm\sqrt{|k|}\sinh\theta & \cosh\theta \end{pmatrix}$$

$$M_{dip} = \begin{pmatrix} \cos\theta & \rho\sin\theta \\ -\frac{1}{\rho}\sin\theta & \cos\theta \end{pmatrix}$$

where θ is the bending angle of the dipoles.
The magnets in an accelerator are placed with a distance from one another, called *drift region*. The transfer matrix for a drift region between magnets is:

$$M_{drift} = \begin{pmatrix} 1 & s \\ 0 & 1 \end{pmatrix}$$

In order to 'move' from one point to another within a sequence of magnets, the principle is to multiply the transfer matrices of each element *in the right order* as demonstrated in Fig. (9.12)[7].

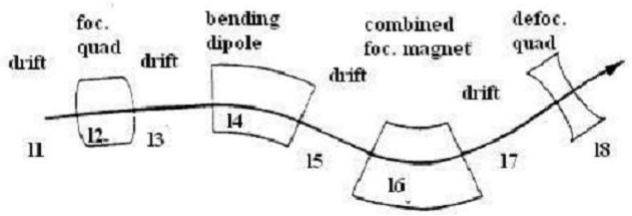

Figure 9.12: *The circulation of the particles through a sequence of dipole and quadrupole magnets*

The complete transfer matrix of this sequence of magnetic elements is:
$M = M_8 * M_7 * M_6 * M_5 * M_4 * M_3 * M_2 * M_1$
where M_i, $i = 1, .., 8$ are theh transfer matices of the elements of the lattice.

9.4 Betatron Oscillations

As a particle circulates through the ring, it preforms an oscillation about the nominal trajectory. This transverse oscillation about the orbit is described by *Hill's differential equation* and is known as *betatron oscillation*.

Substituting $1/\rho = 0$ and $\Delta p/p = 0$ in equation (9.18), equation (9.26)-(*Hill's differential equation*) is obtained [2] :

$$x''(s) - k(s)x(s) = 0 \tag{9.26}$$

where the quadrupole strength (k), is a function of a position in the orbit (s).

The solution of this trajectory equation is:

$$x(s) = Au(s)\cos(\Psi(s) + \phi) \tag{9.27}$$

The term $u(s)$ is considered to be equal to $u(s) = \sqrt{\beta(s)}$, where $\beta(s)$ is a periodical function of position, known as *beta function*: $\beta(s) = u^2(s)$, and will be analyzed in the following paragraph. The constant amplitude factor A and the phase ϕ are constants of integration and are determined by the initial conditions. The trajectory function, $x(s)$, describes a transverse oscillation around the orbit (betatron oscillation), The functions $u(s)$ (amplitute) and phase $\Psi(s)$ -known as *betatron phase*- are functions of the particle position in the orbit s and therefore have a different value at every point around the orbit [2]. Additionally, the amplitude factor A can be replaced by what is called emittance: $A = \sqrt{\epsilon}$. The emittance describes the area occupied by the beam which maintains the same through the ring and will be analysed in section (9.5).Hence, equation (9.27) becomes :

$$x(s) = \sqrt{\epsilon}\sqrt{\beta(s)}\cos(\Psi(s) + \phi) \tag{9.28}$$

The beta function $\beta(s)$ describes the variation of the beam's characteristics in both planes-vertical and horizontal- as the beam circulates through the sequence of magnets in the ring. Thus, it depends on the beam focusing or defocusing, which varies with position. It is a measure of the beam cross-section whereas, the emittance, ϵ, is constant throughout the whole beam transport system. The particles oscillate around the orbit,but they do not all follow the same trajectory. However, the transverse motion of the particles takes place within a range marked out by a position-dependent amplitude called *Envelope* and is expressed by equation (9.29)

$$E(s) = \sqrt{\epsilon\beta(s)} \tag{9.29}$$

This is demonstrated in Fig. (9.13) [2]:

It is interesting to see how the beta functions change in each plane as the position changes.
The first derivative of the trajectory function is:

$$x'(s) = \frac{-\sqrt{\epsilon}}{\sqrt{\beta(s)}}[\alpha(s)\cos(\Psi(s) + \phi) + \sin(\Psi(s) + \phi)] \tag{9.30}$$

with

$$\alpha(s) = -\frac{\beta'(s)}{2} \tag{9.31}$$

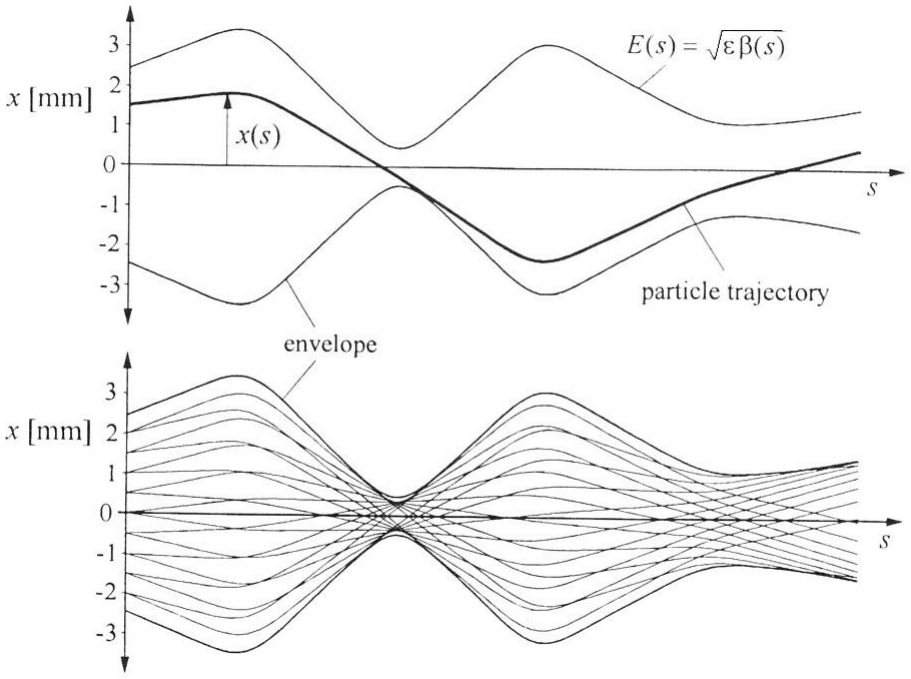

Figure 9.13: *The amplitude of the particle oscillation has a boundary defined by the Envelope*

representing the first derivative of the beta-function.
Since the beta function is periodical, it can be said that $\beta(s + C) = \beta(s)$.
where C is the circumference of the accelerator. This means that the beta function will have the same value for a certain point in the accelerator after each turn of the beam. Also, the betatron phase function $\Psi(s)$ for a point s, is calculated from the beta function as shown in equation (2.32)[7]:

$$\Psi(s) = \int_{s_0}^{s} \frac{1}{\beta(s)}\, ds \tag{9.32}$$

The same procedure is followed in order to calculate the betatron phase function for another point $s + C$:

$$\Psi(s + C) = \int_{s_0}^{s+C} \frac{1}{\beta(s)}\, ds = \int_{s_0}^{s} \frac{1}{\beta(s)}\, ds + \int_{s}^{s+C} \frac{1}{\beta(s)}\, ds \tag{9.33}$$

Thus, the phase advance per period is [2]:

$$\Delta\Psi = \mu = \Psi(s+C) - \Psi(s) = \int_s^{s+C} \frac{1}{\beta(t)}\, dt \tag{9.34}$$

It is clear that it demonstrates the change in the betatron phase per revolution.

The number of betatron oscillations per revolution is known as Tune and is expressed by equation (9.35):[7]

$$Q = \frac{N\mu}{2\pi} = \frac{\Delta\Psi}{2\pi} = \frac{1}{2\pi} \oint \frac{ds}{\beta(s)} \tag{9.35}$$

where N is the number of periods, μ is the phase advance and $\Delta\Psi$ indicates the phase advance for one complete revolution. The number of periods is indicated by the number of identical magnet structures in a lattice.
Since the oscillation of the particles and the amplitude of these oscillations can be obtained from the beta functions, it is important to understand how the beta function behaves while the particles are travelling through the ring.
This is demonstrated in Fig. (9.14) [2]:

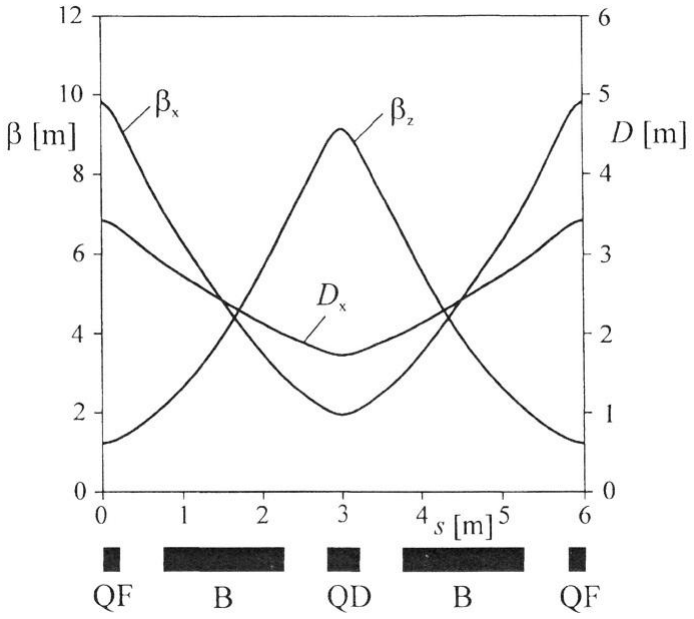

Figure 9.14: *Circulation of the beam through the magnet structure. Evolution of the beta functions*

It is easy to see that when the particles pass through a focusing quadrupole (QF), the beta function in the horizontal plane reaches a maximum, whereas in the vertical plane, it reaches a minimum. Respectively, when the beam passes through a defocusing quadrupole (DF), the vertical beta function reaches a maximum, whereas the horizontal reaches a minimum. This behaviour can be observed more clearly in Fig. (9.15) [4].

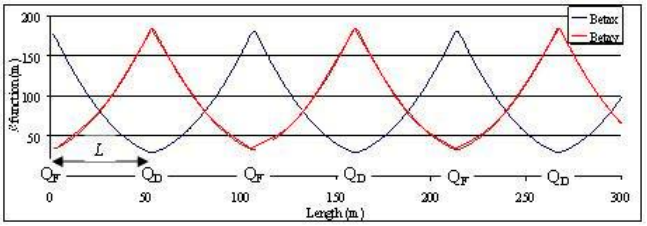

Figure 9.15: *Circulation of the beam through the magnet structure. The beta functions oscillate along the ring, reaching maximum and minimum values in the quadrupoles*

9.5 Emittance

Under linear forces, any particle moves on *ellipse phase space* $(x, x'), (y, y')$. The phase space is a space that consists of all possible values of position and momentum variables. The ellipse rotates and moves between magnets, but its area is preserved. The area of the ellipse defines the *emittance* [9]. The emittance represents the phase-space volume occupied by the beam.

Using equations (9.28) and (9.30), an expression describing the particle motion in the $x - x'$ phase space plane is obtained with no dependence on the phase Ψ [2]:

$$\cos(\Psi(s) + \phi) = \frac{x}{\sqrt{\epsilon}\sqrt{\beta(s)}} \tag{9.36}$$

and

$$\sin(\Psi(s) + \phi) = \frac{\beta(s)x'}{\sqrt{\epsilon}} + \frac{\alpha(s)x}{\sqrt{\epsilon}\sqrt{\beta(s)}} \tag{9.37}$$

By using the general relation $\sin^2\theta + \cos^2\theta = 1$ equation (2.38) is obtained:

$$\frac{x^2}{\beta(s)} + (\frac{\alpha(s)}{\sqrt{\beta(s)}x} + \sqrt{\beta(s)}x')^2 = \epsilon \tag{9.38}$$

while

$$\gamma(s) = \frac{1 + \alpha^2(s)}{\beta(s)} \tag{9.39}$$

From equations (9.38) and (9.39), equation (9.40) is acquired:

$$\gamma(s)x^2(s) + 2\alpha(s)x(s)x'(s) + \beta(s)x'^2(s) = \epsilon \tag{9.40}$$

where $\alpha(s)$ is expressed by equation (9.31) and $\gamma(s)$ is expressed by equation (9.39). Equation (9.40) is the general equation of an ellipse in the $x - x'$ plane, as shown in Fig. (9.16) [2].

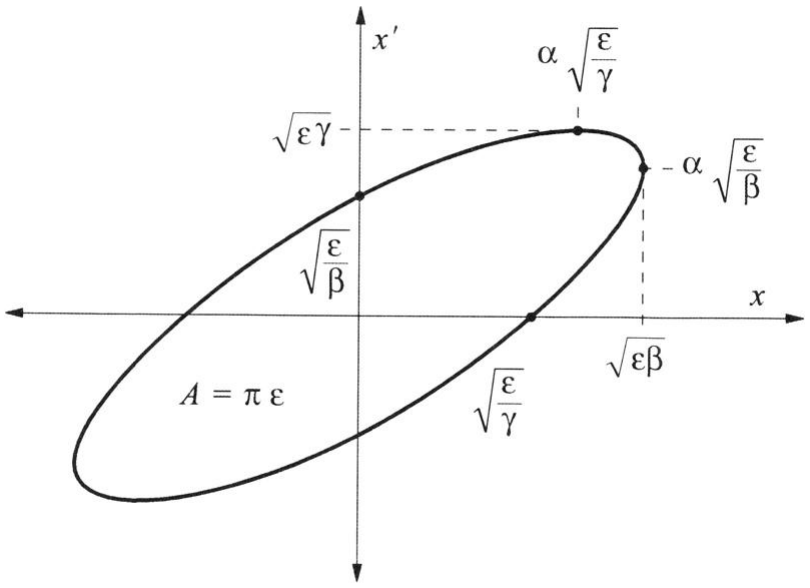

Figure 9.16: *The emittance is defined by the area of the phase space ellipse.*

The area $A = \pi\epsilon$ of the phase space ellipse is expressed by the emittance ϵ, multiplied by a factor π. According to Liouville's theorem, as a particle changes position, the ellipse changes shape with the amplitude of the beta function but the area of the ellipse remains the same.

However, a beam is a set of millions of particles, moving with various amplitudes and each corresponding to a different ellipse in the phase space plane. The horizontal particle distribution is described by a Gaussian distribution:

$$\rho(x, z) = \frac{Ne}{2\pi\sigma_x\sigma_z} exp(\frac{-x^2}{2\sigma_x^2} - \frac{z^2}{2\sigma_z^2}) \tag{9.41}$$

where N is the number of particle of charge e in the beam and σ_x, σ_y are the horizontal and vertical beam sizes. The horizontal particle distribution $\rho(x)$ is demonstrated in Fig. (9.17) [2]:

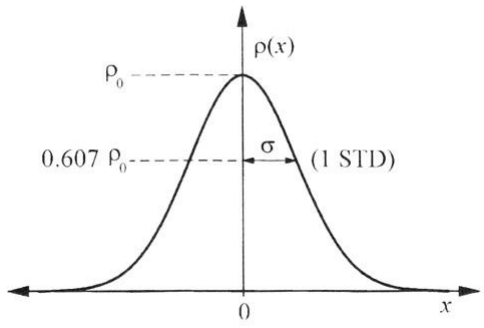

Figure 9.17: *Horizontal particle distribution.*

where $0.607\rho_0$ represents the distance from the beam axis where the particle density has decreased by $exp(-1/2)$.

All particles which lie exactly one standard deviation σ from the beam axis may be assigned to an emittance ϵ_{std} via the relation: $\sigma(s) = \sqrt{\epsilon_{std}\beta(s)}$ It is important that in an accelerator, even particles undergoing very large betatron oscillations are kept within the phase space ellipse. What defines how large the phase space ellipse is allowed to be, is the value of $\sqrt{\beta(s)}$ which is proportional to the width of the beam and not the aperture of a vacuum chamber .

9.6 Matching of Beam Optics

During the design of a lattice and its system of beam optics, the values of the optical functions, $\beta(s), \alpha(s), \gamma(s)$ which are mentioned in previous sections, are fixed in advance. The evolution of the optical functions through the magnetic structure is computed by using the matrix equations and certain simulation programs.
This is a very important procedure and has an effect on many issues. For example, it helps to ensure that the beta function will stay within reasonable limits and as a result, the particles will not hit the wall of the vacuum chamber. A significant part of this process is to choose the appropriate quadrupole strengths in order for the optical functions to have the desired form and values at the end of the structure. This procedure is known as *matching of beam optics* [2].

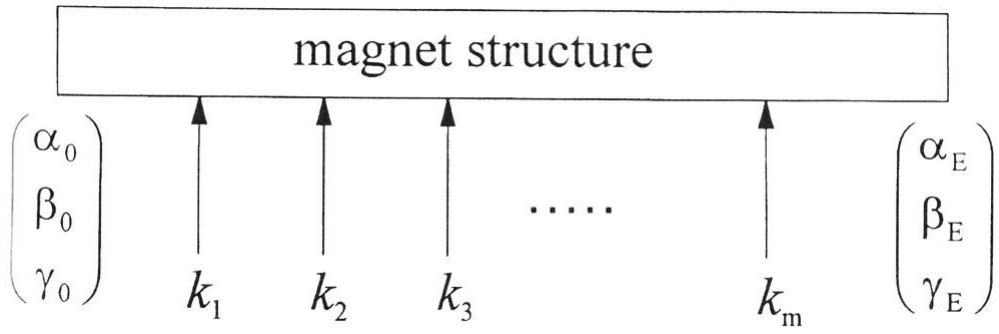

Figure 9.18: *Matching of beam optics. The quadrupole strengths are defined so that the optical functions acquire the desired value at the end of the lattice.*

9.7 Periodicity Conditions

In circular accelerators, there is not a defined beginning or end of the structure. However, due to their periodicity, the optical functions must repeat continuously. Additionally, the optical functions are reflected through the symmetry points of the lattice as it is demonstrated in Fig. (9.19), at which the optical functions must have the same values [2], which sets another constraint. Thus, the optical functions can defined around the ring.

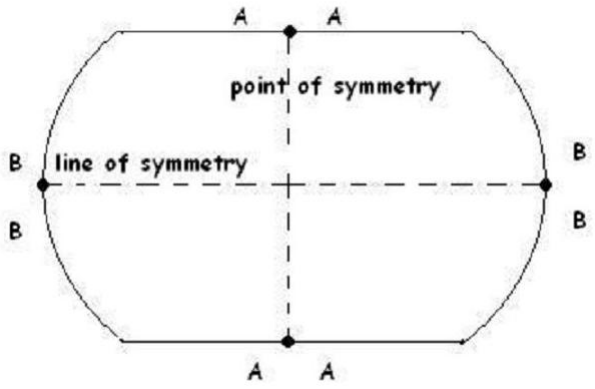

Figure 9.19: *The points of symmetry encountered in the accelerator, establish periodicity conditions, causing the particles to circulate periodically.*

9.8 FODO cell

The purpose of the arrangement of magnets in a circular accelerator -and in this case, in a synchrotron- is to steer the beam in a controlled way, bend and focus it whenever needed. The simplest arrangement of magnets is the *FODO structure*, shown in Fig. (9.20) [2]. The ring consists of a number of identical cells, each consisting of two dipoles to bend the beam in a circular path and quadrupoles arranged with alternating polarity between them, to consecutively focus and defocus the beam as needed. The alternating polarity is indicated by the fact that a quadrupole, only focuses the beam in one place, while it defocuses it in the other. Between the magnets, is a *drift region* which has no magnetic field and is indicated by $'0'$, hence the name of the structure(F.0.D.0).

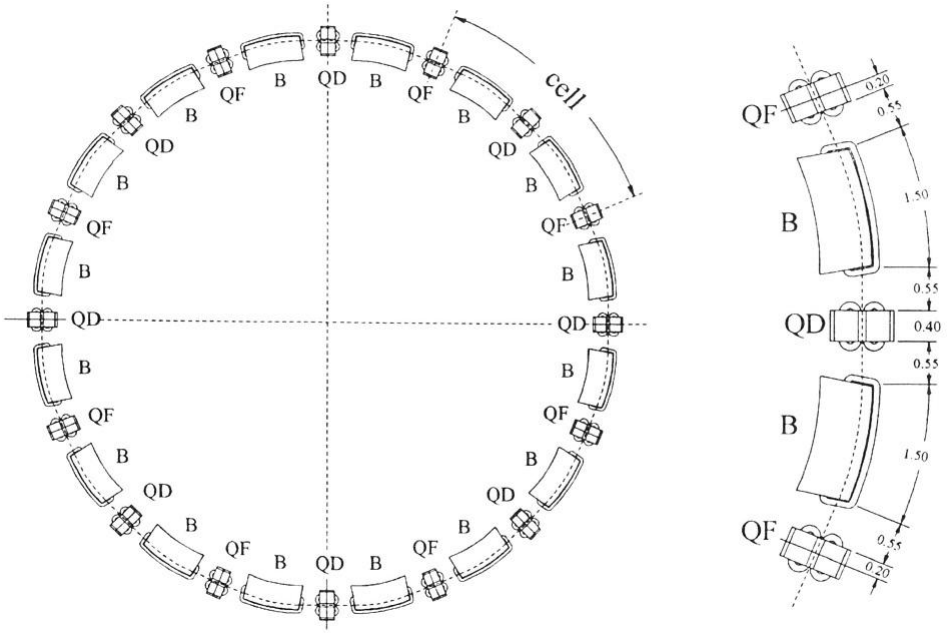

Figure 9.20: *A synchrotron consisting of a sequence of FODO cells.*

It is important to understand how the beam circulates through a FODO cell using transfer matrices. Considering the quadrupoles as focusing and defocusing lenses and following the thin lens approximation ($f \geq\geq l$, where f is the focal length of the quadrupole and l is the quadrupole length) and not taking into account the dipoles, the transfer matrices for the quadrupoles and the drift sections

are [7]:

$$M_F = \begin{pmatrix} 1 & 0 \\ -1/f & 1 \end{pmatrix}$$

$$M_{drift} = \begin{pmatrix} 1 & L_f/2 \\ 0 & 1 \end{pmatrix}$$

$$M_D = \begin{pmatrix} 1 & 0 \\ +1/f & 1 \end{pmatrix}$$

where f is the focal length of the quadrupoles, L_f is the length of the FODO cell, M_F is the transfer matrix of the focusing quadrupole, M_{drift} is the transfer matrix of the drift section and M_D is the transfer matrix of the defocusing quadrupole. Thus, the whole transfer matrix from the beginning to the end of the FODO cell is:

$$M = M_F M_0 M_D M_0 M_F = \begin{pmatrix} 1 - \frac{L_f(2f+L_f)}{4f^2} & L_f + \frac{L_f^2}{4f} \\ \frac{-4f^2+L_f^2}{4f^3} & 1 - \frac{L_f(2f+L_f)}{4f^2} \end{pmatrix}$$

where M_0 is the transfer matrix for the drift space between the magnets.

Also, the cosine of the phase advance is expressed by equation (2.42):

$$\cos\mu = \frac{1}{2}TrM = 1 - 2\frac{\rho^2}{f'^2}\sin^2\theta = 1 - \frac{L_f^2}{8f^2} \tag{9.42}$$

where μ as mentioned before is the phase advance.
It occurs from equation (9.42), that the phase advance per cell can be defined by the cell length and the focal length of the quadrupoles

9.9 Strong Focusing

The following assumptions are made in order to study the effect of the strong focusing of the magnets in a FODO cell:

1. The short drift spaces between the dipoles and the quadrupoles are neglected.

2. F and D(Focusing and Defocusing) quadrupoles are considered to have the same strength 1/f and are treated as thin lenses.

The parameters used are:

- Half cell length: $l_f = L_f/2$
- Bending strength: $\frac{1}{\rho}$
- Strength of half a quadrupole: $\pm\frac{1}{f'} = \pm\frac{1}{2f}$

As already mentioned, a typical FODO cell consists of a sequence of magnets: A focusing quadrupole, a dipole, a defocusing quadrupole, a dipole and again a focusing quadrupole. In order to examine the effect of both, the quadrupole and the dipole magnets, on a beam travelling through a FODO cell, a half cell is considered; that is from the middle of the focusing quadrupole to the middle of the defocusing quadrupole. This is described by multiplying the transfer matrices of each magnet, in the order that the beam passes through them (Fig. (9.21)[7]):

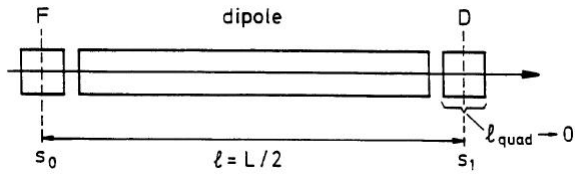

Figure 9.21: *Half FODO cell.*

The transfer matrix from the middle of the first focusing quadrupole to the middle of the defocusing quadrupole is [7]:

$$M(s_1/s_0) = \begin{pmatrix} 1 & 0 \\ 1/f' & 1 \end{pmatrix} \begin{pmatrix} 1 & \rho\sin\theta \\ 0 & 1 \end{pmatrix} \begin{pmatrix} 1 & 0 \\ -1/f' & 1 \end{pmatrix}$$

where

$$M_b = \begin{pmatrix} 1 & \rho\sin\theta \\ 0 & 1 \end{pmatrix}$$

is the matrix for the dipole, ρ is the bending radius of the dipole and θ is the bending angle $\theta = \frac{L_b}{\rho}$. Which gives:

$$M(s_1/s_0) = \begin{pmatrix} 1 - \frac{\rho}{f'}\sin\theta & \rho\sin\theta \\ -\frac{\rho}{f'^2}\sin\theta & 1 + \frac{\rho}{f'}\sin\theta \end{pmatrix}$$

In this approach, the weak focusing caused by the dipole magnets has not been taken into account. However, when an accelerator operates at a low energy (in the

MeV range), the weak focusing should be taken into account. This case will be analysed in Chapter 12.

For the whole FODO cell the transformation matrix is $M(s_0) = M(s_2/s_1)M(s_1/s_0)$ which gives:

$$M(s_0) = \begin{pmatrix} 1 - \frac{2\rho^2}{f'^2}\sin^2\theta & 2\rho\sin\theta + \frac{2\rho^2}{f'}\sin^2\theta \\ -\frac{2\rho}{f'^2}\sin\theta + \frac{2\rho^2}{f'^3}\sin^2\theta & 1 - \frac{2\rho}{f'^2}\sin^2\theta \end{pmatrix}$$

and the phase advance is expressed by equation (9.43) :

$$\cos\mu = \frac{1}{2}TrM = 1 - 2\frac{\rho^2}{f'^2}\sin^2\theta = 1 - \frac{L_f^2}{8f^2} \tag{9.43}$$

as $\theta << 1$

Taking into account equations (9.42) and (9.43), the solution is the same as it was when treating the dipoles as drift spaces.

In the middle of the focusing quadrupole, the beta function reaches a maximum value $\hat{\beta}$ [7], whereas in the middle of the defocusing quadrupole it reaches a minimum value $\check{\beta}$. The first derivative -slope- of β, (β') is zero, so $\alpha = 0$ and $\gamma = 1/\beta$ according to equations (9.28) and (9.36).

The transformation matrix applied, in order to 'transfer' from point s_0 to point s_1 of the lattice ($s_0 \rightarrow s_1$) is the following:

$$M(s_1/s_0) = \begin{pmatrix} C & S \\ C' & S' \end{pmatrix} = \begin{pmatrix} \sqrt{\check{\beta}/\hat{\beta}}\cos(\Delta\Phi) & \sqrt{\hat{\beta}\check{\beta}}sin(\Delta\Phi) \\ -\frac{1}{\sqrt{\hat{\beta}\check{\beta}}}sin(\Delta\Phi) & \sqrt{\hat{\beta}/\check{\beta}}cos(\Delta\Phi) \end{pmatrix}$$

where $\Delta\Phi = \mu/2$ Since the matrix above, is equal to $M(s_1/s_0)$, equation (9.44) derived:

$$\frac{S'}{C} = \hat{\beta}/\check{\beta} = \frac{1 + \frac{\rho}{f'}sin\phi}{1 - \frac{\rho}{f'}sin\phi} \tag{9.44}$$

Taking into account equation (9.44), as well as the fact that $|\cos\mu| < 1$, μ must take values between 0 and π, the maximum and minimum beta functions can be calculated as functions of μ:

$$\hat{\beta} = L_f\frac{1 + \sin\mu/2}{\sin\mu} \tag{9.45}$$

$$\check{\beta} = L_f\frac{1 - \sin\mu/2}{\sin\mu} \tag{9.46}$$

The phase advance,μ, for which the beta function attributes a maximum value is found by differentiating equation (9.45). After solving equation

$$d\hat{\beta}/d\mu = 0 \tag{9.47}$$

the value of the phase advance μ is obtained and it is equal to $\mu = 76.35$. This shows that the phase advance is between 60 and 90 degrees.

9.10 Stability Diagram

In order to ensure the correct function of the accelerator, it is important to define the values of the phase advance in each plane, taking into account the quadrupole strengths. The region of values of the phase advance is called *stable region* of the lattice.
Taking into account that the quadrupole strengths for the focusing ($k = F$) and the defocusing ($k = D$) quadrupoles are different, for the horizontal motion, matrix $M(s_1/s_0)$ is also equal to:

$$\begin{pmatrix} C & S \\ C' & S' \end{pmatrix} = \begin{pmatrix} 1-F & l \\ -\frac{(F-D+FD)}{l} & 1+D \end{pmatrix}$$

from where equations (9.48) and (9.49) are obtained:

$$-C'S = F - D + FD = sin^2\frac{\mu_x}{2} \tag{9.48}$$

$$D - F + FD = sin^2\frac{\mu_y}{2} \tag{9.49}$$

Taking into account equations (9.48), (9.49) and that $0 \leq \sin^2 \mu/2 \leq 1$, equations (9.50) and (9.51) are acquired:

$$0 \leq F - D + FD \leq 1 \tag{9.50}$$

$$0 \leq D - F + FD \leq 1 \tag{9.51}$$

Which leads to: $F = \frac{D}{1+D}$, $F = 1$, $D = \frac{F}{1+F}$ and $D = 1$. The stable region is demonstrated in Fig. (9.22)[7]

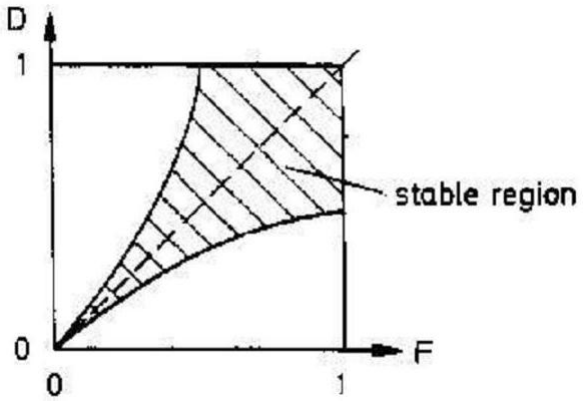

Figure 9.22: *Stability Diagram.*

9.11 Dispersion

Despite the fact that beam optics are calculated starting with particles of a nominal momentum, this is not the case in reality. Particles enter the ring with slightly different energies and thus, have a momentum deviation about this nominal value, equal to $\Delta p/p \neq 0$. As a result, when particles of different momentum enter a dipole, they experience different forces and exit the dipole at different angles. This, consequently, leads to particles travelling on dispersive trajectories which deviate from the nominal orbit. This effect is known as *dispersion*. From equation (9.15), it is obtained that momentum deviation is important only when the dipole strength $\frac{1}{\rho}$ is not zero, since the existence of dipoles is responsible for the dispersion [2, 10].

The dispersion function should be defined. Assuming a homogeneous field with no gradient($k = 0$), equation (9.18) becomes [2]:

$$x'' + \frac{1}{\rho^2}x = \frac{1}{\rho}\frac{\Delta p}{p} \tag{9.52}$$

where ρ is the bending radius.

Considering for simplicity a special trajectory $D(s)$ for which $\frac{\Delta p}{p} = 1$, the dispersion function is:

$$D''(s) + \frac{1}{\rho^2}D(s) = \frac{1}{\rho} \tag{9.53}$$

. Clearly, the dispersion function depends only on the dipole strength $\frac{1}{\rho}$, while the quadrupole strength k is not a part of the function. This is expected, since

the dipoles are the magnets creating the dispersion, whereas, quadrupoles have no such effect on the particles [10].

In conformance with the above, it is interesting to see how the transfer matrices for the quadrupole and the dipole magnets become, when the dispersion is taken into account:

Quadrupole Magnet:

$$M_{quad} = \begin{pmatrix} \cosh\theta & \frac{1}{\sqrt{|k|}}\sinh\theta & 0 \\ \pm\sqrt{|k|}\sinh\theta & \cosh\theta & 0 \\ 0 & 0 & 1 \end{pmatrix}$$

Dipole Magnet:

$$M_{dip} = \begin{pmatrix} \cos\theta & \rho\sin\theta & \rho(1-\cos\theta) \\ -\frac{1}{\rho}\sin\theta & \cos\theta & \sin\theta \\ 0 & 0 & 1 \end{pmatrix}$$

where θ, represents the bending angle ($\theta = L_b/\rho$).

From the above, it can be infered that the quadrupoles have nothing to do with dispersion, whereas dipoles are the ones who cause the dispersion when the off-momentum particles pass through them. As mentioned in previous sections, when particles with momentum deviation enter a dipole, they are bend in different angles, and therefore exit the magnet also in different angles, creating a beam that requires focusing. The following matrices, represent the transfer matrix of half a FODO cell:

$$\begin{pmatrix} C & S & D \\ C' & S' & D' \\ 0 & 0 & 1 \end{pmatrix} = \begin{pmatrix} 1 & 0 & 0 \\ 1/f' & 1 & 0 \\ 0 & 0 & 1 \end{pmatrix} \begin{pmatrix} 1 & \rho\sin\theta & \rho(1-\cos\theta) \\ 0 & 1 & 2\tan\theta/2 \\ 0 & 0 & 1 \end{pmatrix} \begin{pmatrix} 1 & 0 & 0 \\ -1/f' & 1 & 0 \\ 0 & 0 & 1 \end{pmatrix} = \begin{pmatrix} a & b & c \\ d & e & f \\ 0 & 0 & 1 \end{pmatrix}$$

where:

$a = 1 - \frac{\rho}{f'}\sin\theta$

$b = \rho\sin\theta$

$c = \rho(1 - cos\theta)$

$d = \frac{\rho}{f'^2} \sin\theta$

$e = 1 + \frac{\rho}{f'} \sin\theta$

$f = \frac{\rho}{f'}(1 - \cos\theta) + 2\tan\theta/2$

9.12 Tune and Optical Resonances

9.12.1 Periodic Solution of Hill's differential equation

In circular accelerators, the beam encounters the same magnetic structure, once every full revolution, thus the particles experience forces periodically. For example, the quadrupoles cause the particles to oscillate transversely which may under certain conditions lead to resonances. *Resonances* are beam instabilities due to perturbation terms in the equation of motion and they can be caused by dipoles, quadrupoles and sextupoles or octupoles.If this happens, the amplitude of the oscillations will increase and the particles may hit the wall of the vacuum chamber and as a result, be lost.
The trajectory of particles with no momentum deviation ($\Delta p = 0$) is described by Hill's differential equation:

$$x''(s) + K(s)x(s) = 0 \tag{9.54}$$

The focusing function $K(s)$ in a circular machine is periodic with a period C, where C is the circumference of the ring:

$$K(s) = 1/\rho^2(s) - k(s) \tag{9.55}$$

and thus, $K(s+C) = K(s)$, where L is the circumference of the ring. The solution of equation (9.54) is obtained by using *Floquet's Theorem*[2, 12]:

$$x(s) = \sqrt{\epsilon}\sqrt{\beta(s)}\cos[\Psi + \phi] \tag{9.56}$$

The beta function is also periodic with the same period as K(s). This means that $\beta(s + C) = \beta(s)$, as mentioned in section (9.4).

The resonant behaviour depends on the betatron phase $\Delta\Psi$ over one complete revolution. Thus, the tune, which defines the number of oscillations a particle undergoes over one complete revolution (section 9.4)[2, 12], is expressed by equation (9.57):

$$Q = \Delta\Psi/2\pi = \frac{1}{2\pi}\oint \frac{ds}{\beta(s)} \tag{9.57}$$

where $\Delta\Psi$ is the phase advance for a full revolution:$\Delta\psi = \Psi(s+C) - \Psi(s)$ as already mentioned in section (9.4). However, due to the periodicity of the beta function, the tune is independent of position s. The transfer matrix for a full revolution is:

$$M_{s\to s+C} = \begin{pmatrix} \cos\mu + \alpha(s)\sin\mu & \beta(s)\sin\mu \\ -\gamma(s)\sin\mu & \cos\mu - \alpha(s)\sin\mu \end{pmatrix}$$

with $\mu = 2\pi Q$
In order to study the resonances, the variable

$$\phi = \frac{\Psi(s)}{Q} = \frac{1}{Q}\oint \frac{ds}{\beta(s)} \tag{9.58}$$

is introduced which increases by 2π per revolution.
The particle amplitude, $x(s)$, is replaced by the normalised value:

$$n(s) = x(s)/\sqrt{\beta(s)} \tag{9.59}$$

After calculations and by multiplying equation (9.54) with $\beta^{3/2}(s)Q^2$, the transformed equation of motion is derived:

$$\frac{d^2n}{d\phi^2} + Q^2 n = 0 \tag{9.60}$$

Equation (9.60) applies for particles with nominal momentum and for a lattice with no field errors. However, in reality, this becomes:

$$\frac{d^2n}{d\phi^2} + Q^2 n = \beta^{2/3}Q^2\frac{\Delta B}{RB_{z_0}} \tag{9.61}$$

where Q is the tune value, B is the magnetic field and ρ the bending radius. Using Floquet's theorem equation (9.62) is obtained:

$$n(\phi) = \frac{Q}{2\sin\pi Q}\int \beta^{3/4}\frac{\Delta B}{RB_{z_0}}\cos[Q(\pi+\phi+\theta)]d\theta \tag{9.62}$$

for a full revolution, with ϕ given from equation (9.58).

It is clear from equation (9.62) that as the tune approaches a whole number, the amplitude of the particle oscillations $n(\phi)$ grows without limit since $\lim \sin(\pi Q) = 0$. As a result of this rapid and infinite increase of the oscillations' amplitude, the particles may be lost. What happens physically is that the beam receives a kick at the same phase on every turn and just spirals outwards [12]. The region around an integer value of Q is called *integer stopband*.

Depending on the tune value, integer, half integer and one-third integer resonances can be encountered [2]. In reality, the magnets manufactured do not agree exactly with the model. As a result, there are always non-negligible deviations from the ideal field. These deviations are called *field errors*. The resonance caused by a dipole field error is the strongest and is known as *Integer Resonance*-$Q = n$. Specifically, assuming that there is only one magnet with a field error, when the particle beam circulates through the ring and passes through the faulty dipole, it undergoes an angular deflection. If the tune is an integer, the beam will encounter the faulty magnet at the exact same point in evergy revolution. Therefore, the angular deflection increases with each revolution. The oscillation amplitude increases linearly with the number of revolutions and at some point, the particle hit the wall of the vacuum chamber. *Half-Integer Resonance* is caused by quadrupole field errors and it takes place when Q takes a half integer value, $Q = n + 1/2$. Last, a sextupole magnet can cause what is known as *One-Third Integer Resonance* with $Q = n + 1/3$. The resonances induced by dipoles and quadrupoles are called *linear resonances* since they are caused by field errors of linear elements (quadrupoles,dipoles). However, resonances caused by non linear fields(sextupoles, octupoles) are used to compensate for particular beam dynamics problems and are known as *higher order resonances*, which will no be discussed in the framework of this study.

9.12.2 The Tune Diagram

The field errors caused by the accelerator magnets are usually not known precisely and thus, it is difficult to determine the strength of a resonance. It is definite though, that the strength of a resonance decreases sharply with the order of the resonance. This means for example, that integer and half integer resonances cause the beam to resonate, increase it's oscillation amplitude and hit the wall of the vaccum chamber. Thus, integer and half integer resonances should be avoided while the beam can survive all the other resonances. In an accelerator it is possible to

have all multipole fields [2]. Thus, there are always resonances when $aQ = p$, where a,p are integers that demonstrate the order of the resonance.
Every lattice has two tune values: The horizontal-Q_x and the vertical-Q_y which are generally different. As a result, the resonance conditions for each plane are also different. Equation (2.63) determines the condition for optical resonance in both planes:

$$mQ_x + nQ_y = p(m, n, p = integers) \tag{9.63}$$

.
The sum $|m| + |n|$ is called *order* of the resonance and the pair of Q_x and Q_y is known as *working point* and should be chosen to avoid resonances. The lines in Fig. (9.23)[2] represent the optical resonances and thus, the working point should be chosen to be far from these lines.

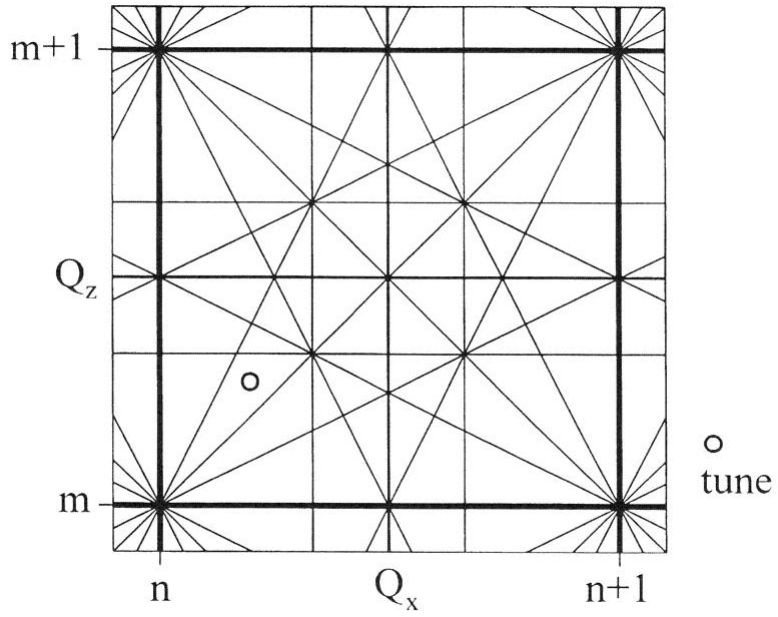

Figure 9.23: *Tune Diagram demonstrating resonances up to third order.*

In the tune diagram (Fig. (9.23)), resonances up to 3rd order ($|m| + |n| \leq 3$) are demonstrated.

9.13 Chromaticity

Chromaticity refers to the dependence of the focusing function on momentum[13].It is important to understand how the optics change for the off-momentum particles with a deviation $\Delta p \neg 0$. The following assumption is made: $\Delta p << p_0$. The off-momentum particles, with $p = p_0 + \Delta p$ have a different betatron oscillation frequency and experience a different focusing strength from the quadrupoles which is expressed by:

$$k = -\frac{e}{p}g = -\frac{e}{p_0 + \Delta p}g = k_0 + \Delta k \tag{9.64}$$

This can be regarded as a quadrupole error, caused by a slight alteration in the quadrupole strength k equal to $\Delta k = \frac{\Delta p}{p}k_0$
This error however, causes a tune shift per path element ds:

$$dQ = \frac{\Delta p}{p}\frac{1}{a\pi}k_0\beta(s)ds \tag{9.65}$$

The variation in the tune with the relative momentum deviation is known as *chromaticity*:

$$\xi = \frac{\Delta Q}{\Delta p/p} = -\frac{1}{4\pi}\oint k(s)\beta(s)ds \tag{9.66}$$

The chromaticity increases with the beam focusing, especially with strong focusing quadrupoles (high quadrupole strength k), where the beta functions have significantly large values [7]. Even for small values of momentum deviation, the tune shift may be damagingly large by 'hitting' optical resonances which cause the particles to be lost.

The chromaticity is compensated for using *sextupole* magnets [2, 10], at points where the dispersion is non-zero and the particle trajectories are described by:
$x_D = D(s)\frac{\Delta p}{p}$
Sextupoles generate a non-linear field which, along the $x-$ axis is expressed by:

$$G_y(x) = \frac{g'x^2}{2} \tag{9.67}$$

with $g' = \frac{6\mu_0 nI}{\rho^3}$ where μ_0 is the magnetic permeability, n is the number of the coils and I indicates the current in the coils. In figure (9.24) [5], the magnetic field lines in a sextupole are demonstrated:

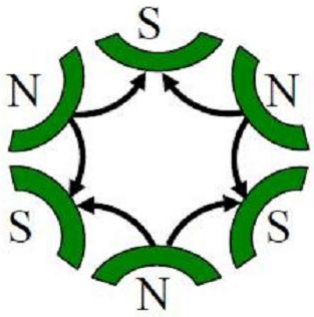

Figure 9.24: *The magnetic field lines in a sextupole.*

The sextupole focusing strength depends on the transverse beam position and the magnetic field produced by the sextupoles can be calculated from the equations (9.68) and (9.69):

$$\vec{B_x} = g'\hat{x}\hat{y} \tag{9.68}$$

$$B_y = \frac{1}{2}g'(\hat{x}^2 - \hat{y}^2) \tag{9.69}$$

and the sextupole strength is:

$$m = \frac{e}{p}g'x \tag{9.70}$$

In Fig. (9.25) [2], the chromaticity correction is demonstrated:

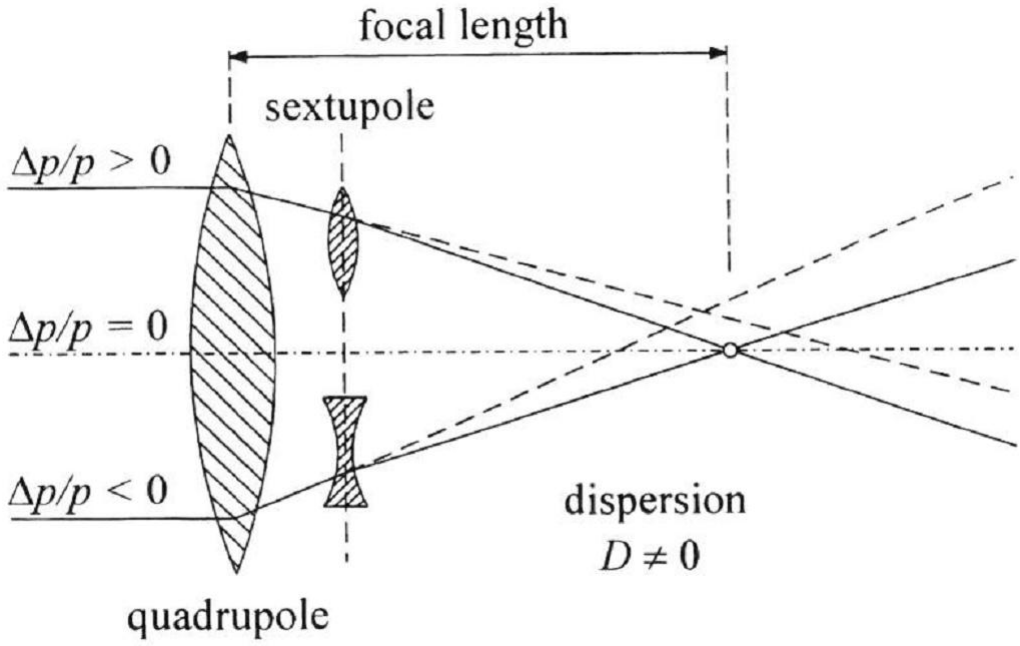

Figure 9.25: *Chromaticity correction. The particles with no momentum deviation are not influenced by the magnetic field of the sextupole.*

The particles with no momentum deviation travel along the axis and are not affected by the sextupole field. The field gradient is zero on the axis. The particles with $\Delta p/p > 0$ sense a very weak focusing effect from the quadrupoles but as they pass through the sextupole, they experience a displacement

$$x = \frac{\Delta p}{p} D \tag{9.71}$$

In other words, these particles experience an extra focusing effect from the sextupoles with strength $k_{sext} = mD\frac{\Delta p}{p}$. Respectively, the same thing applies for particles with negative momentum deviation,but with the sign reversed.
Thus the total chromaticity is:

$$\xi_{tot} = \frac{1}{4\pi} \oint [m(s)D(s) + k(s)]\beta(s)ds \tag{9.72}$$

Chromaticity causes instability of the beam and is generally not desired in a machine. However, this subject exceeds the framework of this study and will not be further analyzed.

9.14 Methodology and Tools

The design of the medical synchrotron employs consideration of all the parameters mentioned in this chapter. These parameters mainly concern the linear characteristics of the lattice [2]. Certain actions should be taken for a proper function of the accelerator. These actions involve the following:
(1)Specification of the characteristics of the magnets and determination of the values of the optical functions in order to ensure the stability of the lattice and
(2) Suppression of the dispersion.

There are simulation programs that for given variables perform simulation and propose valid results assuring the stability of the lattice.

The program used, to determine these values and consequently for the accelerator design is MAD. This is a program language and simulation a tool which allows the user to define various elements around a ring and compute the corresponding optic parameters. It is able to handle very large and very small accelerators and solves various problems on such machines. The version of MAD being used is MAD-X, the succesor of MAD-8 [11]. Using MADX, various tasks, nessecary for the proper function of an accelerator, can be performed, such as: suppression of the dispersion, chromaticity correction, simulation and correction of possible machine imperfections, calculation of the optics parameters for a machine description, definition and computation of the desired properties of the machine etc *mad*. This is done with *MADX code* (MADX scripts), written by the user, depending on the objective of his work. The machine description depends on the following parameters, to which, *predetermined values* have been assigned:

(1) the *desired output energy*
(2) the *number of dipoles-*N_b being used and
(3) the *bending angle-*θ
while the accelerated particles are defined (in this case, protons). The *characteristics of the magnets (i.e the quadrupole strengths,the dipole and quadrupole length)* as well as the *drift spaces* between them and the *phase advance* are given **initial values** as input, which may be varied during the design and simulation procedure. Thus, for a specific output energy and particles, different magnet characteristics are required. MAD-X performs the matching of the beam optics for the given characteristics of the magnetic elements and produces an output. The aim is to define the nessecary quadrupole strengths in order to have a stable lattice and a

[2]There are more optics parameters and properties of linear and non linear dynamics needed to be considered and these may slighty differentiate the process, but these are out of the scope of the present study.

stable circulation of the beam. MAD-X uses recursive algorithms to perform the matching of the beam optics, in other words, define and compute the desired properties of the accelerator (e.g define the quadrupole strengths in order to obtain the desired form and values for the optical functions at the end of the structure-section (9.6)). By matching, recalculations are performed in order to achieve quadrupole strength values that, given the predetermined values (output energy, number of dipoles, bending angle), provide a stable circulation of the beam.
In the case where, the initial values of the quadrupole strengths are close to the nessecary-output values, then a solution has been reached and the strengths for the given characteristics of the lattice (magnet lengths, drift spaces, phase advance) are defined. In the case where, the initial values are not close to the nessecary values, different input values need to be assigned to the quadrupole strengths. Afterwards, the matching procedure is carried out again in order to reach a solution and define the quadrupole strengths. This process may need to be repeated several times before reaching a solution. However, it is possible that a lattice with the initial characteristics can never be stable. Thus, if the matching procedure does not provide a solution despite the change of the input quadrupole strengths, the magnet length and phase advance need to be redefined as well. When MADX performs the matching, except from the output values, it creates a file, known as *twiss file*, that contains the values of $\beta_{x,y}$, $\alpha_{x,y}$, $\gamma_{x,y}$, $d_{x,y}$, $\xi_{x,y}$ etc., at the end of each magnet element. This way, it is possible to observe the effect of the magnet structure on the particle beam.
The code written in MADX consists of the following standard parts, in the order they are written by the user and performed by the program . First, the machine description is needed in order to calculate the optics paremeters. This is carried out with the following steps:(1) determination of the fixed values (particle type, output energy, number of dipoles and bending angle)
(2)initial values for the magnet size (eg. dipole and quadrupole length), length of the drift spaces, quadrupole strengths
(3)definition of the magnets used (quadrupoles are defined by their: name, length and strength, dipole are defined by their: name, length and bending angle)
(4) determination of the length of the magnet sequences in the lattice (e.g. Length of a FODO cell: the sum of the magnet and drift lengths, length of an Arc: sum of the length of the FODO cells used etc).
(5)definition of each magnet sequence (sequence length and position of each magnet).
After having described the machine, definition and computation of the desired properties of such a machine and simulation of the beam dynamics in the designed machine take place: (6)Matching of a sequence with several constraints, depending on the purpose of the script. The matching is performed based on commands

written by the user.
(7)Any other actions can be carried out depending again, on the purpose of the script (e.g plots of the beta functions and dispersion, commands for dispersion suppression, chromatcity correction).
Parts of the scripts written in MADX during this study can be seen in the following Tables:

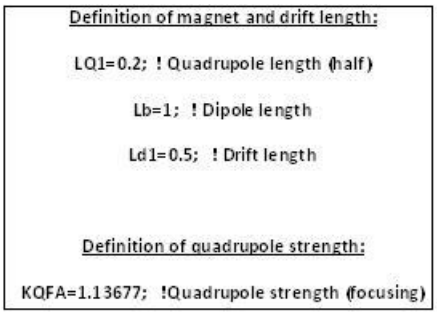

Figure 9.26: *Definition of element length and quadrupole strength*

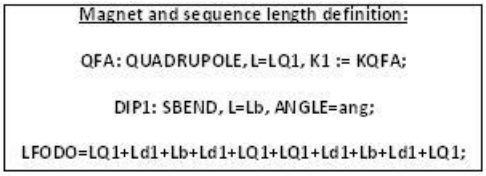

Figure 9.27: *Magnet and Magnet Sequence Length definition*

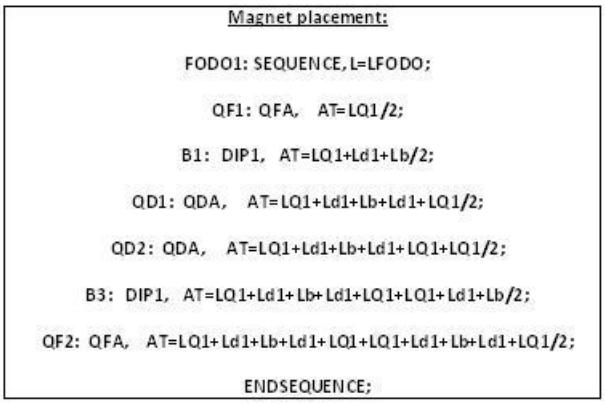

Figure 9.28: *Magnet Placement*

The whole scripts written for the purpose of this thesis can be found in the appendix.

Chapter 10

Determination of Lattice Characteristics

10.1 Parameterization

This study elaborates a design for a medical synchrotron producing a proton beam of kinetic energy T=300 MeV and is suitable for hadron therapy. The proposed accelerator is not completely circular. It consists of two arcs and two straight sections. The definition of the values of the parameters used in the lattice is based on the structure of the arc and the straight section. As previoulsy described, the number of FODO cells, the number of dipole and quadrupole magnets used as well as their size must be determined. The aim of the *parameterization* process is to come up with equations through which, given the value of one parameter the definition of the others is possible. Moreover, the effect of the variation of one parameter on the others should be examined and a lower limit for the values that may be attributed to each characteristics of the lattice (i.e dipole length, number of dipoles, bending radius etc.) should be determined. The equations used are the following:

$$C = L_{arc} + L_{str} \tag{10.1}$$

where C the circumference of the ring and is equal to the sum of the length of the arcs -L_{arc}- and the length of the straight sections -L_{str}. Each arc consists of a number of FODO cells. The length of both arcs in the ring is expressed by equation (10.2):

$$L_{arc} = N_{arc} L_f \tag{10.2}$$

where N_{arc} represents the number of FODO cells in both arcs and L_f represents the length of one full FODO cell. These are expressed by equations (10.3) and (10.4).
As mentioned in section (9.8), a FODO cell consists of a focusing quadrupole, a dipole magnet, a defocusing quadrupole, and another dipole and drift space between them. Consequently, the number of FODO cells in the arcs, is expressed by the total number of dipoles divided by two (equation (10.3)):

$$N_{arc} = N_b/2 \tag{10.3}$$

where N_b represents the number of dipoles in both arcs.
The length of a FODO cell (L_f) is expressed by equation (10.4) as follows:

$$L_f = 2(L_b + 2L_d + L_q) \tag{10.4}$$

where L_b, L_d and L_q are the lengths of the dipoles,drift spaces and quadrupoles respectively.
Taking into account equations (10.1) and (10.2), the circumferance (C) of the ring can be expressed by equation (10.5):

$$C = N_{arc}L_{fodo} + L_{str} \tag{10.5}$$

Substituting equations (10.3) and (10.4) into equation (10.5) and presuming for simplicity that the ring consists only of arcs and no straight sections, the circumference of the ring is:

$$C = N_bL_b + 2N_bL_d + N_bL_q \tag{10.6}$$

The bending angle is expressed by equation (9.7), while equation (9.8) gives the bending radius ρ. Combining both, equation (9.7) and (9.8), equation (10.7) is obtained:

$$\theta = L_b/\rho = 2\pi/N_b \tag{10.7}$$

Another important parameter which needs to be considered is the Filling Factor. The Filling Factor indicates the ratio of the length of the ring's circumference that is covered by dipoles over the total circumference of the ring. It is expressed by:

$$FF = \rho/R = (N_bL_b)/C \tag{10.8}$$

where R is the radius of the ring. Substituting equation (3.6) into equation (10.8) the Filling Factor becomes:

$$FF = L_b/(L_q + 2L_d + L_b) = 2L_b/L_f \tag{10.9}$$

If the Filling Factor has a large value, the rest of the elements used in the lattice will be fairly small, since most of the ring will be covered by dipoles. The construction of a ring with a small Filling Factor is easier, since most of the ring will be covered by dipoles and the rest of the elements will be small. Thus, in designing a compact synchrotron, it is prefered theta the Filling Factor has the maximum possible value. Of course, the FF will always be less than 1 since the whole ring cannot be covered by dipoles. According to equation (10.8), the Filling Factor depends on the dipole length L_b, the number of dipoles N_b and the bending radius ρ. Since the bending radius is expressed by the following formula: $\rho = \frac{\beta E}{B}$, it is clear that the Filling Factor also depends on the magnetic field B. The influence of the dipole length and the number of dipoles on the FF and the magnetic field B is demonstrated in Fig. (10.1) and (10.2):

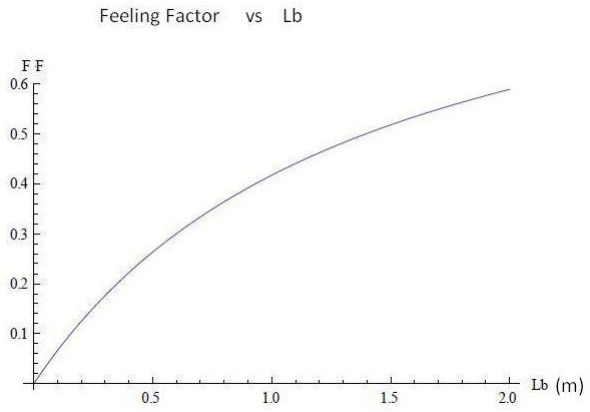

Figure 10.1: *The Filling Factor with respect to the dipole length L_b.*

In particular, in Fig. (10.1), the dependence of the Filling Factor on the dipole length is demonstrated. Clearly, the value of the Filling Factor increases with the dipole length, according to equation (3.8)
The magnetic field of the dipoles of conventional magnets, as already mentioned in section (8.2), can reach a maximum value of $B = 1,7$ Tesla [10]. The relation between the magnetic field and the bending radius is:

$B\rho = \beta E/0.2998$ (eq. (9.9))

where $B\rho$ is the magnetic rigidity, E is the total particle energy and $\beta = \sqrt{1-(E_0^2/E^2)}$. The dependence of the dipole length and the number of dipoles

on the magnetic field is demonstrated in Fig. (10.2).

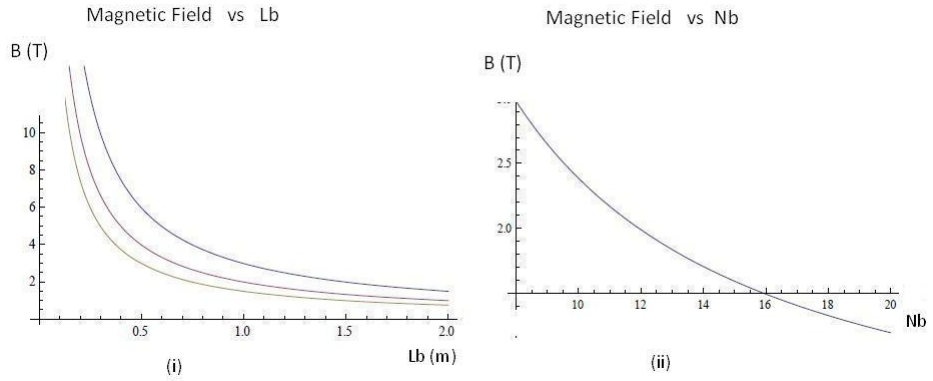

Figure 10.2: *The magnetic field with respect to the number of dipoles N_b and the dipole length L_b.*

In Fig. (10.2-i) the dependence of the magnetic field on the dipole length is demonstrated. The lowest line corresponds to $N_b = 16$ the middle one to $N_b = 12$ and the highest one to $N_b = 8$.
Last, according to Fig. (10.2-ii), keeping the dipole length constant, it can be observed that if the number of dipoles decreases, then a higher magnetic field is required. This behaviour is expected since the dependence of the magnetic field on the dipole number and dipole length -obtained from equations (9.7), (9.8) and (9.9) (section (9.2.1))-, denotes that the magnetic field B produced by the dipole magnets, decreases (becomes weaker) when the dipole length or the number of dipoles increase (longer or more dipoles in the lattice). Equations (9.7), (9.8) and (9.9) are given again below:

$$\begin{aligned} \theta &= \frac{2\pi}{N_b} (2.7) \\ \rho &= \frac{L_b}{\theta} (2.8) \\ B\rho &= \frac{\beta E}{0.2998} (2.9) \end{aligned} \tag{10.10}$$

Substituting equation (9.8) into equation (9.9), equation (10.10) is derived:

$$B = \frac{\beta E \theta}{0.2998 L_b} \tag{10.11}$$

Substituting equation (9.7) into equation (10.10), equation (10.11) is obtained:

$$B = \frac{\beta E 2\pi}{0.2998 L_b N_b} \tag{10.12}$$

The magnetic field B is inversely proportional to the length and to the number of dipoles as well. This realtion justifies the asymptotic behaviour of Fig. (10.2).

As mentioned in the beginning of this chapter, it is important for the minimum values of the dipole length and bending radius to be defined, for a given output energy. Setting a lower limit to these parameters, makes obtaining a more accurate perception of the limits on the optics parameters possible . Considering equations (10.7) and (9.9), the minimum values that should be used for the dipole length and the bending radius are expressed by equation (10.12):

$$L_{bmin} = \theta_{min}\rho_{min} = (2\pi/N_b)(\beta E/(0.2998B)) \tag{10.13}$$

where θ is the bending angle and $\rho = \frac{\beta E}{(0.2998B)}$
All the calculations, plots and results that will be presented in the following chapters have been done by using protons with a kinetic energy of $T = 300$ MeV. According to equation (9.11) ($E = E_0 + T$), the total particle energy E is: $E = E_0 + T = 0.938 + 0.3 = 1.238$ GeV, where 0.938 is the proton mass in GeV (inertia energy). The output energy of the medical synchrotron will be $E = 1.238GeV$.
For this case, the minimum value for the dipole length and the bending radius can be calculated.
The minimum number of FODO cells in an arc is two. Therefore, the minimum number of dipoles is $N_b = 8$.
The minimum bending radius is possible, for the maximum magnetic field B, since ρ and B are inversily proportional. Thus, for an output energy of $E = 1.238$ GeV, the minimum bending radius ρ can be calculated as follows:

$\rho_{min} = \frac{\beta E}{0.2998 B_{max}} = \frac{0.65 \times 1.238}{0.2998 \times 1.7} = 1.585$ m
where B_max is equal to 1.7 Tesla (the maximum achievable magnetic field by conventional magnets)
Therefore, $\rho \geq 1.585$ m.

Thus, the minimum dipole length is $L_{bmin} = 1.24$ m.

The values of these parameters may be changed depending on the structure of the lattice, in order to assure the stable circulation of the particle beam. This parameterization is very useful since it sets a lower limit for these values, justifies and makes the selection of the values easier. However, this parameterization can be used for the calculation of the values of the above parameters, for different type of particles and different output energies.

10.2 Different energies and different particles

The above parameterization process, applies for protons of different kinetic energy and for other particles as well. In the following, three different cases are presented.
Parameters for protons of T=200 MeV
When the kinetic energy of the protons is chosen to be $T = 200$ MeV, then the total output energy of the synchrotron would be calculated to be: $E = E_0 + T = 0.938 + 0.2 = 1.138$ GeV and the value of β would be $\beta = \sqrt{1 - (0.938^2/1.138^2)} = 0.566$.
Substituting the values of β and E into equation (2.9) ($B\rho = \frac{\beta E}{0.2998}$), the magnetic rigidity $B\rho$ can be calculated. The result is:
$B\rho = 2.15$ Tm.
Parameters for protons of T=250 MeV
When the kinetic energy of the protons is chosen to be $T = 250$ MeV, then the total output energy of the synchrotron would be calculated to be: $E = E_0 + T = 0.938 + 0.25 = 1.188$ GeV and the value of β would be $\beta = \sqrt{1 - (0.938^2/1.188^2)} = 0.61367$.
Substituting the values of β and E into equation (10.10) the magnetic rigidity $B\rho$ is:
$B\rho = 2.43$ Tm
Table (2) summarizes the results:

T(MeV)	B ρ(Tm)
200	2.15
250	2.43
300	2.69

Table 10.1: Energy-Magnetic Rigidity

The bending angle can be determined from equation (10.7) for a specific dipole length and for a given number of dipoles number of dipoles. Then, the magnetic field required for the given parameters of the ring can be calculated. **Parameters for Carbon** In this case, what changes is the E_0, that is the mass of the particle

in energy units since carbon has a much larger mass than protons. The mass of carbon in GeV is $E_0 = 11.2$ GeV. Thus, for a kinetic energy of $T = 0.3$ GeV the total output energy is $E = 11.2 + 0.3 = 11.5$ GeV and the value of β would be $\beta = \sqrt{1 - (11.2^2/11.5^2)} = 0.2269$.
Substituting the values of β and E into equation (10.10) the magnetic rigidity $B\rho$ is:
$B\rho = 8.7$ Tm.
If the magnetic field required is $B > 1.7$ Tesla, then superconducting magnets must be used since as already mentioned, conventional magnets can only give a magnetic field up to 1.7 Tesla.

Chapter 11

Dispersion

As already mentioned, the synchrotron of this study consists of two arcs and two straight sections. The arc consists of FODO cells (minimum two) where, dipoles are responsible for the bending of the beam and quadrupoles perform the focusing. However, in the straight section bending of the beam is not required and therefore, it is a sequence of quadrupole magnets only.

The beam circulation through a FODO cell is demonstrated in Fig. (11.1) and (11.2) where the evolution of the beta functions and the phase advance can be seen:

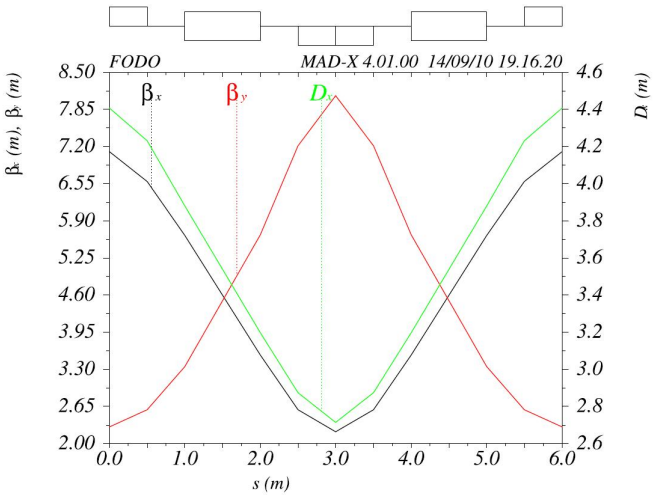

Figure 11.1: *Evolution of the beta functions and the dispersion through a FODO cell.*

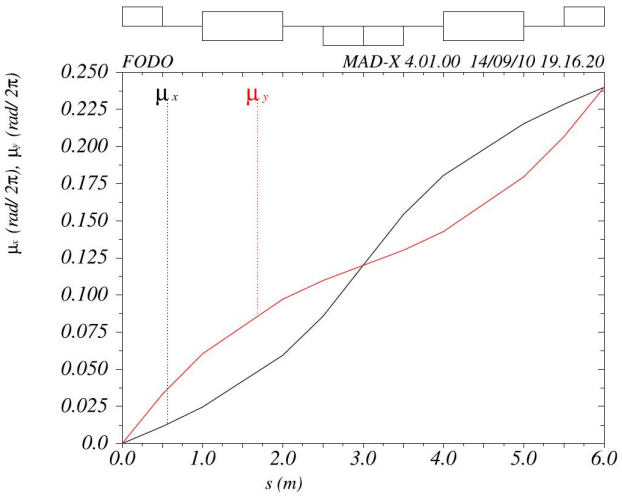

Figure 11.2: *Evolution of the phase advance through a FODO cell.*

As it can be observed in Fig. (11.1), the dispersion in the FODO cell reaches large values. As mentioned in Chapter (9), dispersion is caused by the fact that particles enter the arc with different momentum and therefore, they are bent by a different angle by the dipoles. However, it is important that the dispersion is suppressed before entering a straight section in order to create a homogeneous beam. This way, the particles to exit the ring with the same angle and not deviate from the ideal orbit.

There are many ways to suppress the dispersion to zero. Dispersion suppressors can be made from FODO cells, additional quadrupoles in the FODO structure, electrostatic deflectors (structures that use electric fields for the modification of the particle path) etc. [16, 17]. However, in the case of a medical accelerator, which needs to be as compact as possible, adding any other structures (i.e quadrupoles, electrostatic deflectors) will increase the circumference of the ring. Therefore, the dispersion should be suppressed only by using the FODO cells which constitute the arc. Thus, more than two FODO cells per arc are required in order to sufficiently suppress the dispersion. This can be achieved by using two methods: The *missing dipole method* and the *resonant lattice method* both of which will be analysed in the following sections.

11.1 Dispersion suppression

11.1.1 Missing Dipole method

As already mentioned, dispersion is caused by dipole fields. Therefore, the most convenient way to suppress the dispersion is at the exit of an arc. The purpose is to maintain the dispersion suppressed to zero until the next bend. In the straight sections there are no dipoles, thus there is no cause of dispersion. This can be done by removing a dipole almost at the end of an arc. The dispersion function, defined in equation (9.53) ($D''(s) + \frac{1}{\rho^2}D(s) = \frac{1}{\rho^2}$), makes a small amplitute oscillation around a value determined by the strength of the dipole field. By reducing the strength of a dipole magnet, the dispersion begins to oscillate around it's new equilibrium point. In the case of removing a dipole magnet completely, this pointis zero. Therefore, the dispersion function begins to oscillate around zero, and gradually reaches zero. The second last dipoles at each end of the arc are being removed in order to achive this.
Considering the compact requirement, the arc in this design consists of only four FODO cells. The general layout is presented in Fig. (11.3):

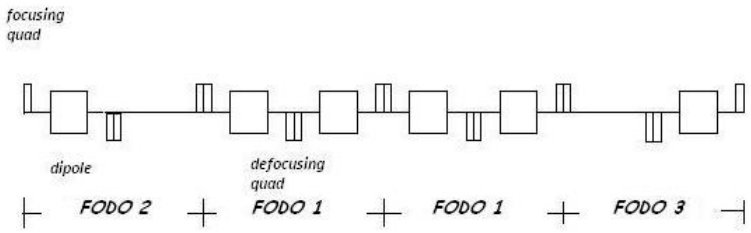

Figure 11.3: *Expected general layout of the ring*

As it can be seen in Fig. (11.3) the arc consists of two normal FODO cells in the middle (FODO 1) and two FODO cells with a missing dipole in each end (FODO 2 and FODO 3). The place in the FODO cell where the dipole is missing, is compensated by a drift section, having length equal to the length of the dipole. The arc contains 6 dipoles: Two in each normal FODO cell and one in each FODO cell with a missing dipole. Therefore the whole ring consists of 12 dipoles. Now, equation (10.3) becomes

$$N_{arc} = N_b/2 + 2 \tag{11.1}$$

Since the number of dipoles N_b is known, the minimum dipole length can be calculated from equation (10.12):

$L_{bmin} = \theta_{min}\rho_{min} = (2\pi/N_b)(\beta E/(0.2998B_{max})) \Rightarrow L_{bmin} = 0.829$ m for $E = 1.238$ GeV, $N_b = 12$ and $B_{max} = 1.7$ Tesla which is the maximum achievable field with conventional magnets.
As it can be seen from the script 'Missing Dipole', in the index, the dipole length used in this case is $L_b = 1$ m. Given the number of dipoles and the dipole length, the bending radius and thus, the magnetic field of the dipoles can be calculated according to equations (10.11) and (9.9) which are presented again, respectively:

$$\begin{aligned} B &= \frac{\beta E 2\pi}{0.2998 L_b N_b} \\ B\rho &= \frac{\beta E}{0.2998} \end{aligned} \tag{11.2}$$

Substituting the number of dipoles, with $N_b = 12$ and the dipole length with $L_b = 1$ m into equation (10.11), the magnetic field is calculated: $B = 1.41$ Tesla. Moreover, substituting the magnetic field B into equation (9.9), the bending radius is obtained: $\rho = 1.91$ m.
In order to suppress the dispersion, except the extraction of two dipoles, a change in the quadrupole strengths is also needed. The focusing quadrupole strengths are the same in both versions of the FODO cells (the normal FODO cell and the FODO cell with the missing dipole). However, the defocusing quadrupole strengths are different between the normal FODO cells and the ones with the missing dipole. Of course, since FODO 2 and FODO 3 are symmetrical, the quadrupole strengths are the same.
Only FODO 1 is matched to a phase advance of 0.24 in both planes. Figures (11.4)-(11.9) demonstrate the circulation of the beam through FODO 1, FODO 3 and through the whole arc as well.

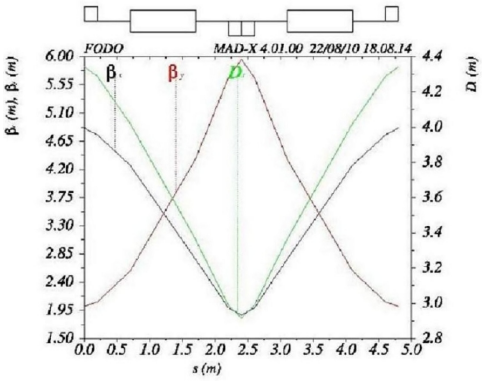

Figure 11.4: *Evolution of the beta functions and the dispersion through FODO1.*

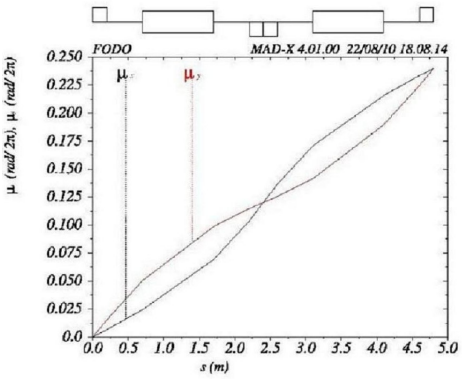

Figure 11.5: *Evolution of the phase advance through FODO1.*

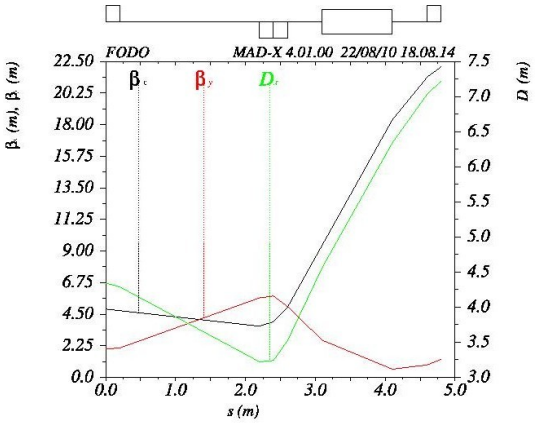

Figure 11.6: *Evolution of the beta functions and the dispersion through FODO3.*

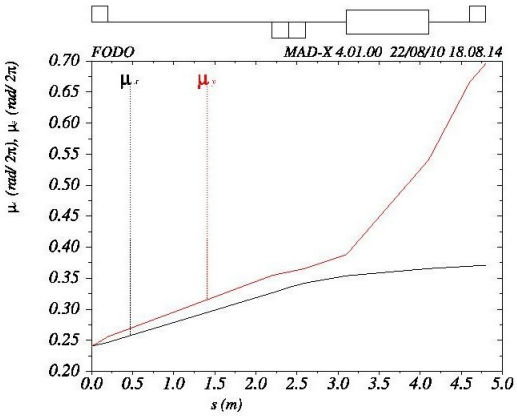

Figure 11.7: *Evolution of the phase advance through FODO3.*

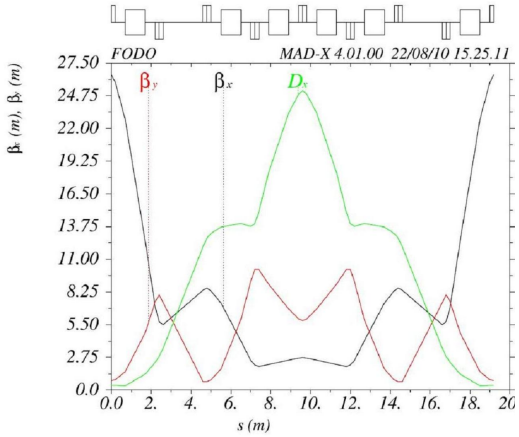

Figure 11.8: *Evolution of the beta functions and the dispersion through the arc.*

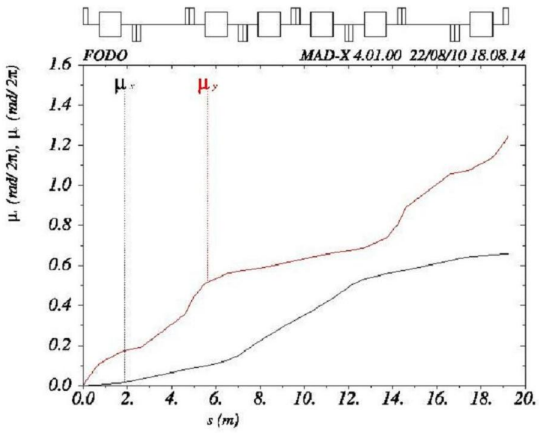

Figure 11.9: *Evolution of the phase advance through the arc.*

In Fig. (11.4), (11.6) and (11.8), the black and red lines demonstrate the evolution of the beta function in the horizontal and vertical plane, respectively, whereas the green line demonstrates the evolution of the dispersion function in the horizontal plane. In Fig. (11.5),(11.7) and (11.9), the black and red lines represent the horizontal and vertical phase advance, respectively.
As it can be observed in Fig. (11.8), the dispersion at the end of the arc is close to zero. The exact value of the beam dispersion at the end of the arc is 0.15 m. This is the lowest achievable value for the dispersion. This may be resolved by adding extra elements except from the FODO cells in the arc; specifically, by adding quadrupoles with different quadrupole strengths. However, as mentioned above, this option is contradictory with the requirement of the compact ring, since the circumference of the ring should be around 50 m. Of course, this is impossible to achieve by adding more elements to the original design. Therefore, the missing dipole method cannot be used in this case to suppress the dispersion. The program code written in MADX for this method can be found in the Appendix (FODOcell-MD).

11.1.2 Resonant Lattice

Due to the inability to use the missing dipole method, an attempt was made to suppress the dispersion by constructing what is called a 'resonant lattice'.
The arc consists of 4 identical FODO cells. In order to eliminate the dispersion, the FODO cells must have a phase advance of $\pi/2$ each, resulting in a total hor-

izontal phase advance of 2π at the end of the arc. Ths can be achieved with a minimum number of FODO cells equal to 4. This results in a compact lattice with zero dispersion of the beam. The disadvantage of this method, is the lack of arc tunability [14] due to the integer tune value (Q=1) at the end of each arc, based on equation (9.35).
However, the lack of arc tunability will not be further analyzed in the framework of this thesis. The straight section consists of 2 half focusing quadrupoles on each side and a triplet of quadrupoles in the middle.
The half focusing quads in each end of the straight section have the same strengths (KQFA) as the ones in each end of the arc due to symmetry reasons. The focusing quadrupole in the middle of the straight section have a different strength (KQFB), and the defocusing quadrupoles in the triplet have different defocusing strengths as well (KQDB) than the defocusing quads in the arc (KQDA). The structure of the arc in the case of resonant lattice is illustrated in Fig. (11.10):

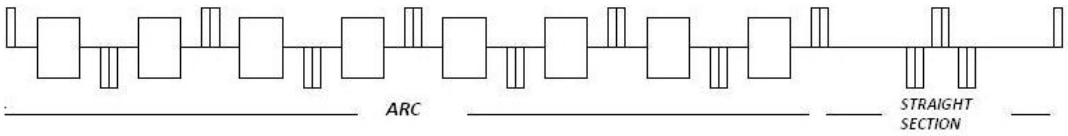

Figure 11.10: *The structure of a half resonant lattice.*

The parameterization procedure is presented, in order to calculate the appropriate values for the parameters of the lattice. They are defined according to the following lattice structure:

- Each arc consists of 4 FODO cells, all identical. Therefore, each arc contains 8 dipoles, thus, the whole ring contains 16 dipoles.

- The straight section consists of 2 half focusing quads and a triplet.

- The perimeter of the ring is then expressed by: $C = 2L_{arc} + 2L_{str}$

- The number of FODO cells in the arc is expressed by: $N_{arc} = N_{dip}/2$, thus $L_{arc} = N_{arc} * L_f$

- The length of the straight section is: $L_{str} = 8 * L_{Q1} + 2 * L_{d2} + 2 * L_{d3}$ where L_{Q1} is the length of half a quad

- L_{d2} is the length between the focusing quad and the triplet

- L_{d3} is the length between the quads that the triplet consists of.

As already mentioned in Chapter (9), the number of periods of a ring is indicated by the number of identical magnet structures. Therefore, in this case, the number of periods is $N = 2$, since each period is defined by one arc and one straight section. The minimum dipole length is defined by the bending angle and the magnetic field, according to the following formulas:

$B\rho = \frac{\beta E}{0.2998}$ (eq. (3.10)) where $\beta = \sqrt{1 - \frac{E_0^2}{E^2}} = \sqrt{1 - \frac{0.938^2}{1.238^2}}$

For the maximum achievable magnetic field with conventional magnets $B_{max} =$ 1.7 Tesla

thw minimum bending radius can be calculated from equation:

$$\rho_{min} = \frac{\beta E}{0.2998 B_{max}} = 1.585 \tag{11.3}$$

m

The minimum dipole length L_b can be calculated by the equation (10.12), as shown below:

$L_{bmin} = \theta_{min}\rho_{min} = \frac{2\pi}{16}1.585 = 0.62$ m, where θ is given by: $\theta = \frac{L_b}{\rho} = \frac{2\pi}{N_b}$

However, in case the desired output energy increases or the accelerated particles are carbon ions instead of protons, the required dipole length will be greater (equation 9.9). Moreover, the quadrupole strengths depend on the dipole length as well. This dependence can be observed by substituting equations (9.7) and (9.8) into equation (9.16):

$$k = \frac{0.2998 \times g \times 2\pi}{B \times L_b \times N_b} \tag{11.4}$$

. Clearly, for the same number of dipoles, but for a greater dipole length, the quadrupole strengths receive smaller value. Therefore, in order to be able to accelerate different particles or even protons to higher energies with the *same accelerating structure*, the actual dipole length is selected to be $L_b = 1$ m in order to obtain a more flexible design.
Given the number of dipoles and the dipole length, the bending radius and thus, the magnetic field of the dipoles can be calculated according to equations (10.10) and (9.9):
$\rho = 2.54$ m and $B = 1.06$ Tesla.
The length of the quadrupole magnets is selected to be 0.4 m. Taking into account the above calculation, the length of each arc is 19.2 m whereas the length of each straight section is 5.7 m.

Since the dispersion is caused by dipoles, which only have an effect on the beam in the horizontal plane, the most important constraint is to keep the horizontal phase advance equal to 0.25. During the matching, the phase advance of the FODO cell is varied in both planes: $\mu_x : [0.23, 0.27]$ and $\mu_y : [0.2, 0.47]$. This way, it is possible to calculate through MADX, the different values for the quadrupole strengths depending on the phase advance (see Appendix: Table 1-KFD), as well as the different values for the tune, the dispersion and the beta functions (see Appendix: Table 2-RST2).
The ring is matched to initial conditions. For symmetry reasons, as a constraint, the beta functions at the end of the ring are required to have the same values as in the beginning of the ring. This leads to a definition of the quadrupole strengths of the straight section.
Afterwards, the previously defined quadrupole strengths are used as initial values. Then, the ring is matched again but this time not to initial conditions.

This method, as already mentioned, renders zero dispersion when the phase advance is set to 90 degrees ($\mu_x = \mu_y = 0.25$). For a phase advance of 0.25 in both, the horizontal and vertical plane, the quadrupole strengths are: KQFA = 1.137 m^{-2} (focusing quadrupole in the arc), KQDA=-1.47 m^{-2} (defocusing quadrupole in the arc), KQFB=2.766 m^{-2} (focusing quadrupole in the straight section) and KQDB=-1.97 m^{-2} (defocusing quadrupole in the straight section). In Fig. (11.11-11.14) the circulation of the beam through the *half* ring is demonstrated:

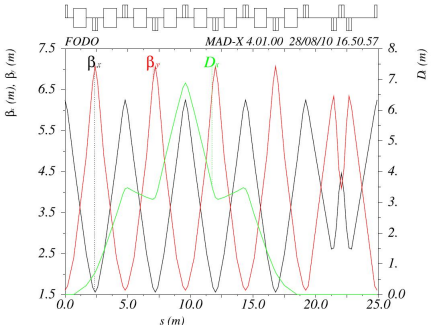

Figure 11.11: *The evolution of the beta functions and the dispersion for a phase advance of 90 degrees.*

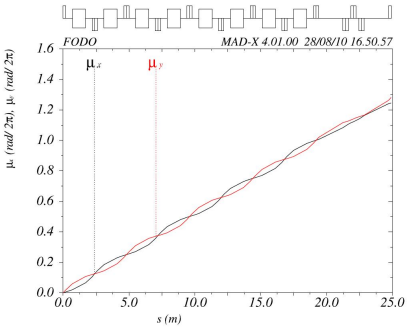

Figure 11.12: *Phase Advance of 90 degrees.*

It can be observed that in Fig. (11.11), that at the end of the arc the dispersion of the beam is zero. This happens because this figure demonstrates the beta functions and the dispersion, when the phase advance is 0.25, as it can also be seen in Fig. (11.12). The maximum beta functions are approximately β_x= 6.2 m in the horizontal plane and β_y= 7 m in the vertical plane.

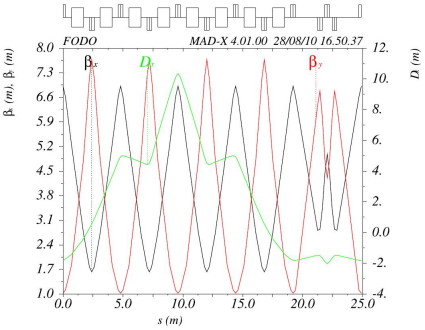

Figure 11.13: *The evolution of the beta functions and the dispersion when the phase advance is not 90 degrees.*

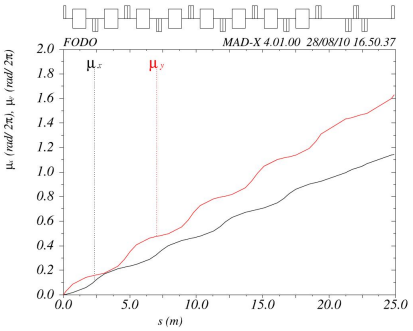

Figure 11.14: *Phase Advance ≠ 90 degrees.*

On the contrary, in Fig. (11.13), the dispersion of the beam is almost equal to 2 m which of course is due to the fact that the phase advance is not close to 0.25. Specifically, the phase advance is μ_x= 0.23 and μ_y= 0.44 for the horizontal and vertical plane, respectivelly. Thus, these figures prove that the resonant lattice method suppresses the dispersion when the phase advance is set to 90 degrees.

Having analyzed the significance of the tune values for the stable circulation of the particle beam, it is interesting to observe the change that ocuurs in the beta functions, the dispersion and the phase advance as the tune changes for a half ring (Fig. (11.15)-(11.22)). As already mentioned, the phase advance in each FODO cell is varied in both planes: $\mu_x : [0.23, 0.27]$ and $\mu_y : [0.2, 0.47]$.
In Fig. (11.15) and (11.16), the evolution of the beta functions (β_x and β_y, respectivelly) for different tune values is demonstrated:

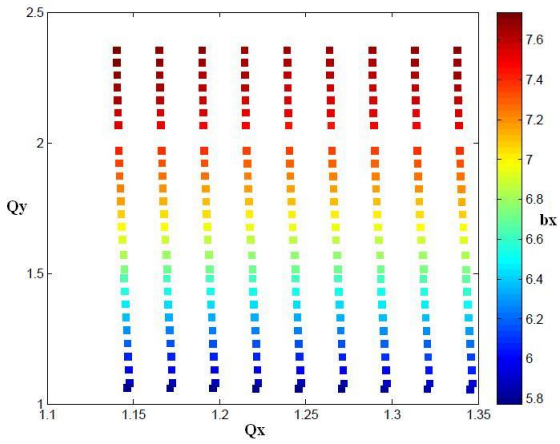

Figure 11.15: *The tune (Q_x,Q_y) with respect to the beta function in the horizontal plane (b_x).*

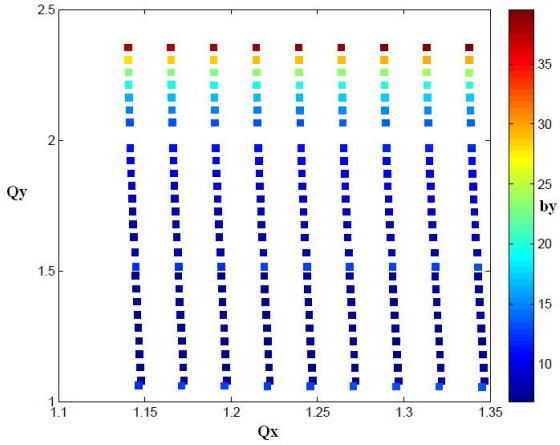

Figure 11.16: *The tune (Q_x,Q_y) with respect to the beta function in the vertical plane (b_y).*

For each value of Q_x (Q_x=1.14, 1.16, 1.19 etc.), the value of Q_y is scanned through Q_y: [1, 2.35]. The different colors indicate the different values of the beta function in the horizontal plane. In Fig. (11.16), β_x varies between 5.8 mm and 7.6 mm. However, in Fig. (11.16), β_y varies between 6.9 mm and 37.5 mm. Therefore, the difference in color cannot be easily discerned. For each value of Q_x and for Q_y between 1 and 2, β_y has relativelly low values (7-10 mm). However, for $Q_y = 1$, 1.5 and 1.97, the dots are light blue and the amplitute of the particle oscillation in the vertical plane (β_y) is approximately 12 mm. These pairs of tune values ($[Q_x, Q_y]$=[1.14,1],[1.14,1.5],[1.14,1.97],[1.16,1] etc.) indicate resonances of the beam. Further increase in Q_y causes a more evident increase in β_y which reaches 37.5 mm.

In Fig. (11.17) and (11.18), the evolution of the phase advance (μ_x and μ_y,

respectivelly) for different tune values is demonstrated:

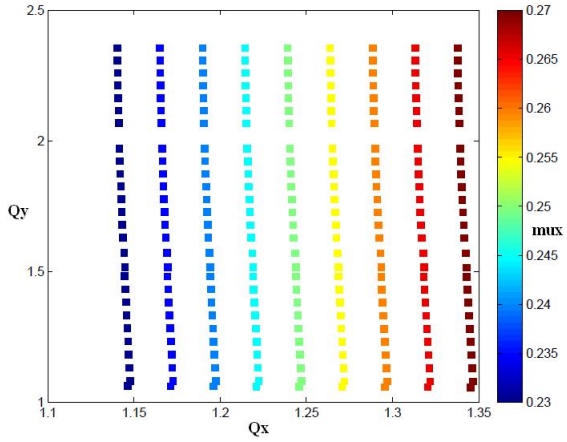

Figure 11.17: *The tune (Q_x,Q_y) with respect to the phase advance in the horizontal plane (μ_x).*

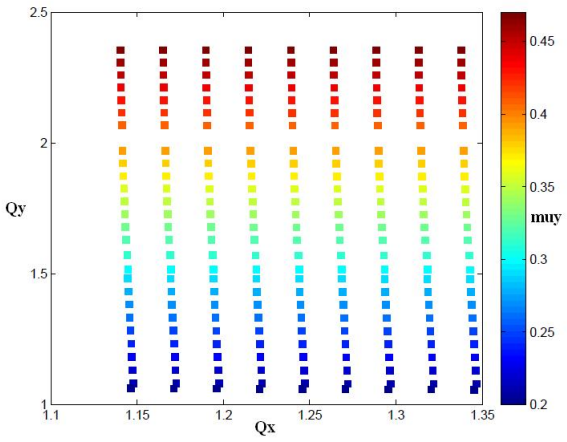

Figure 11.18: *The tune (Q_x,Q_y) with respect to the phase advance in the vertical plane (μ_y).*

In Fig. (11.17), it can be observed that the horizontal phase advance increases with Q_x. It is independent of the value of the vertical tune Q_y.
The same behaviour is observed in Fig. (11.18) where the vertical phase advance is presented. Its evolution is independent of Q_x. This is expected since the total phase advance indicates the tune values multyplies by 2π.

In Fig. (11.19) and (11.20), the tune, as well as the phase advance, in relation with the dispersion is presented:

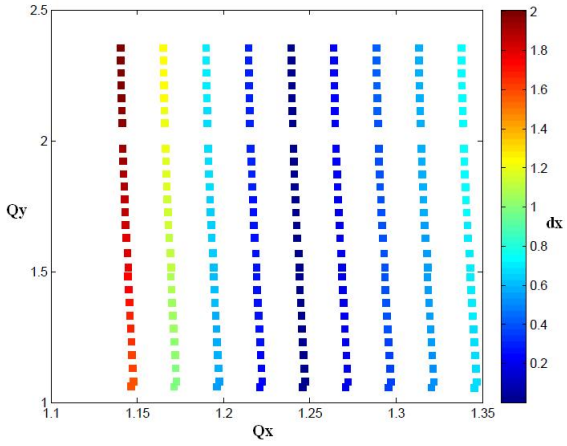

Figure 11.19: *The tune (Q_x,Q_y) with respect to the dispersion in the horizontal plane (d_x).*

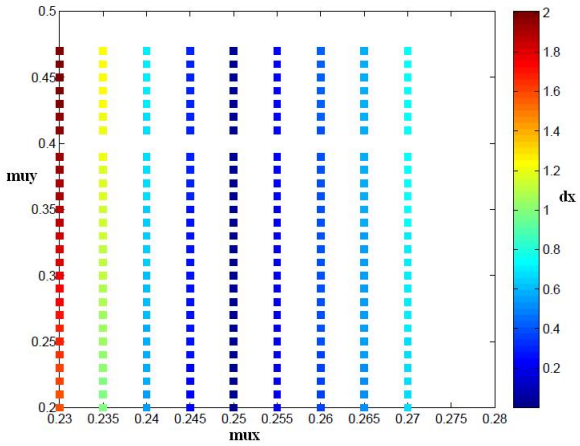

Figure 11.20: *The phase advance (μ_x,μ_y) with respect to the dispersion in the horizontal plane (d_x).*

As it can be observed from Fig. (11.19) and (11.20), the dispersion d_x, depends mostly on the horizontal tune Q_x and phase advance μ_x as expected. The dispersion initially has high values, then reaches a minimum when $Q_x = 1.25$ and starts to increase again for $Q_x \geq 1.25$. This behaviour of course is expected, since for $Q_x = 1.25$, the phase advance in the horizontal plane is $\mu_x = 0.25$. The dispersion is almost independent of the vertical tune and phase advance, which is logical, since dispersion is caused by dipole magnets,which act upon the beam only in the horizontal plane. The values of the dispersion function in relation with the tune and the phase advance can also be seen in the Appendix (Table 2-RST2).

Moreover, the evolution of the phase advanced in relation to the tune (horizontal and vertical) is demonstrated in Fig. (11.21) and (11.22) :

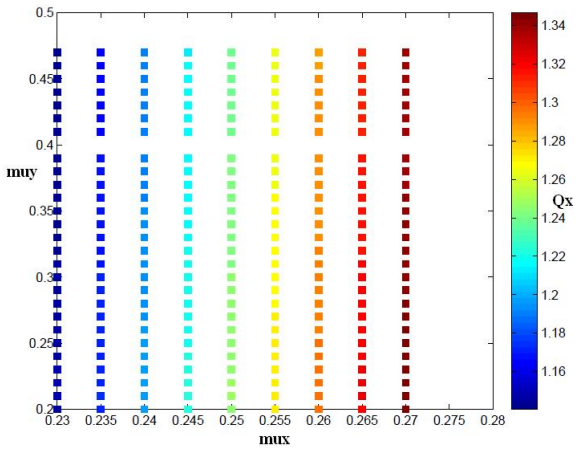

Figure 11.21: *Evolution of the phase advance (μ_x,μ_y), with respect to the tune in the horizontal plane (Q_x).*

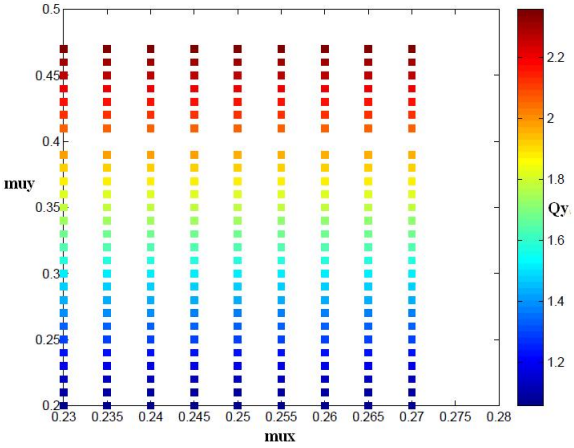

Figure 11.22: *Evolution of the phase advance in both planes, with respect to the tune in the vertical plane (Q_y).*

The horizontal tune, Q_x, depends on the horizontal phase advance and increases along with it. Respectively, the same applies for Fig. (11.22). This is expected since the tune demonstrates the total phase advance of the ring.
It is important to mention that the above diagrams refer to the half ring, for simplicity. For the whole ring, the values are double, since the lattice is symmetrical.

In Fig. (11.23) optical resonances up to third order are demonstrated:

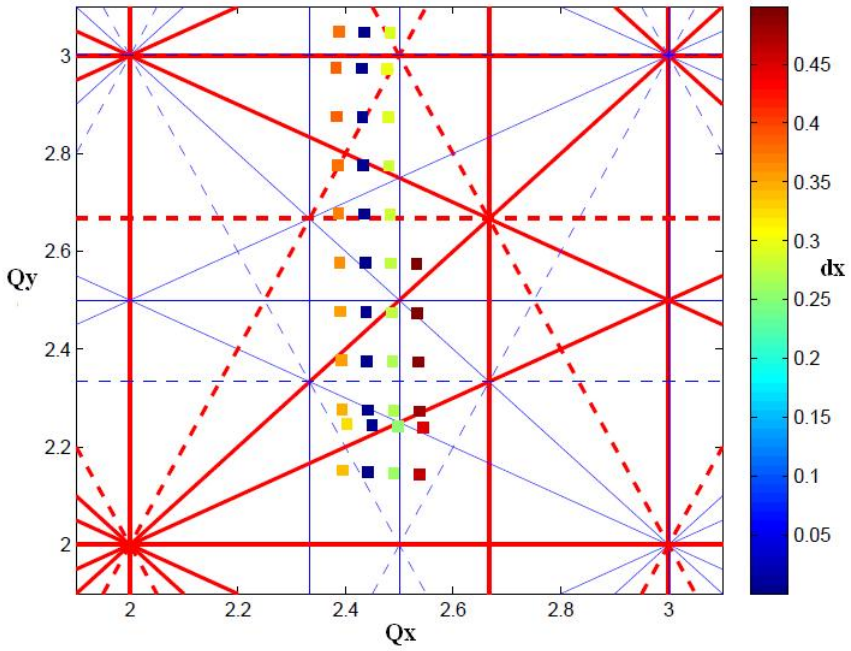

Figure 11.23: *The Tune Diagram, demonstrating up to third order resonances.*

As it has already been explained in Chapter (9),section (9.12), it is important to avoid optical resonances. The condition for optical resonance in both planes is expressed by equation (9.63): $mQ_x + nQ_y = p$ where m, n, p are integers and $|m| + |n|$ is called *order* of the resonance.
The solid red and blue lines indicate systematic [1] and non-systematic resonances,respectivelly, while dashed lines indicate skew resonances[2].
In order to provide a stable operation, a pair of values for Q_x and Q_y must be chosen that is far from resonances.
For example, it is evident that the tune must not take values near $Q_x = Q_y$=2 or 3. Also, as it can be seen in Fig.(11.23), the dispersion is zero for Q_x=2.45 and Q_y=2.36. These tune values are given by a phase advance of μ_x=0.25 and μ_y=0.23 respectivelly. When the vertical phase advance is set to 0.25 as well, the dispersion

[1] *Systematic* resonances appear when the p is an integer multiple of the number of periods. In this case, as already mentioned, the number of periods is N=2. For example, for Q_x=2, equation (9.63) gives: $n \times Q_x = p \Rightarrow p = 1 \times 2$ and indicates a first order ($m = 0$, therefore the order of the resonance is determined only by n), systematic resonance.

[2] Skew resonances are caused by rotated magnets but since in this case only normal magnets are used, skew resonances exeed the framework of this study.

of the beam is zero. However, when both μ_x and μ_y are equal to 0.25, the beam hits optical resonances, as it can be seen from Fig. (11.23), where $Q_x = 2.45$ and $Q_y = 2.56$ (blue line). Therefore, these values should be avoided.

As a result of this method, the final lattice is displayed in Fig. (11.24):

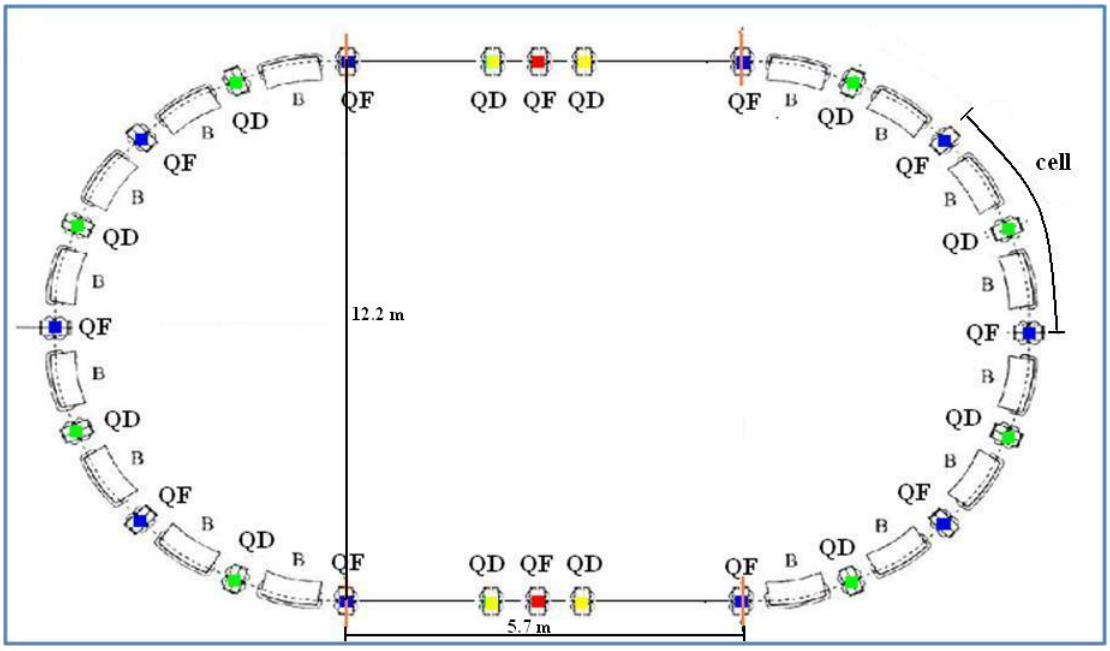

Figure 11.24: *The lattice, consists of two arcs and two straight sections.*

Each arc, consists of 4 identical FODO cells and has a total length of 19.2 m. Each straight section consists of two half focusing quadrupoles at each end and a quadrupole triplet in the middle and has a total length of 5.7 m. The different colours correspond to different quadrupole strengths. The program code written in MADX for this method can be found in the Appendix(FODOm). The total length could have been less if superconducting magnets were used. However, this would increase the cost and since one of the prerequisites is to have a low cost synchrotron, conventional magnets were used.

Chapter 12

Analytical Calculations for a FODO cell

12.1 Weak Focusing

This subject has already been presented in section (9.9), for the case of high energy accelerators (TeV range), where the weak focusing is negligible and has not been taken into account during the calculations of the transfer matices. However, since the accelerator of this study is a medical synchrotron which functions in the MeV range, weak focusing constitutes an important factor which should be considered. According to equation (9.9): $B\rho = \beta E/0,2998$, the bending radius ρ has a very large value for high energy accelerators. For this reason, the factor $1/\rho^2$ representing the weak focusing is negligible and therefore, is not taken into account. Since the accelerator of this study functions in the (MeV) range, the bending radius of the ring is significantly smaller. Thus, the weak focusing $(1/\rho^2)$ caused by the dipoles should be taken into account while examining the beam circulation in the synchrotron design. During the matching process, MADX takes into account this situation, but it is a seamless to the user. For the completeness of the study, the beam circulation through a FODO cell is discussed and the determination of the transfer matrices of the magnets in a FODO cell is presented, taking into account the weak focusing.
In Fig. (12.1), a half FODO cell is presented:

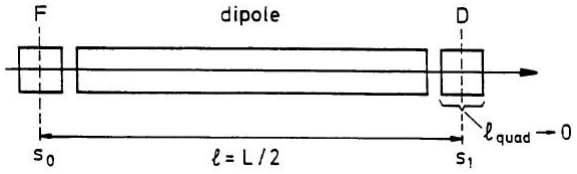

Figure 12.1: *Half FODO cell.*

As demonstrated in Chapter 2, the transfer matrix for a whole FODO cell is:

$$M(s_0) = \begin{pmatrix} 1 - \frac{2\rho^2}{f'^2} sin^2\theta & 2\rho sin\theta + \frac{2\rho^2}{f'} sin^2\theta \\ -\frac{2\rho}{f'^2} sin\theta + \frac{2\rho^2}{f'^3} sin^2\theta & 1 - \frac{2\rho}{f'^2} sin^2\theta \end{pmatrix}$$

This is obtained by multiplying the matrices of the focusing quadrupoles, the drift spaces, the dipoles and the defocusing quadrupoles:

$$M_F = \begin{pmatrix} 1 & 0 \\ -1/f & 1 \end{pmatrix}$$

$$M_{dip} = \begin{pmatrix} 1 & \rho sin\theta \\ 0 & 1 \end{pmatrix}$$

$$M_D = \begin{pmatrix} 1 & 0 \\ +1/f & 1 \end{pmatrix}$$

where f is the focal length of the quadrupoles, M_F is the transfer matrix for a focusing quadrupole, M_{dip} is the transfer matrix for a dipole magnet and M_D is the transfer matrix for a defocusing quadrupole. As already mentioned in Chapter (9), section (9.2), the focal length, f, for a focusing quadrupole is positive, whereas the focal length for a defocusing quadrupole is negative.
However, this approach refers to accelerators in the TeV range where from equation:
$B\rho = \beta E/0.2998$ (eq. (9.9))
it is clear that the bending radius ρ has a very large value since it increases proportionally with the particle energy E. Therefore, the value of $1/\rho^2$ which determines the weak focusing of the dipoles is negligible.
On the contrary, in medical accelerators, the weak focusing of the bending magnets cannot be neglected. These accelerators function in the MeV zone which means that ρ has a rather small value as well.

Taking into account the weak focusing, the transfer matrix for the dipole becomes:

$$M_{dip} = \begin{pmatrix} 1 & \rho sin\theta \\ -\sin\theta/\rho & 1 \end{pmatrix}$$

whereas the transfer matrices for the quadrupoles remain the same. The transfer matrix for the whole FODO cell for this case is:
$M = M_2 M_1$ where

$$M_1 = \begin{pmatrix} 1 & 0 \\ 1/f & 1 \end{pmatrix} \begin{pmatrix} 1 & \rho sin\theta \\ -\frac{\sin\theta}{\rho} & 1 \end{pmatrix} \begin{pmatrix} 1 & 0 \\ -1/f & 1 \end{pmatrix}$$

Which gives:

$$M_1 = \begin{pmatrix} 1 + \frac{\rho\sin\theta}{f} & \rho\sin\theta \\ -\frac{\sin\theta}{\rho} - \frac{\rho\sin\theta}{f^2} & 1 - \frac{\rho\sin\theta}{f} \end{pmatrix}$$

and

$$M_2 = \begin{pmatrix} 1 & 0 \\ -1/f & 1 \end{pmatrix} \begin{pmatrix} 1 & \rho sin\theta \\ -\sin\theta/\rho & 1 \end{pmatrix} \begin{pmatrix} 1 & 0 \\ 1/f & 1 \end{pmatrix}$$

Which gives:

$$M_2 = \begin{pmatrix} 1 - \frac{\rho\sin\theta}{f} & \rho\sin\theta \\ -\frac{\sin\theta}{\rho} - \frac{\rho\sin\theta}{f^2} & 1 + \frac{\rho\sin\theta}{f} \end{pmatrix}$$

Therefore, by multiplying M_2 with M_1 the transfer matrix for the whole FODO cell is obtained:

$$M = \begin{pmatrix} \rho\sin\theta(-\frac{\sin\theta}{\rho} - \frac{\sin\theta}{f^2}) + (1 - \frac{\sin\theta}{f})(1 + \frac{\sin\theta}{f}) & 2\rho\sin\theta(1 + \frac{\sin\theta}{f}) \\ 2(-\frac{\sin\theta}{\rho} - \frac{\sin\theta}{f^2})(1 - \frac{\sin\theta}{f}) & \rho\sin\theta(-\frac{\sin\theta}{\rho} - \frac{\sin\theta}{f^2}) + (1 - \frac{\sin\theta}{f})(1 + \frac{\sin\theta}{f}) \end{pmatrix}$$

The trace of M is expressed by: $Tr(M) = 2\rho\sin\theta(-\frac{\sin\theta}{\rho} - \frac{\rho\sin\theta}{f^2}) + 2(1 - \frac{\rho\sin\theta}{f})(1 + \frac{\rho\sin\theta}{f})$
Moreover, taking into account the dispersion and the drift spaces between the magnets, the transfer matrices become:

$$M_{Fd} = \begin{pmatrix} 1 & 0 & 0 \\ -1/f & 1 & 0 \\ 0 & 0 & 1 \end{pmatrix}$$

$$M_{Dd} = \begin{pmatrix} 1 & 0 & 0 \\ 1/f & 1 & 0 \\ 0 & 0 & 1 \end{pmatrix}$$

$$M_{dipd} = \begin{pmatrix} 1 & \rho\sin\theta & \rho(1-\cos\theta) \\ -\sin\theta/\rho & 1 & 2\tan\theta/2 \\ 0 & 0 & 1 \end{pmatrix}$$

$$M_{drift} = \begin{pmatrix} 1 & L/2 & 0 \\ 0 & 1 & 0 \\ 0 & 0 & 1 \end{pmatrix}$$

The transfer matrix for the half cell is:

$$M_d = \begin{pmatrix} A & B & C \\ D & E & F \\ 0 & 0 & 1 \end{pmatrix}$$

where:

$A = \frac{L(2f_f+L)L_d^3-2L_d(3L(2f_f+L)+2L_d^2)\rho^2+24(f_f+L+L_d)\rho^4}{24f_f\rho^4}$

$B = L + L_d - \frac{L_d^3}{(6\rho^2)} + + \frac{((L^2(L_d^3-\rho L_d\rho^2))}{(24\rho^4)}$

$C = \frac{(LL_d^3+12L_d(L+L_d)\rho^2)}{(24\rho^3)}$

$D = \frac{((2f_d+L)(2f_f+L)L_d^3-2L_d(3(2f_d+L)(2f_f+L)+2L_d^2)\rho^2+24(f_d+f_f+L+L_d)\rho^4)}{(24f_df_f\rho^4)}$

$E = \frac{(L(2f_d+L)L_d^3-2L_d(3L(2f_d+L)+2L_d^2)\rho^2+24(f_d+L+L_d)\rho^4)}{(24f_d\rho^4)}$

$F = \frac{((2f_d+L)L_d^3+12L_d(2f_d+L+L_d)\rho^2)}{(24f_d\rho^3)}$

and $f_f = 1/f$, $f_d = -1/f$ and $\theta = L_d/\rho$.

In this case a solution is difficult to be obtained due to the third order equations. Thus, the calculation of the phase advance, the beta functions and all the values that need to be defined in order to have a complete image of how the beam circulates through the accelerator, is possible by using MADX.

12.2 Stability Diagram

The stability of a FODO cell is a very important factor which depends on the strengths of the focusing and defocusing quadrupoles and the way they are related to the phase advance. The strengths of the focusing and defocusing quadrupole can be defined as :

$$\frac{l}{f_1'} = F \tag{12.1}$$

and

$$\frac{l}{f_2'} = D \tag{12.2}$$

respectively
where l is the quadrupole length and $1/f'$ is the strength of half quadrupole. The transformation matrix for the half FODO cell ($s_0 \rightarrow s_1$) is :

$$\begin{pmatrix} C & S \\ C' & S' \end{pmatrix} = \begin{pmatrix} \sqrt{\check{\beta}/\hat{\beta}}cos(\Delta\theta) & \sqrt{\hat{\beta}\check{\beta}}sin(\Delta\theta) \\ -\frac{1}{\sqrt{\hat{\beta}\check{\beta}}}sin(\Delta\theta) & \sqrt{\hat{\beta}/\check{\beta}}cos(\Delta\theta) \end{pmatrix}$$

where $\Delta\theta = \mu/2$ and μ is the phase advance.
For the horizontal motion the matrix above is equal to:

$$\begin{pmatrix} C & S \\ C' & S' \end{pmatrix} = \begin{pmatrix} 1-F & l \\ -\frac{(F-D+FD)}{l} & 1+D \end{pmatrix}$$

From this, we obtain:

$$-C'S = F - D + FD = sin^2\frac{\mu_x}{2} \tag{12.3}$$

$$D - F + FD = sin^2\frac{\mu_y}{2} \tag{12.4}$$

In an attempt to define the dependence of the quadrupole strengths on the phase advance, the phase advance was scanned in both, the horizontal and the vertical

plane from 0.24 to 0.38 rad. The program code written in MADX for the calculations of the quadrupole strengths for the different values of the phase advance, can be found in the Appendix (Table 3-Tableplot).

After calculations by using Mathematica, this dependence is demonstrated in Fig. (12.2) :

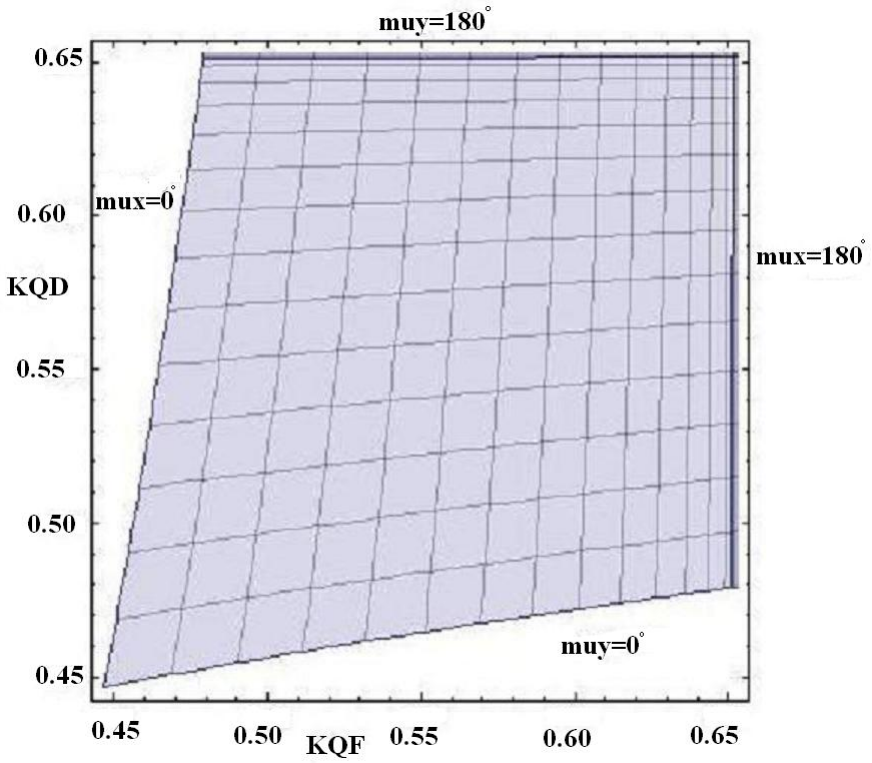

Figure 12.2: *Stability Diagram.*

The boundaries in the plot represent the horizontal and vertical phase advance, μ_x and μ_y respectively. The area between the two lines, is the stability region, that is to say, the values the quadrupole strengths can take in order for the lattice to be stable.
In addition to this, using Matlab, Fig. (12.3) and (12.4) demonstrate the evolution of the beta functions in both planes as the phase advance changes.

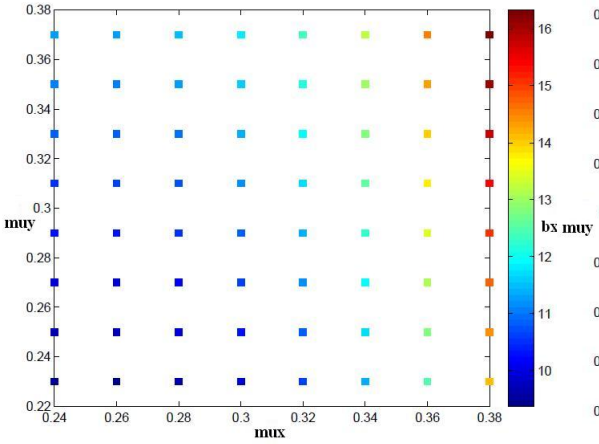

Figure 12.3: *The phase advance (mux, muy) with respect to the horizontal beta function (bx).*

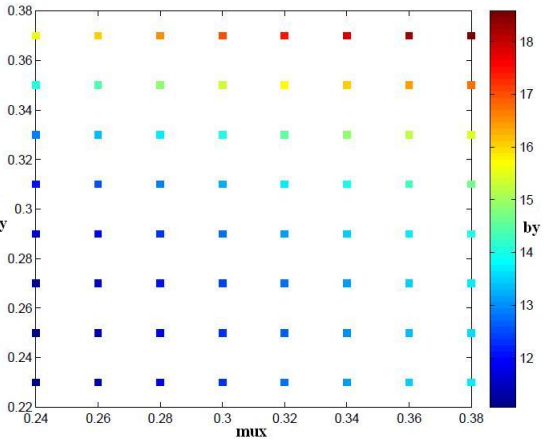

Figure 12.4: *The phase advance (mux, muy) with respect to the vertical beta function (by).*

As it can be observed in Fig. (12.3), the beta function (bx)in the horizontal plane increases with the horizontal phase advance (mux). The same happens for the beta function in the vertical plane, in Fig. (12.4).

Chapter 13

Conclusion

There are many factors that should be taken into account when designing an accelerator. Such factors are the output energy, the characteristics of the elements used, the magnetic field etc. Moreover, it is important to define the tune in order assure the stability of the lattice and to ensure the suppression of the dispersion so that the particles of the output beam travel without momentum deviation. Summarizing, the outcome of this approach, is a proton synchrotron with a circumference of 49.8 m and a maximum kinetic energy 300 MeV. The dipoles have a length of 1 m and produce a magnetic field of 1.06 Tesla which can be achieved with conventional magnets. The dispersion is successfully suppressed to zero for a phase advance of 90 degrees with the resonant lattice method. The maximum beta functions are approximately β_x= 6.2 mm in the horizontal plane and β_y= 7 mm in the vertical plane. The results can also be seen in the following Table:

Input Parameters	**Results**
Particles: Protons	
T=300 MeV	
N_{dip}=16	B=1.06 Tesla
L_{dip}=1 m	C=49.8 m
N_{quad}=24	Dispersion=0
L_{quad}=0.4 m	
μ_x=0.25, μ_y=0.23	

Figure 13.1: *Results*

However, concepts such as injection and extraction of the beam as well as analysis of the non-linear dynamics need to be examined, but exceed the purpose of

this study. As mentioned in the abstract, this project has been conducted in the framework of a bachelor thesis and therefore, due to time limitations, thorough investigation of this field has been difficult. This dissertation constitutes a preliminary stage of the design of a medical synchrotron where of course further research is needed.

Bibliography

[1] G. Cuttone, *Applications of Particle Accelerators in Medical Physics.* https://espace.cern.ch/partnersite/Bibliography

[2] Klaus Wille, *The Physics of Particle Accelerators, an introduction* . Oxford University Press Inc, New York, 1st Edition, 2000.

[3] Gerald Dugan, *Introduction to Accelerator Physics, lecture 1.* USPAS Jan. 2002
http://www.lns.cornell.edu/ dugan/USPAS/.

[4] S. Prestemon, P. Ferracin and E. Todesco, *Magnet Specifications in Circular Accelerators.* USPAS June 2007.

[5] David Robin, *Fundamental Accelerator Theory, Simulations and Measurement Lab, Lecture 3: Charged Particle Optics-Matrix Representation of the Accelerator Elements.* Michigan State University Lansing June 4-15, 2007.

[6] J. Rossbach, P. Schmuser *Basic Course on Accelerator Optics*
http://adweb.desy.de/ rossbach/uni/CERN.pdf.

[7] *CAS, CERN Accelerator School, Fifth General Accelerator Physics Course.* University of Jyvaskyla, Finland September 1992, S. Turner.

[8] Y. Papaphillippou, N. Catalan Casheras *Magnet design* USPAS, Cornell University, Ithaca, NY, 2005

[9] Y. Papaphillippou, N. Catalan Casheras *Phase space concepts* USPAS, Cornell University, Ithaca, NY, 2005.

[10] Helmut Wiedemann, *Particle Accelerator Physics.* Springer-Verlag 3rd Edition, 2007.

[11] http://mad.web.cern.ch/mad/

[12] E. J. N. Wilson, *An Introduction to Particle Accelerators*. Oxford University Press Inc, New York, 2001

[13] Gerald Dugan, *Introduction to Accelerator Physics, lecture 8*. USPAS Jan. 2002
http://www.lns.cornell.edu/ dugan/USPAS/.

[14] J. Wei, A. Fedotov, Y. Papaphilippou, *Physics and Design of High Intensity Circular Accelerators*. Brookhaven National Laboratory June 28, 2002
.

[15] W. Bartmann, M. Benedikt, C. Carli, B. Goddard, S. Hancock, J.M. Jowett, A. Koschik, Y. Papaphilipou, *Optics considerations for PS2*. Brookhaven National Laboratory October 4th, 2007
http://yannis.web.cern.ch/yannis/talks/PS2optics.pdf.

[16] H. Homeyer, Ch. Petit-Jean-Genaz, *EPAC 92, Berlin 24-28 March,1992, Volume 1*. Frontiers, 1992.

[17] M. Ikegami, Y. Iwashita, H. Souda, M. Tanabe, and A. Noda, *Electrostatic deflectors and dispersion suppressors: Their formulation and application to a storage ring*. PHYSICAL REVIEW SPECIAL TOPICS - ACCELERATORS AND BEAMS 8, 124001 (2005),

[18] Alex Chao, *A Handbook of Accelerator Physics and Engineering*. World Scientific Pub Co Inc 1999.

[19] W. Chou, *A SIMPLE TRANSITION-FREE LATTICE OF AN 8 GEV PROTON SYNCHROTRON* Fermilab, Batavia, IL 60510, U.S.A FERMILAB-CONF-09-175-AD

[20] Michael Benedikt, Johannes Gutleber, Marcus Palm, Werner Pirkl, Ulrich Dorda, Adrian Fabich,Wr. Neustadt, *Overview of the MedAustron Design and Technology Choices*
https://espace.cern.ch/be-dep/Lists/IPAC101/Attachments/99/Dorda-MOPEA020.pdf

[21] G.Zschornack, F.Grossmann, V.P.Ovsyannikov, A.Schwan, F.Ullmann, E.Tanke, P.Urschutz, *STATUS OF ELECTRON BEAM ION SOURCES FOR PARTICLE THERAPY*
http://www.dreebit.com/publications/$38_{Z}schornack_{1m}edicine.pdf$

Appendix

```
! FODO test
! March 2010
!*****************************

TITLE, 'FODOcell_MD';

BEAM, PARTICLE=PROTON,energy=1.238;
option,-echo -info;
Nb=12;         ! Number of dipoles
ang=2*pi/Nb;    ! Bending angle

LQ1=0.2;       ! Quadrupole length (half)
KQFA=0.5;
KQFB=1.2;      ! Quadrupole strength (focusing)
KQD3=-2;     ! Quadrupole strength (defocusing)
KQD=-2;
Ld1=0.5;       ! Drift length 1
Lb=1;          ! Dipole length

QFA: QUADRUPOLE, L=LQ1, K1 := KQFA;
QFB: QUADRUPOLE, L=LQ1, K1 := KQFB;
QD: QUADRUPOLE, L=LQ1, K1 := KQD;
QD3: QUADRUPOLE, L=LQ1, K1 := KQD3;
DIP1: SBEND, L=Lb, ANGLE=ang;

LFODO=LQ1+Ld1+Lb+Ld1+LQ1+LQ1+Ld1+Lb+Ld1+LQ1;
```

```
FODO1: SEQUENCE, L=LFODO;
  QF1:  QFA,    AT=LQ1/2;
  B1:   DIP1,   AT=LQ1+Ld1+Lb/2;
 !B2:   DIP1,  AT=LQ1+Ld1+Lb+Lb/2;
  QD1:  QD,     AT=LQ1+Ld1+Lb+Ld1+LQ1/2;
  QD2:  QD,     AT=LQ1+Ld1+Lb+Ld1+LQ1+LQ1/2;
  B3:   DIP1,   AT=LQ1+Ld1+Lb+Ld1+LQ1+LQ1+Ld1+Lb/2;
  !B4:  DIP1,  AT=LQ1+Ld1+Lb+Ld1+LQ1+LQ1+Ld1+Lb+Lb/2;
  QF2:  QFA,    AT=LQ1+Ld1+Lb+Ld1+LQ1+LQ1+Ld1+Lb+Ld1+LQ1/2;
ENDSEQUENCE;

FODO2: SEQUENCE, L=LFODO;
  QF12:  QFA,   AT=LQ1/2;
  B12:   DIP1,  AT=LQ1+Ld1+Lb/2;
  !B22:  DIP1,  AT=LQ1+Ld1+Lb+Lb/2;
  QD12:  QD3,    AT=LQ1+Ld1+Lb+Ld1+LQ1/2;
  QD22:  QD3,    AT=LQ1+Ld1+Lb+Ld1+LQ1+LQ1/2;
  QF22:  QFA,   AT=LQ1+Ld1+Lb+Ld1+LQ1+LQ1+Ld1+Lb+Ld1+LQ1/2;
ENDSEQUENCE;

FODO3: SEQUENCE, L=LFODO;
  QF13:   QFA,    AT=LQ1/2;
  QD13:   QD3,     AT=LQ1+Ld1+Lb+Ld1+LQ1/2;
```

```
 QD23:  QD3,    AT=LQ1+Ld1+Lb+Ld1+LQ1+LQ1/2;
 B33:   DIP1,   AT=LQ1+Ld1+Lb+Ld1+LQ1+LQ1+Ld1+Lb/2;
 !B43:  DIP1,   AT=LQ1+Ld1+Lb+Lb+Ld1+LQ1+LQ1+Ld1+Lb+Lb/2;
 QF23:  QFA,    AT=LQ1+Ld1+Lb+Ld1+LQ1+LQ1+Ld1+Lb+Ld1+LQ1/2;
ENDSEQUENCE;
ARC: SEQUENCE, REFER=START, L=4*LFODO;
   FODO2, AT=0;
   FODO1, AT=LFODO;
   FODO1, AT=2*LFODO;
   FODO3, AT=3*LFODO;
ENDSEQUENCE;
USE,sequence=FODO1;
USE,sequence=FODO2;
USE,sequence=FODO3;
USE,sequence=ARC;
select,flag=twiss,column=name,s,betx,bety,alfx,alfy,dx,dpx,mux,muy;
MATCH,SEQUENCE=FODO1;
 GLOBAL, q1=0.24, q2=0.24;
 VARY,NAME=KQFA,STEP=1E-6;
 VARY,NAME=KQD,STEP=1E-6;
 LMDIF,CALLS=500,TOLERANCE=1e-21;
 !JACOBIAN,CALLS=30,TOLERANCE=1e-21;
  ENDMATCH;

 twiss,sequence=FODO1,file=fodo1.dat;
 savebeta, label=fm,place=#e,sequence=FODO1;
 twiss, sequence=FODO1;
```

```
 show, fm;
plot,haxis=s,vaxis1=betx,bety,vaxis2=dx,colour=100;    !,interpolate=true;
plot,haxis=s,vaxis=mux,muy,colour=100;!,interpolate=true;
twiss,sequence=FODO3,beta0=fm,file=fodo3d.dat;
savebeta,label=bg,place=#e,sequence=FODO3;
twiss,sequence=FODO3,beta0=fm;
show, bg;
plot,haxis=s,vaxis1=betx,bety,vaxis2=dx,colour=100; !,interpolate=true;
plot,haxis=s,vaxis=mux,muy,colour=100;!,interpolate=true;

twiss,sequence=ARC;!,beta0=bg,dx=0,dpx=0,file=arc.dat;
plot,haxis=s,vaxis1=betx,bety,vaxis2=dx,colour=100;    !,interpolate=true;
plot,haxis=s,vaxis=mux,muy,colour=100;!,interpolate=true;
******
```

Fodo3d

Twiss Table which presents the evolution of the values of the beta functions (bx,by), the dispersion (dx) etc.
through FODO 3 of the Missing Dipole Lattice (Chapter 4).

```
@ NAME             %05s "TWISS"
@ TYPE             %05s "TWISS"
@ SEQUENCE         %05s "FODO3"
@ PARTICLE         %06s "PROTON"
@ MASS             %le         0.938272013
@ CHARGE           %le                   1
@ ENERGY           %le               1.238
@ PC               %le        0.8076444946
@ GAMMA            %le         1.319446795
@ KBUNCH           %le                   1
@ BCURRENT         %le                   0
@ SIGE             %le                   0
@ SIGT             %le                   0
@ NPART            %le                   0
@ EX               %le                   1
@ EY               %le                   1
@ ET               %le                   1
@ LENGTH           %le                 4.8
@ ALFA             %le                   0
@ ORBIT5           %le                   0
@ GAMMATR          %le                   0
@ Q1               %le        0.3708652855
@ Q2               %le        0.6960715079
@ DQ1              %le                   0
@ DQ2              %le                   0
@ DXMAX            %le         7.222574962
@ DYMAX            %le                   0
@ XCOMAX           %le                   0
@ YCOMAX           %le                   0
@ BETXMAX          %le         22.12352471
@ BETYMAX          %le          5.78501522
@ XCORMS           %le                   0
@ YCORMS           %le                   0
@ DXRMS            %le         5.342054569
@ DYRMS            %le                   0
@ DELTAP           %le                   0
@ SYNCH_1          %le                   0
@ SYNCH_2          %le                   0
@ SYNCH_3          %le                   0
@ SYNCH_4          %le                   0
@ SYNCH_5          %le                   0
@ TITLE            %04s "FODO"
@ ORIGIN           %19s "MAD-X 4.01.00 Linux"
@ DATE             %08s "13/02/11"
@ TIME             %08s "21.03.03"
```

* NAME	S	BETX	BETY	ALFX	ALFY	DX	DPX	MUX	MUY
$ %s	%le	%le	%le	%le	%le	%le	%le	%le	%le
"FODO3$START"	0	4.859741206	2.013256803	3.390082777e-16	-1.731788182e-16	4.341352978	-2.220446049e-16	0.24	0.24
"QF13"	0.2	4.748625599	2.083525496	0.550987352	-0.3542370118	4.287744308	-0.5349806645	0.2466007201	0.2556310938
"DRIFT_1"	2.2	3.642751442	5.661203254	0.001949726296	-1.434601867	3.217782979	-0.5349806645	0.3264409907	0.3545623602
"QD13"	2.4	3.952480687	5.78501522	-1.591674598	0.832139016	3.2389262	0.7478205441	0.3349461497	0.3600517427
"QD23"	2.6	4.985097469	5.030432874	-3.708362793	2.839621022	3.520915557	2.090847299	0.3422156518	0.3658752684
"DRIFT_0"	3.1	9.433262979	2.641242649	-5.187968226	1.938759429	4.566339206	2.090847299	0.353830349	0.3877758045
"B33"	4.1	18.35425434	0.5654469784	-2.902476002	0.1370362422	6.343392891	1.38168839	0.3653907828	0.5403108115
"DRIFT_0"	4.6	21.38509795	0.8788415328	-3.159211219	-0.763825351	7.034237086	1.38168839	0.3694078792	0.6658011032
"QF23"	4.8	22.12352471	1.28403224	-0.5024149016	-1.278813277	7.222574962	0.4978046502	0.3708652855	0.6960715079
"FODO3$END"	4.8	22.12352471	1.28403224	-0.5024149016	-1.278813277	7.222574962	0.4978046502	0.3708652855	0.6960715079

```
TITLE, 'FODOm';


BEAM, PARTICLE=PROTON,energy=1.238;

option,-echo -info;

Nb=16;         ! Number of dipoles

ang=2*pi/Nb;    ! Bending angle


KQFA=1.13677;       !Quadrupole strength (focusing)

KQFB=2.76554;

KQDA=-1.47329;        ! Quadrupole strength (defocusing)

KQDB=-1.9732;

LQ1=0.2;       ! Quadrupole length (half)

Ld1=0.5;       ! Drift length 1

Ld2=1.845;

Ld3=0.205;

Lb=1;          ! Dipole length

QFA: QUADRUPOLE, L=LQ1, K1 := KQFA;

QFB: QUADRUPOLE, L=LQ1, K1 := KQFB;

QDA:  QUADRUPOLE, L=LQ1, K1 := KQDA;

QDB: QUADRUPOLE, L=LQ1, K1 := KQDB;

DIP1: SBEND, L=Lb, ANGLE=ang;

LFODO=LQ1+Ld1+Lb+Ld1+LQ1+LQ1+Ld1+Lb+Ld1+LQ1;

LARC=4*LFODO;

LSTR=LQ1+Ld2+LQ1+LQ1+Ld3+LQ1+LQ1+Ld3+LQ1+LQ1+Ld2+LQ1;


FODO1: SEQUENCE, L=LFODO;

  QF1:  QFA,    AT=LQ1/2;
```

```
 B1:  DIP1,  AT=LQ1+Ld1+Lb/2;
 QD1:  QDA,    AT=LQ1+Ld1+Lb+Ld1+LQ1/2;
 QD2:  QDA,    AT=LQ1+Ld1+Lb+Ld1+LQ1+LQ1/2;
 B3:  DIP1,  AT=LQ1+Ld1+Lb+Ld1+LQ1+LQ1+Ld1+Lb/2;
 QF2:  QFA,   AT=LQ1+Ld1+Lb+Ld1+LQ1+LQ1+Ld1+Lb+Ld1+LQ1/2;
ENDSEQUENCE;

ARC: SEQUENCE, REFER=START, L=LARC;
   FODO1, AT=0;
   FODO1, AT=LFODO;
   FODO1, AT=2*LFODO;
   FODO1, AT=3*LFODO;
ENDSEQUENCE;

STR: SEQUENCE, L=LSTR;
   QFS1:  QFA,  AT=LQ1/2;
   QDS1a: QDB,  AT=LQ1+Ld2+LQ1/2;
   QDS1b: QDB,  AT=LQ1+Ld2+LQ1+LQ1/2;
   QFS2a: QFB,  AT=LQ1+Ld2+LQ1+LQ1+Ld3+LQ1/2;
   QFS2b: QFB,  AT=LQ1+Ld2+LQ1+LQ1+Ld3+LQ1+LQ1/2;
   QDS2a: QDB,  AT=LQ1+Ld2+LQ1+LQ1+Ld3+LQ1+LQ1+Ld3+LQ1/2;
   QDS2b: QDB,  AT=LQ1+Ld2+LQ1+LQ1+Ld3+LQ1+LQ1+Ld3+LQ1+LQ1/2;
   QFS3:  QFA,  AT=LQ1+Ld2+LQ1+LQ1+Ld3+LQ1+LQ1+Ld3+LQ1+LQ1+Ld2+LQ1/2;

ENDSEQUENCE;
HRING: SEQUENCE, REFER=START, L=LARC+LSTR;
     ARC, AT=0;
```

```
    STR, AT=LARC;
ENDSEQUENCE;




USE, sequence=FODO1;
USE, sequence=ARC;
USE, sequence=STR;
USE, sequence=HRING;

select,flag=twiss,column=name,s,betx,bety,alfx,alfy,dx,dpx,mux,muy,k1l,k2l;

create, table=RST2,column=mx,my,mix,miy,Qx,Qy,bxm,bym,Dx;!,KQFA,KQD,KQFB,KQDB;
create, table=KFD,column=KQFF,KQDF,KQFS,KQDS,mx,my;
create, table=match,column=mix,mx,my,miy;
create, table=mtbp,column=Qx,Qy,bxm,bym,mx,my;
test1(KQF,KQFF,i): macro={KQFA = table(KFD,KQFF,i);}
test2(KFD,KQDF,i): macro={KQD =  table(KFD,KQDF,i);}
test3(KFD,KQFS,i): macro={KQFB = table(KFD,KQFS,i);}
test4(KFD,KQDS,i): macro={KQDB = table(KFD,KQDS,i);}

i=1;
mx=0.225;
my=0.2;
while(mx<0.27)
{
  mx=0.005+mx;
```

```
 my=0.2;


if (mx>0.23 && my==0.2)
{
 exec,test1(KFD,KQFF,$i);
 exec,test2(KFD,KQDF,$i);
 exec,test3(KFD,KQFS,$i);
 exec,test4(KFD,KQDS,$i);
 value, KQFA;
 value, KQD;
 value, KQFB;
 value, KQDB;
 i=i+28;
}
 while(my<0.48)
{
 MATCH,SEQUENCE=FODO1;
 GLOBAL, q1=mx,q2=my;
 VARY,NAME=KQFA,STEP=1E-6;
 VARY,NAME=KQDA,STEP=1E-6;
 LMDIF,CALLS=500,TOLERANCE=1e-21;
 !JACOBIAN,CALLS=30,TOLERANCE=1e-21;
ENDMATCH;
savebeta, label=ef1,place=#s sequence=FODO1;
twiss,sequence=FODO1,file=fodo1.dat;
KQFF:=KQFA;
KQDF:=KQDA;
```

```
mix=table(summ,q1);

miy=table(summ,q2);

use,sequence=ARC;

select,flag=twiss,column=dx,dpx;


savebeta,label=boa,place=#s, sequence=ARC;

savebeta,label=eoa,place=#e, sequence=ARC;

twiss,sequence=ARC,beta0=ef1,dx=0,dpx=0,file=arc-rl.dat;

select,flag=twiss,clear;

twiss,sequence=ARC,beta0=ef1,dx=0,dpx=0,file=arc-rl.dat;


MATCH,SEQUENCE=HRING;

CONSTRAINT,SEQUENCE=HRING,range=#e,betx=boa->betx,bety=boa->bety;
VARY,NAME=KQFB,STEP=1E-6;

VARY,NAME=KQDB,STEP=1E-6;

LMDIF,CALLS=500,TOLERANCE=1e-21;

JACOBIAN,CALLS=30,TOLERANCE=1e-21;

ENDMATCH;


savebeta,label=eor,place=#e, sequence=HRING;

twiss,sequence=HRING;

select,flag=twiss,clear;

twiss,sequence=STR,beta0=eor,file=ster.dat;


Dx=table(summ,dxmax);

select,flag=twiss,clear;

twiss,sequence=HRING,file=hringb.dat;

KQFS:=KQFB;
```

```
KQDS:=KQDB;

Qx=table(summ,q1);

Qy=table(summ,q2);

bxm=table(summ,betxmax);

bym=table(summ,betymax);

plot,haxis=s,vaxis1=betx,bety,vaxis2=dx,colour=100; !,interpolate=true;

plot,haxis=s,vaxis=mux,muy,colour=100;!,interpolate=true;

savebeta,label=bos,place=#s, sequence=STR;

fill, table=KFD;

fill, table=RST2;

fill, table=match;

fill, table=mtbp;

my=my+0.01;

            }


           }

write,table=KFD,file=KFD;

write, table=match,file=match;

write,table=RST2,file=RST2;

write,table=mtbp,file=mtbp;

*******
```

Table 1-Fodo

Presents the variation of the quadrupole strengths in the Resonant Lattice,
caused by the change in the phase advance: 0.23<mx<0.27 and 0.2<my<0.48.
This is done to study the dispersion suppression in the resonants lattice (Chapter 11).

```
@ NAME             %03s "KFD"
@ TYPE             %04s "USER"
@ TITLE            %04s "FODO"
@ ORIGIN           %19s "MAD-X 4.01.00 Linux"
@ DATE             %08s "13/02/11"
@ TIME             %08s "21.02.39"
*               KQFF               KQDF               KQFS               KQDS                 MX                 MY
$                %le                %le                %le                %le                %le                %le
       0.9457146532       -1.190017458        2.858381018       -1.958352105               0.23                0.2
       0.9630860235       -1.241404207        2.657295103        -1.80602173               0.23               0.21
       0.9799662839       -1.292915015        2.685176327       -1.845563364               0.23               0.22
       0.9963242965       -1.344384983        2.712382382       -1.884586867               0.23               0.23
        1.012134929       -1.395652623        2.738819965       -1.922955868               0.23               0.24
        1.027378164       -1.446559459        2.764407008       -1.960543753               0.23               0.25
        1.042038331       -1.496949782        2.789072502       -1.997233713               0.23               0.26
        1.056103434       -1.546670507        2.812756262       -2.032918767               0.23               0.27
        1.069564576       -1.595571157        2.835408616       -2.067501741               0.23               0.28
         1.08241546       -1.643503921        2.856990009       -2.100895173               0.23               0.29
        1.094651951       -1.690323804        2.820881503       -2.084815763               0.23                0.3
        1.106271708        -1.73588884        2.853986585       -2.127138529               0.23               0.31
        1.117273859       -1.780060366        2.915053991       -2.193205217               0.23               0.32
        1.127658714       -1.822703339        2.932139802       -2.221152501               0.23               0.33
        1.137427534       -1.863686697        2.948088953       -2.247609787               0.23               0.34
         1.14658231       -1.902883747        2.962909714       -2.272541406               0.23               0.35
        1.155125586       -1.940172581        2.976615557       -2.295918506               0.23               0.36
        1.163060302       -1.975436497        2.989224258       -2.317718382               0.23               0.37
        1.170389658       -2.008564442        3.000757002       -2.337923775               0.23               0.38
        1.177116992       -2.039451444        3.011237487       -2.356522166               0.23               0.39
        1.183245683       -2.067999049        3.011237487       -2.356522166               0.23                0.4
        1.188779064       -2.094115738        3.029143879       -2.388867312               0.23               0.41
        1.193720344       -2.117717339        3.036622135       -2.402606436               0.23               0.42
        1.198072545       -2.138727406        3.043151311       -2.414722008               0.23               0.43
        1.201838449       -2.157077582         3.04875552       -2.425215072               0.23               0.44
        1.205020553       -2.172707922        3.053456899       -2.434087629               0.23               0.45
        1.207621027       -2.185567187        3.057275086       -2.441342168               0.23               0.46
         1.20964169       -2.195613096        3.060226771       -2.446981275               0.23               0.47
      0.9768192325       -1.200561811        2.855755257       -1.960090412              0.235                0.2
      0.9933623856       -1.251120506        2.659644699       -1.811471308              0.235               0.21
        1.009462832       -1.301851631        2.687012514          -1.850406              0.235               0.22
        1.025087225       -1.352588075        2.713738625       -1.888864202              0.235               0.23
        1.040208223       -1.403166139        2.739728453       -1.926707809              0.235               0.24
        1.054803649       -1.453425188        2.764898599       -1.963808423              0.235               0.25
        1.068855755       -1.503207431        2.789176688       -2.000047426              0.235               0.26
        1.082350569       -1.552357811        2.812501153       -2.035316031              0.235               0.27
         1.09527733       -1.600723985        2.834820937       -2.069515262              0.235               0.28
        1.107627996       -1.648156401        2.856095116       -2.102555884              0.235               0.29
         1.11939681        -1.69450844         2.82074462       -2.086967221              0.235                0.3
        1.130579925       -1.739636635        2.853110452        -2.12860865              0.235               0.31
        1.141175076       -1.783400934         2.91337621       -2.193975853              0.235               0.32
        1.151181298       -1.825665018        2.930243027       -2.221677042              0.235               0.33
        1.160598672       -1.866296654        2.945992141       -2.247910908              0.235               0.34
        1.169428118       -1.905168079        2.960630683       -2.272640301              0.235               0.35
        1.177671198       -1.942156408        2.974171051       -2.295834963              0.235               0.36
         1.18532996       -1.977144053         2.98663001       -2.317470857              0.235               0.37
        1.192406796       -2.010019158        2.998027804       -2.337529477              0.235               0.38
        1.198904314       -2.040676025        3.008387261       -2.355997138              0.235               0.39
        1.204825239       -2.069015551        3.008387261       -2.355997138              0.235                0.4
        1.210172317       -2.094945636        3.026090249       -2.388124752              0.235               0.41
        1.214948238       -2.118381594        3.033484756       -2.401775199              0.235               0.42
        1.219155569       -2.139246529         3.03994136       -2.413814391              0.235               0.43
        1.222796697       -2.157471692         3.04548367       -2.424242674              0.235               0.44
         1.22587378       -2.172996804        3.050133392       -2.433061438              0.235               0.45
        1.228388707       -2.185770346        3.053909802       -2.440272662              0.235               0.46
        1.230343067       -2.195749814        3.056829294       -2.445878513              0.235               0.47
        1.007753014       -1.210851899        2.853149583       -1.961811626               0.24                0.2
        1.023502871       -1.260617484        2.661848651       -1.816773476               0.24               0.21
        1.038853707       -1.310599151        2.688709441       -1.855118771               0.24               0.22
        1.053770601       -1.360628214        2.714959767       -1.893026183               0.24               0.23
        1.068224558       -1.410539319        2.740504124       -1.930356308               0.24               0.24
        1.082191726       -1.460170152         2.76525808       -1.966979342               0.24               0.25
        1.095652692        -1.50936126        2.789148158        -2.00277519               0.24               0.26
        1.108591867       -1.557955967        2.812111642        -2.03763354               0.24               0.27
        1.120996937       -1.605800378        2.834096296       -2.071453867               0.24               0.28
        1.132858382       -1.652743462        2.855059998       -2.104145375               0.24               0.29
        1.144169048       -1.698637208        2.820447239       -2.089034944               0.24                0.3
         1.15492378       -1.743336842        2.852081085       -2.130006331               0.24               0.31
        1.165119092       -1.786701094        2.911545674       -2.194681237               0.24               0.32
        1.174752885       -1.828592513        2.928188805       -2.222137082               0.24               0.33
        1.183824192       -1.868877823        2.943733094       -2.248147846               0.24               0.34
        1.192332963       -1.907428297        2.958184616       -2.272674991               0.24               0.35
        1.200279876       -1.944120167        2.971554761       -2.295686927               0.24               0.36
        1.207666167        -1.97883504        2.983859348       -2.317158356               0.24               0.37
        1.214493486       -2.011460322         2.99511773       -2.337069577               0.24               0.38
        1.220763773       -2.041889654        3.005351912       -2.355405792               0.24               0.39
        1.226479148       -2.070023329        3.005351912       -2.355405792               0.24                0.4
        1.231641814       -2.095768715        3.022843802       -2.387314324               0.24               0.41
        1.236253982       -2.119040646        3.030151178       -2.400875325               0.24               0.42
        1.240317793       -2.139761807        3.036532171       -2.412837411               0.24               0.43
        1.243835264       -2.157863085        3.042009909       -2.423200243               0.24               0.44
        1.246808239       -2.173283888        3.046605683       -2.431964624               0.24               0.45
        1.249238343       -2.185972437        3.050338422       -2.439132031               0.24               0.46
        1.251126948       -2.195886016        3.053224239       -2.444704224               0.24               0.47
        1.038498999        -1.22089087         2.85054951       -1.963508114              0.245                0.2
         1.05348863       -1.269896436         2.66389958       -1.821925687              0.245               0.21
        1.068118688         -1.3191575         2.69025895       -1.859698254              0.245               0.22
        1.082353213       -1.368504335        2.716037014       -1.897068751              0.245               0.23
        1.096162031       -1.417770404        2.741137644       -1.933896849              0.245               0.24
        1.109520024       -1.466792128        2.765475653       -1.970051674              0.245               0.25
        1.122406483       -1.515408756        2.788976705       -2.005411948              0.245               0.26
        1.134804519       -1.563462312         2.81157715       -2.039866094              0.245               0.27
         1.14670054       -1.610797623        2.833223761       -2.073312264              0.245               0.28
        1.158083788       -1.657262422        2.853873391       -2.105658298              0.245               0.29
        1.168945922       -1.702707514        2.819977901       -2.091013489              0.245                0.3
         1.17928066       -1.746986996        2.850886663       -2.131326101              0.245               0.31
        1.189083451       -1.789958538        2.909550179       -2.195315977              0.245               0.32
        1.198351197       -1.831483695        2.925964631       -2.222527231              0.245               0.33
           1.207082       -1.871428262        2.941299013       -2.248315217              0.245               0.34
        1.215274947       -1.909662652        2.955558424       -2.272640096              0.245               0.35
        1.222929914       -1.946062302         2.96875332       -2.295469023              0.245               0.36
        1.230047402       -1.980508087        2.980898632        -2.3167755              0.245               0.37
        1.236628389       -2.012886747         2.99201288       -2.336538695              0.245               0.38
        1.242674201       -2.043091313        3.002117293       -2.354742743              0.245               0.39
        1.248186402       -2.071021529        3.002117293       -2.354742743              0.245                0.4
        1.253166698       -2.096584266         3.01938994       -2.386430628              0.245               0.41
        1.257616851        -2.11969392        3.026606601       -2.399901406              0.245               0.42
         1.26153861       -2.140272787        3.032908765       -2.411785646              0.245               0.43
         1.26493365       -2.158251413        3.038319098       -2.422082349              0.245               0.44
         1.26780352       -2.173568916        3.042858498       -2.430791744              0.245               0.45
        1.270149596       -2.186173276        3.046545561       -2.437914824              0.245               0.46
        1.271973054       -2.196021577        3.049396128       -2.443452953              0.245               0.47
        1.069040011       -1.230681818        2.847940235        -1.96517229               0.25                0.2
        1.083300777       -1.278958748        2.665789615       -1.826925278               0.25               0.21
         1.09723761       -1.327526785        2.691652357       -1.864140935               0.25               0.22
        1.110813958       -1.376215606        2.716960996       -1.900987753               0.25               0.23
        1.123998865        -1.42485789        2.741619056       -1.937324811               0.25               0.24
         1.13676631       -1.473289155        2.765540841       -1.973020456               0.25               0.25
        1.149094602       -1.521347667        2.788651383       -2.007952492               0.25               0.26
        1.160965835        -1.56887443        2.810886296        -2.04200831               0.25               0.27
        1.172365385       -1.615713242        2.832191547       -2.075084945               0.25               0.28
        1.183281471       -1.661710814        2.852523124       -2.107089062               0.25               0.29
        1.193704757       -1.706716955         2.81932428       -2.092897204               0.25                0.3
```

1.203627998	-1.750584804	2.849514412	-2.132562221	0.25	0.31
1.213045723	-1.793171113	2.907376459	-2.195874354	0.25	0.32
1.221953962	-1.834336567	2.923556891	-2.222841749	0.25	0.33
1.230349995	-1.873946144	2.938675945	-2.248407263	0.25	0.34
1.238232141	-1.911869492	2.952737824	-2.27252984	0.25	0.35
1.24559956	-1.947981338	2.965752123	-2.295175457	0.25	0.36
1.25245209	-1.982161896	2.977732948	-2.316316483	0.25	0.37
1.258790098	-2.014297303	2.988698044	-2.335931006	0.25	0.38
1.264614352	-2.044280035	2.998667913	-2.354002145	0.25	0.39
1.269925908	-2.072009333	2.998667913	-2.354002145	0.25	0.4
1.274726012	-2.097391615	3.015712668	-2.385467778	0.25	0.41
1.279016017	-2.12034087	3.022834809	-2.398847536	0.25	0.42
1.282797308	-2.140779035	3.029054724	-2.410653172	0.25	0.43
1.286071242	-2.158636343	3.034394643	-2.420883049	0.25	0.44
1.288839093	-2.173851643	3.038875089	-2.429536841	0.25	0.45
1.291102011	-2.186372686	3.042514343	-2.43661507	0.25	0.46
1.292860981	-2.196156375	3.04532799	-2.442118714	0.25	0.47
1.099358713	-1.240227787	2.845306539	-1.966796573	0.255	0.2
1.112920395	-1.287805885	2.667510311	-1.831769436	0.255	0.21
1.12619036	-1.335707274	2.692880369	-1.868443167	0.255	0.22
1.139131831	-1.383761404	2.717721688	-1.904778909	0.255	0.23
1.151713412	-1.431800512	2.741937689	-1.94063543	0.255	0.24
1.163908486	-1.479659517	2.765442395	-1.975880561	0.255	0.25
1.175694659	-1.527175981	2.788160412	-2.010391421	0.255	0.26
1.18705325	-1.574190137	2.810026808	-2.044054581	0.255	0.27
1.197968827	-1.620544971	2.830986914	-2.076766154	0.255	0.28
1.208428782	-1.666086368	2.850996006	-2.108431794	0.255	0.29
1.218422952	-1.710663313	2.818473065	-2.094680179	0.255	0.3
1.227943283	-1.754128137	2.847950484	-2.133708644	0.255	0.31
1.236983516	-1.796336808	2.905010062	-2.19635028	0.255	0.32
1.245538928	-1.83714926	2.920950733	-2.223074498	0.255	0.33
1.25360608	-1.876429754	2.935848648	-2.248417803	0.255	0.34
1.261182609	-1.914047265	2.949707198	-2.272338004	0.255	0.35
1.268267041	-1.949875884	2.962535186	-2.294799973	0.255	0.36
1.274858618	-1.98379524	2.974345965	-2.31577501	0.255	0.37
1.280957158	-2.01569092	2.985156558	-2.335240181	0.255	0.38
1.286562922	-2.045454901	2.994986794	-2.353177636	0.255	0.39
1.291676503	-2.072985966	2.994986794	-2.353177636	0.255	0.4
1.296298728	-2.098190117	3.011794435	-2.384419344	0.255	0.41
1.300430572	-2.120980972	3.018818001	-2.397707253	0.255	0.42
1.304073087	-2.141280137	3.024952022	-2.409433498	0.255	0.43
1.307227334	-2.159017556	3.03021832	-2.419595826	0.255	0.44
1.309894335	-2.174131828	3.034637064	-2.428193374	0.255	0.45
1.312075027	-2.186570495	3.038226236	-2.435226208	0.255	0.46
1.313770224	-2.19629029	3.041001181	-2.440694933	0.255	0.47
1.129437625	-1.24953177	2.842632685	-1.968373336	0.26	0.2
1.142328546	-1.29643938	2.669052573	-1.836455164	0.26	0.21
1.154956879	-1.343699378	2.693932999	-1.872601136	0.26	0.22
1.167285931	-1.391141297	2.718308314	-1.908437765	0.26	0.23
1.179284152	-1.438597217	2.742082062	-1.943823757	0.26	0.24
1.190924592	-1.485901723	2.765168192	-1.978626653	0.26	0.25
1.202184395	-1.532891913	2.787491071	-2.012723097	0.26	0.26
1.213044326	-1.579407465	2.808985404	-2.045999036	0.26	0.27
1.223488337	-1.62529075	2.829596042	-2.07834983	0.26	0.28
1.233503169	-1.670387003	2.849277706	-2.109680285	0.26	0.29
1.243077989	-1.71454454	2.817409838	-2.096356197	0.26	0.3
1.25220407	-1.757615022	2.846179828	-2.134758958	0.26	0.31
1.26087449	-1.799453754	2.902435206	-2.19673724	0.26	0.32
1.269083879	-1.839920028	2.918129921	-2.223218891	0.26	0.33
1.276828174	-1.878877485	2.932800443	-2.24834018	0.26	0.34
1.284104419	-1.916194509	2.946449436	-2.272057868	0.26	0.35
1.290910574	-1.951744632	2.95908499	-2.294335792	0.26	0.36
1.297245355	-1.985406957	2.970719765	-2.315144245	0.26	0.37
1.303108085	-2.017066586	2.981370128	-2.334459328	0.26	0.38
1.308498568	-2.04661504	2.991055286	-2.352262271	0.26	0.39
1.313416977	-2.073950689	2.991055286	-2.352262271	0.26	0.4
1.317863759	-2.098979159	3.007615956	-2.383278287	0.26	0.41
1.321839543	-2.121613726	3.014536611	-2.396473474	0.26	0.42
1.325345074	-2.141775696	3.020580844	-2.4081195	0.26	0.43
1.328381144	-2.159394744	3.025770092	-2.41821352	0.26	0.44
1.330948542	-2.174409242	3.030124195	-2.426754151	0.26	0.45
1.333048006	-2.186766538	3.033660856	-2.433741021	0.26	0.46
1.334680192	-2.196423207	3.036395193	-2.439174371	0.26	0.47
1.159259147	-1.258596704	2.839902297	-1.969894855	0.265	0.2
1.171506278	-1.304860819	2.670406565	-1.840979241	0.265	0.21
1.183517166	-1.351503636	2.694799465	-1.876610815	0.265	0.22
1.195255457	-1.398355024	2.718709248	-1.911959651	0.265	0.23
1.206689688	-1.445247149	2.742039776	-1.946884606	0.265	0.24
1.217792803	-1.492014486	2.764705115	-1.981253134	0.265	0.25
1.228541692	-1.538493881	2.786629576	-2.014941595	0.265	0.26
1.238916757	-1.584524647	2.807747662	-2.04783548	0.265	0.27
1.248901509	-1.629948712	2.828003906	-2.079829563	0.265	0.28
1.258482192	-1.674610817	2.847352611	-2.110827944	0.265	0.29
1.267647445	-1.718358752	2.816118921	-2.097918677	0.265	0.3
1.276387994	-1.761043631	2.84418604	-2.135706335	0.265	0.31
1.284696368	-1.802520212	2.899634625	-2.197028239	0.265	0.32
1.292566646	-1.842647242	2.915076667	-2.223267825	0.265	0.33
1.299994235	-1.881287832	2.92951304	-2.248167199	0.265	0.34
1.30697566	-1.918309853	2.942945764	-2.271682147	0.265	0.35
1.313508388	-1.953586347	2.95538229	-2.293775543	0.265	0.36
1.319590667	-1.986995955	2.966834659	-2.314416739	0.265	0.37
1.32522138	-2.018423341	2.97731864	-2.333580923	0.265	0.38
1.330399922	-2.047759625	2.986852875	-2.351248456	0.265	0.39
1.335126089	-2.074902802	2.986852875	-2.351248456	0.265	0.4
1.33939998	-2.099758157	3.003155998	-2.382036881	0.265	0.41
1.343221913	-2.122238657	3.009969094	-2.395138416	0.265	0.42
1.34659235	-2.142265331	3.015919361	-2.406703345	0.265	0.43
1.349511837	-2.159767613	3.021027884	-2.41672825	0.265	0.44
1.35198095	-2.174683664	3.025314196	-2.425211253	0.265	0.45
1.354000246	-2.186960654	3.028795742	-2.432151554	0.265	0.46
1.355570231	-2.196555012	3.031487429	-2.437549048	0.265	0.47
1.188805577	-1.267425477	2.837098238	-1.971353255	0.27	0.2
1.200434636	-1.313071836	2.6715616	-1.845338183	0.27	0.21
1.211851285	-1.359120699	2.69546808	-1.880467919	0.27	0.22
1.223019715	-1.405402479	2.718911886	-1.91533963	0.27	0.23
1.233908755	-1.45174963	2.741797383	-1.949812507	0.27	0.24
1.244491436	-1.497996713	2.764038927	-1.983754098	0.27	0.25
1.254744575	-1.543980499	2.785560939	-2.017040643	0.27	0.26
1.264648378	-1.589540103	2.80629788	-2.049557344	0.27	0.27
1.274186065	-1.634517166	2.826194114	-2.081198526	0.27	0.28
1.283343528	-1.678756075	2.845203665	-2.111867727	0.27	0.29
1.292109003	-1.722104218	2.814583217	-2.099360612	0.27	0.3
1.300472783	-1.764412279	2.841951192	-2.136543465	0.27	0.31
1.30842695	-1.80553457	2.896589385	-2.197215731	0.27	0.32
1.315965128	-1.845329387	2.911771447	-2.223213619	0.27	0.33
1.32308227	-1.883659391	2.925966342	-2.247891049	0.27	0.34
1.32977446	-1.920392013	2.939175532	-2.271202913	0.27	0.35
1.336038736	-1.955399872	2.95140591	-2.29311119	0.27	0.36
1.341872935	-1.988561202	2.962668965	-2.313584351	0.27	0.37
1.347275551	-2.019760284	2.972979935	-2.332596728	0.27	0.38
1.352245616	-2.048887877	2.982356953	-2.350127859	0.27	0.39
1.356782587	-2.075841642	2.982356953	-2.350127859	0.27	0.4
1.360886249	-2.100526557	2.998391148	-2.38068663	0.27	0.41
1.364556639	-2.122855311	3.005091685	-2.393693511	0.27	0.42
1.367793964	-2.142748682	3.010943494	-2.405176397	0.27	0.43
1.370598544	-2.160135883	3.01596734	-2.415131324	0.27	0.44
1.372970759	-2.174954883	3.020182474	-2.423555935	0.27	0.45
1.374911001	-2.187152689	3.023606105	-2.430449022	0.27	0.46
1.376419641	-2.196685597	3.026252946	-2.435810145	0.27	0.47

Table 2-rst2

Presents the variation of the Tune(Qx,Qy), the maximum beta functions (Bxm,Bym)
and the dispersion (Dx)in the Resonant Lattice,
caused by the change in the phase advance: 0.23<mx<0.27 and 0.2<my<0.48.
This is done to study the dispersion suppression in the resonant lattice (Chapter 11).

@ NAME %04s "RST2"
@ TYPE %04s "USER"
@ TITLE %04s "FODO"
@ ORIGIN %19s "MAD-X 4.01.00 Linux"
@ DATE %08s "13/02/11"
@ TIME %08s "21.02.39"

* MX	MY	MIX	MIY	QX	QY	BXM	BYM	DX
$ %le	%le	%le	%le	%le	%le	%le	%le	%le
0.23	0.2	0.23	0.2	1.146416873	1.062161348	5.777938659	12.44045238	1.587311512
0.23	0.21	0.23	0.21	1.147750212	1.081466039	5.875816536	6.9523354	1.583629544
0.23	0.22	0.23	0.22	1.147361904	1.13195914	5.974173433	6.880945187	1.604623435
0.23	0.23	0.23	0.23	1.14697114	1.182327875	6.07269531	6.836835382	1.625820092
0.23	0.24	0.23	0.24	1.14657954	1.232569768	6.171071568	6.818941209	1.647148867
0.23	0.25	0.23	0.25	1.146188711	1.282682864	6.268994378	6.826748796	1.668537658
0.23	0.26	0.23	0.26	1.145800237	1.332665773	6.366158305	6.860263712	1.689912992
0.23	0.27	0.23	0.27	1.145415668	1.382517699	6.462260162	6.92000558	1.711200172
0.23	0.28	0.23	0.28	1.145036517	1.432238478	6.556999103	7.007028067	1.732323475
0.23	0.29	0.23	0.29	1.144664246	1.481828589	6.6500769	7.122965863	1.75320641
0.23	0.3	0.23	0.3	1.144766779	1.516268958	6.741198413	12.23923375	1.766247942
0.23	0.31	0.23	0.31	1.144301487	1.571073062	6.830072196	7.85637328	1.788131169
0.23	0.32	0.23	0.32	1.143602456	1.629829542	6.916411249	7.671256926	1.813642978
0.23	0.33	0.23	0.33	1.143271123	1.67891485	6.999933884	7.934458591	1.832795163
0.23	0.34	0.23	0.34	1.142953038	1.727881608	7.080364677	8.247846292	1.851324429
0.23	0.35	0.23	0.35	1.14264926	1.776734071	7.157435509	8.620104833	1.869156902
0.23	0.36	0.23	0.36	1.142360771	1.825477036	7.230886664	9.062581122	1.886220541
0.23	0.37	0.23	0.37	1.142088478	1.8741158	7.300467964	9.590282717	1.902445555
0.23	0.38	0.23	0.38	1.141833212	1.92265612	7.365939942	10.2233802	1.91776482
0.23	0.39	0.23	0.39	1.14159573	1.971104169	7.427075008	10.9895331	1.932114287
0.23	0.4	0.23	0.4	1.143016809	2.006001352	7.57005694	33.59029357	1.890560969
0.23	0.41	0.23	0.41	1.141176792	2.067749958	7.535490449	13.09392598	1.957665359
0.23	0.42	0.23	0.42	1.140996498	2.115961733	7.582385432	14.57306626	1.968757717
0.23	0.43	0.23	0.43	1.140836319	2.164109221	7.624174879	16.49813538	1.97866248
0.23	0.44	0.23	0.44	1.140696673	2.212200041	7.660707429	19.09113177	1.987336541
0.23	0.45	0.23	0.45	1.140577919	2.260241987	7.691849954	22.75183598	1.994741937
0.23	0.46	0.23	0.46	1.140480355	2.308242999	7.717488371	28.28002218	2.000846103
0.23	0.47	0.23	0.47	1.140404225	2.356211132	7.737528345	37.54209656	2.005622088
0.235	0.2	0.235	0.2	1.171277126	1.06146843	5.771672685	12.56805286	0.988465873
0.235	0.21	0.235	0.21	1.172622126	1.081166568	5.867686283	7.021529233	0.9872163318
0.235	0.22	0.235	0.22	1.172226221	1.131661121	5.964261885	6.947468296	0.999834849
0.235	0.23	0.235	0.23	1.171827609	1.182032294	6.061082827	6.90111018	1.012575978
0.235	0.24	0.235	0.24	1.171427954	1.232277577	6.15783588	6.881349211	1.025396498
0.235	0.25	0.235	0.25	1.171028907	1.282394979	6.254210674	6.887639708	1.038252427
0.235	0.26	0.235	0.26	1.170632099	1.332383073	6.349899374	6.919963293	1.051099067
0.235	0.27	0.235	0.27	1.170239129	1.382241029	6.444596572	6.978822669	1.063891097
0.235	0.28	0.235	0.28	1.169851554	1.431968644	6.537999397	7.065261094	1.076582691
0.235	0.29	0.235	0.29	1.169470882	1.481566355	6.629807808	7.180909155	1.089127661
0.235	0.3	0.235	0.3	1.169572242	1.516141134	6.719725049	12.33469445	1.097263879
0.235	0.31	0.235	0.31	1.169098938	1.570861146	6.807458264	7.917801448	1.110321473
0.235	0.32	0.235	0.32	1.16838448	1.629594283	6.892719231	7.730154884	1.125419341
0.235	0.33	0.235	0.33	1.168045282	1.678689825	6.975225212	7.994339942	1.136915206
0.235	0.34	0.235	0.34	1.167719569	1.727667364	7.054699903	8.309095966	1.148034794
0.235	0.35	0.235	0.35	1.167408437	1.776531109	7.13087445	8.683158334	1.158733966
0.235	0.36	0.235	0.36	1.167112904	1.825285811	7.203488534	9.127942747	1.168969733
0.235	0.37	0.235	0.37	1.166833909	1.873936726	7.272291493	9.65855022	1.178700493
0.235	0.38	0.235	0.38	1.166572316	1.922489567	7.337043478	10.29527922	1.187886277
0.235	0.39	0.235	0.39	1.166328909	1.970950466	7.397516608	11.06596677	1.196488982
0.235	0.4	0.235	0.4	1.167697574	2.005717563	7.529157261	35.24519186	1.175260633
0.235	0.41	0.235	0.41	1.165899432	2.067622796	7.504781542	13.18325904	1.211803427
0.235	0.42	0.235	0.42	1.165714569	2.115848188	7.551187698	14.67168249	1.218450297
0.235	0.43	0.235	0.43	1.165550314	2.164009485	7.592545839	16.60897859	1.224384748
0.235	0.44	0.235	0.44	1.165407102	2.212114273	7.628704572	19.21860019	1.229581219
0.235	0.45	0.235	0.45	1.165285307	2.260170321	7.659530761	22.90294923	1.234017212
0.235	0.46	0.235	0.46	1.165185238	2.308185542	7.684910329	28.46704653	1.23767343
0.235	0.47	0.235	0.47	1.165107149	2.356167967	7.704748951	37.78954536	1.240533913
0.24	0.2	0.24	0.2	1.196132757	1.060793873	5.770631288	12.69514133	0.5597602543
0.24	0.21	0.24	0.21	1.197489677	1.080873324	5.864949894	7.09051223	0.5594705458
0.24	0.22	0.24	0.22	1.197086012	1.131368903	5.959905083	7.013846554	0.5664082816
0.24	0.23	0.24	0.23	1.196679389	1.181742102	6.055178403	6.965295351	0.5734148377
0.24	0.24	0.24	0.24	1.196271519	1.231990378	6.15045469	6.943714187	0.5804660753
0.24	0.25	0.24	0.25	1.195864098	1.282111705	6.245421599	6.948527293	0.5875374737
0.24	0.26	0.24	0.26	1.195458802	1.332104622	6.339769345	6.979693739	0.5946041605
0.24	0.27	0.24	0.27	1.195057277	1.381968261	6.433190654	7.037700449	0.6016409606
0.24	0.28	0.24	0.28	1.194661126	1.431702381	6.525380895	7.123581215	0.6086224621
0.24	0.29	0.24	0.29	1.194271904	1.481307381	6.616038401	7.238963313	0.6155230957
0.24	0.3	0.24	0.3	1.194372025	1.516014708	6.70486493	12.43040103	0.6201246421
0.24	0.31	0.24	0.31	1.19389061	1.570651495	6.791566287	7.979391085	0.6272703843
0.24	0.32	0.24	0.32	1.193160455	1.629361447	6.875853053	7.78922563	0.6354837683
0.24	0.33	0.24	0.33	1.192813253	1.678466981	6.957441436	8.054413405	0.6418055633
0.24	0.34	0.24	0.34	1.192479776	1.727455072	7.036054204	8.370557258	0.6479198765
0.24	0.35	0.24	0.35	1.192161159	1.776329888	7.111421704	8.746443658	0.6538024558
0.24	0.36	0.24	0.36	1.191858456	1.825096133	7.183282929	9.193557665	0.6594297015
0.24	0.37	0.24	0.37	1.191572641	1.873759017	7.251386636	9.727094406	0.6647787961
0.24	0.38	0.24	0.38	1.191304606	1.922324213	7.315492483	10.36748103	0.6698278325
0.24	0.39	0.24	0.39	1.191055168	1.970797811	7.375372182	11.14273309	0.6745559398
0.24	0.4	0.24	0.4	1.192373221	2.005424938	7.499055714	37.1326358	0.6644947915
0.24	0.41	0.24	0.41	1.190614961	2.067496414	7.481607102	13.27300178	0.6829717961
0.24	0.42	0.24	0.42	1.190425445	2.11573531	7.527576188	14.77076036	0.6866240611
0.24	0.43	0.24	0.43	1.19025704	2.163910308	7.568548974	16.72034979	0.6898846454
0.24	0.44	0.24	0.44	1.190110197	2.212028968	7.604373935	19.34668469	0.6927395818
0.24	0.45	0.24	0.45	1.189985305	2.260099028	7.634917835	23.05480159	0.6951765793
0.24	0.46	0.24	0.46	1.189882685	2.308128375	7.660066522	28.65499435	0.6971851012
0.24	0.47	0.24	0.47	1.189802602	2.356125016	7.679725618	38.03822487	0.6987564321
0.245	0.2	0.245	0.2	1.22098359	1.0601372	5.774798213	12.8216448	0.2419804769
0.245	0.21	0.245	0.21	1.222352743	1.080586261	5.867581729	7.159239869	0.2419865344
0.245	0.22	0.245	0.22	1.221941137	1.131082475	5.961069164	7.08003325	0.2449105284
0.245	0.23	0.245	0.23	1.221526329	1.18145732	6.054940909	7.029342654	0.2478643626
0.245	0.24	0.245	0.24	1.221110069	1.231708217	6.1488804	7.005986816	0.2508377206
0.245	0.25	0.245	0.25	1.220694102	1.281833109	6.242573753	7.009361438	0.2538201339
0.245	0.26	0.245	0.26	1.220280149	1.331830501	6.335709584	7.039404314	0.2568009966
0.245	0.27	0.245	0.27	1.2198699	1.38169949	6.427979016	7.096587635	0.2597695865
0.245	0.28	0.245	0.28	1.219465008	1.431439795	6.519075862	7.181936598	0.2627150933
0.245	0.29	0.245	0.29	1.219067071	1.481051779	6.608696961	7.2970759	0.2656266525
0.245	0.3	0.245	0.3	1.219165895	1.515889742	6.696542672	12.52626854	0.2676094252
0.245	0.31	0.245	0.31	1.218676253	1.570444216	6.782317496	8.041085232	0.2706122604
0.245	0.32	0.245	0.32	1.2179301	1.629131159	6.865730818	7.848414066	0.2740490331
0.245	0.33	0.245	0.33	1.217574743	1.678246437	6.946497755	8.114622559	0.27671652
0.245	0.34	0.245	0.34	1.217233356	1.727244853	7.024340095	8.43217212	0.2792964206
0.245	0.35	0.245	0.35	1.216907114	1.776130523	7.098987302	8.809900763	0.2817784866
0.245	0.36	0.245	0.36	1.216597105	1.824908111	7.170177586	9.259363395	0.2841527523
0.245	0.37	0.245	0.37	1.216304339	1.87358278	7.237659012	9.795849812	0.2864095879
0.245	0.38	0.245	0.38	1.216029741	1.922160159	7.301190631	10.43991652	0.2885397531
0.245	0.39	0.245	0.39	1.215774156	1.970646297	7.36054363	11.21975844	0.290534449
0.245	0.4	0.245	0.4	1.217043426	2.005122071	7.47862121	39.31297203	0.2868416913
0.245	0.41	0.245	0.41	1.215323013	2.067370893	7.465865965	13.3630679	0.2940847478
0.245	0.42	0.245	0.42	1.215128755	2.115623167	7.511448442	14.87020451	0.2956254065
0.245	0.43	0.245	0.43	1.21495612	2.163811754	7.552080683	16.83214169	0.2970007968
0.245	0.44	0.245	0.44	1.214805576	2.21194418	7.58761093	19.47526178	0.298205041
0.245	0.45	0.245	0.45	1.214677525	2.260028154	7.617905753	23.20724659	0.2992329679
0.245	0.46	0.245	0.46	1.214572306	2.308071536	7.642850847	28.84368434	0.3000801451
0.245	0.47	0.245	0.47	1.214490189	2.356082306	7.662351713	38.28789513	0.3007429071
0.25	0.2	0.25	0.2	1.245829436	1.059497951	5.78418246	12.94748915	3.820054293e-15
0.25	0.21	0.25	0.21	1.24721119	1.080305328	5.875582586	7.227667305	2.174463541e-13
0.25	0.22	0.25	0.22	1.24679145	1.130801819	5.967747723	7.145981538	1.556837982e-13
0.25	0.23	0.25	0.23	1.246368264	1.181177955	6.060357583	7.093203826	7.855770768e-14
0.25	0.24	0.25	0.24	1.245943427	1.231431126	6.153094599	7.068117807	3.332801218e-14
0.25	0.25	0.25	0.25	1.245518727	1.281559245	6.245643675	7.070092077	1.650104671e-13
0.25	0.26	0.25	0.26	1.24509593	1.33156078	6.337692083	7.099044321	2.967146334e-13
0.25	0.27	0.25	0.27	1.244676775	1.381434798	6.428929543	7.155432958	4.387664658e-13
0.25	0.28	0.25	0.28	1.24426296	1.431180979	6.519048446	7.240275395	5.825500299e-13
0.25	0.29	0.25	0.29	1.243856131	1.480799648	6.60774423	7.355194424	7.193249738e-13
0.25	0.3	0.25	0.3	1.243953606	1.515766296	6.694715894	12.6222121	8.067817857e-13
0.25	0.31	0.25	0.31	1.243455602	1.570239406	6.779666644	8.102826778	8.64059341e-13
0.25	0.32	0.25	0.32	1.242693122	1.628903525	6.862304641	7.907664905	8.505768164e-13
0.25	0.33	0.25	0.33	1.242329446	1.678028304	6.942343859	8.174910745	4.326994973e-15
0.25	0.34	0.25	0.34	1.24197999	1.727036811	7.019505026	8.493882218	8.043054032e-15
0.25	0.35	0.25	0.35	1.241645968	1.77593312	7.093516631	8.87346927	4.250405254e-15
0.25	0.36	0.25	0.36	1.241328507	1.824721846	7.164115993	9.325297068	4.924228916e-15
0.25	0.37	0.25	0.37	1.24102865	1.873408109	7.231050368	9.86475053	8.525477016e-15
0.25	0.38	0.25	0.38	1.240747356	1.921997494	7.294078079	10.51251605	1.216201122e-14
0.25	0.39	0.25	0.39	1.240485501	1.970496007	7.352969655	11.2969686	5.561617006e-15
0.25	0.4	0.25	0.4	1.241707796	2.004807111	7.467221043	41.87151724	1.41886276e-14
0.25	0.41	0.25	0.41	1.2400232	2.067246302	7.457494339	13.45337033	5.332105605e-15
0.25	0.42	0.25	0.42	1.239824104	2.115511824	7.502739619	14.96991869	9.841692683e-15
0.25	0.43	0.25	0.43	1.239647152	2.163713877	7.543075205	16.94424598	1.888828544e-14

5-rst2

0.25	0.44	0.25	0.44	1.239492831	2.211859956	7.578348999	19.60420683	3.641614529e-14
0.25	0.45	0.25	0.45	1.239361559	2.259957739	7.608427289	23.36013637	2.051642619e-15
0.25	0.46	0.25	0.46	1.239253686	2.308015056	7.633195532	29.03293335	5.722338416e-15
0.25	0.47	0.25	0.47	1.239169494	2.356039861	7.652559038	38.53831374	1.204358541e-14
0.255	0.2	0.255	0.2	1.270670096	1.058875679	5.798818232	13.0725992	0.1898886901
0.255	0.21	0.255	0.21	1.272064873	1.080030467	5.888979529	7.295749383	0.1933292252
0.255	0.22	0.255	0.22	1.271636791	1.130526909	5.97996157	7.211644448	0.1945420254
0.255	0.23	0.255	0.23	1.271205021	1.180904008	6.071443722	7.156830576	0.1957465199
0.255	0.24	0.255	0.24	1.270771401	1.231159129	6.163107703	7.130057895	0.1969385719
0.255	0.25	0.255	0.25	1.270337765	1.281290151	6.254637431	7.13066919	0.1981142926
0.255	0.26	0.255	0.26	1.269905924	1.331295516	6.345719021	7.158563104	0.1995058858
0.255	0.27	0.255	0.27	1.269477664	1.381174253	6.436040918	7.214185172	0.2017264659
0.255	0.28	0.255	0.28	1.269054729	1.430926011	6.525294175	7.29854575	0.2039304761
0.255	0.29	0.255	0.29	1.268638814	1.480551075	6.613172874	7.413266351	0.2061096661
0.255	0.3	0.255	0.3	1.268734896	1.515644419	6.699374664	12.71814692	0.2076373847
0.255	0.31	0.255	0.31	1.268228376	1.57003715	6.783601429	8.164558488	0.209871743
0.255	0.32	0.255	0.32	1.267449207	1.628678643	6.865560055	7.966922701	0.2124159946
0.255	0.33	0.255	0.33	1.267077034	1.677812676	6.944963299	8.235221104	0.2144138828
0.255	0.34	0.255	0.34	1.266719338	1.726831043	7.021530736	8.55562897	0.2163463677
0.255	0.35	0.255	0.35	1.266377371	1.77573777	7.094989772	8.937088508	0.2182057208
0.255	0.36	0.255	0.36	1.266052299	1.824537427	7.165076717	9.391295471	0.2199844333
0.255	0.37	0.255	0.37	1.265745201	1.87323509	7.23153789	9.933730257	0.2216752555
0.255	0.38	0.255	0.38	1.265457069	1.921836299	7.294130753	10.58520955	0.2232712363
0.255	0.39	0.255	0.39	1.265188809	1.970347018	7.352625047	11.37428886	0.2247657612
0.255	0.4	0.255	0.4	1.266365892	2.004477568	7.464523758	44.93365847	0.2226342191
0.255	0.41	0.255	0.41	1.264715112	2.067122704	7.456465073	13.54382134	0.22742589
0.255	0.42	0.255	0.42	1.264511074	2.115401337	7.501421756	15.06980589	0.2285802752
0.255	0.43	0.255	0.43	1.264329713	2.163616729	7.541503864	17.05655348	0.2296108329
0.255	0.44	0.255	0.44	1.264171534	2.211776341	7.576558858	19.73339409	0.230513155
0.255	0.45	0.255	0.45	1.264036971	2.259887819	7.606452643	23.51332174	0.2312833653
0.255	0.46	0.255	0.46	1.263926387	2.307958965	7.631070355	29.22255662	0.2319181417
0.255	0.47	0.255	0.47	1.263840076	2.355997703	7.65031705	38.7892361	0.232414738
0.26	0.2	0.26	0.2	1.295505356	1.058269952	5.818765179	13.19689879	0.3608795591
0.26	0.21	0.26	0.21	1.296913636	1.079761618	5.907826056	7.363440661	0.3671968468
0.26	0.22	0.26	0.22	1.296476988	1.130257712	5.997758822	7.276974882	0.3694982654
0.26	0.23	0.26	0.23	1.296036411	1.180635471	6.088242721	7.220174593	0.3717868531
0.26	0.24	0.26	0.24	1.295593788	1.230892235	6.178958944	7.191757849	0.3740545846
0.26	0.25	0.26	0.25	1.295150995	1.281025858	6.269590577	7.19104281	0.3762938835
0.26	0.26	0.26	0.26	1.294709893	1.33103475	6.359822688	7.217910059	0.3784976067
0.26	0.27	0.26	0.27	1.294272312	1.380917911	6.449342519	7.272793068	0.3806590265
0.26	0.28	0.26	0.28	1.293840045	1.430674955	6.537839827	7.356695822	0.3827718129
0.26	0.29	0.26	0.29	1.293414834	1.48030613	6.625007338	7.47123913	0.3848300139
0.26	0.3	0.26	0.3	1.293509484	1.515524155	6.710541327	12.81398839	0.3881109556
0.26	0.31	0.26	0.31	1.292994277	1.56983752	6.794142304	8.226223037	0.3897854245
0.26	0.32	0.26	0.32	1.292198023	1.628456592	6.875515806	8.026131881	0.3906228693
0.26	0.33	0.26	0.33	1.291817162	1.677599637	6.954373277	8.295496607	0.3924101282
0.26	0.34	0.26	0.34	1.29145104	1.72662763	7.03043303	8.617353588	0.3941180788
0.26	0.35	0.26	0.35	1.29110095	1.775544554	7.103421266	9.000697553	0.3957426694
0.26	0.36	0.26	0.36	1.290768097	1.824354933	7.173073154	9.457295096	0.3972801156
0.26	0.37	0.26	0.37	1.290453595	1.873063798	7.239133942	10.00272234	0.39872689
0.26	0.38	0.26	0.38	1.290158471	1.921676644	7.301360088	10.65792655	0.4000797154
0.26	0.39	0.26	0.39	1.289883663	1.970199394	7.359520405	11.45164403	0.4019231454
0.26	0.4	0.26	0.4	1.291017243	2.004129986	7.470414529	48.6928709	0.403691515
0.26	0.41	0.26	0.41	1.289398314	2.067000157	7.462787359	13.6343326	0.4066198159
0.26	0.42	0.26	0.42	1.289189224	2.115291756	7.507503462	15.1697684	0.408658063
0.26	0.43	0.26	0.43	1.289003355	2.163520353	7.547374767	17.16895418	0.4104777136
0.26	0.44	0.26	0.44	1.288841231	2.211693371	7.582248179	19.8626969	0.412070969
0.26	0.45	0.26	0.45	1.288703303	2.259818427	7.611989124	23.66665234	0.4134309711
0.26	0.46	0.26	0.46	1.288589948	2.307903288	7.636482336	29.4123679	0.414551844
0.26	0.47	0.26	0.47	1.288501469	2.355955851	7.655632539	39.04041563	0.4154287299
0.265	0.2	0.265	0.2	1.320334991	1.057680348	5.844108947	13.32031088	0.5171095316
0.265	0.21	0.265	0.21	1.321757313	1.079498718	5.932202573	7.430695434	0.5258574659
0.265	0.22	0.265	0.22	1.321311856	1.129994187	6.021215324	7.341925638	0.5291514446
0.265	0.23	0.265	0.23	1.320862233	1.180372326	6.110826449	7.283187551	0.5324309392
0.265	0.24	0.265	0.24	1.320410368	1.230630447	6.200716718	7.253168471	0.5356842387
0.265	0.25	0.265	0.25	1.319958183	1.280766383	6.290568469	7.251163025	0.538900243
0.265	0.26	0.265	0.26	1.319507583	1.330778515	6.380065772	7.277034644	0.5420684461
0.265	0.27	0.265	0.27	1.319060449	1.380665813	6.468894693	7.331205486	0.5451789164
0.265	0.28	0.265	0.28	1.31861862	1.430427861	6.556743684	7.414673801	0.5482222758
0.265	0.29	0.265	0.29	1.318183886	1.480064871	6.643304085	7.529060218	0.5511896766
0.265	0.3	0.265	0.3	1.318277073	1.515405541	6.728270737	12.90965217	0.5558233605
0.265	0.31	0.265	0.31	1.317752986	1.569640577	6.8113427	8.287763037	0.5582695252
0.265	0.32	0.265	0.32	1.316939219	1.628237444	6.892224061	8.08523678	0.5595551248
0.265	0.33	0.265	0.33	1.316549463	1.677389255	6.970624842	8.3556801	0.562140024
0.265	0.34	0.265	0.34	1.316174716	1.726426641	7.046261964	8.678997118	0.564611894
0.265	0.35	0.265	0.35	1.315816311	1.775353539	7.11886029	9.064235279	0.5669646119
0.265	0.36	0.265	0.36	1.315475493	1.824174429	7.188153703	9.523232188	0.5691924463
0.265	0.37	0.265	0.37	1.315153413	1.872894295	7.253886231	10.07165985	0.5712900465
0.265	0.38	0.265	0.38	1.314851132	1.92151859	7.315813182	10.73059621	0.5732524328
0.265	0.39	0.265	0.39	1.314569622	1.970053193	7.373702293	11.52895855	0.5750749906
0.265	0.4	0.265	0.4	1.315661354	2.003759367	7.484971641	53.46714834	0.5783125653
0.265	0.41	0.265	0.41	1.314072348	2.066878707	7.47650688	13.72481525	0.5782839652
0.265	0.42	0.265	0.42	1.313858087	2.115183125	7.521030069	15.2697079	0.5796629514
0.265	0.43	0.265	0.43	1.313667603	2.163424787	7.56073294	17.28133735	0.5808872488
0.265	0.44	0.265	0.44	1.313501442	2.211611081	7.595461732	19.99198772	0.5819540439
0.265	0.45	0.265	0.45	1.313360069	2.259749589	7.625081293	23.8199768	0.5828608885
0.265	0.46	0.265	0.46	1.313243877	2.307848048	7.649475863	29.60217965	0.5836057032
0.265	0.47	0.265	0.47	1.31315318	2.355914323	7.668549764	39.291604	0.584186781
0.27	0.2	0.27	0.2	1.345158759	1.057106455	5.874962051	13.44275763	0.6616598982
0.27	0.21	0.27	0.21	1.346595722	1.079241697	5.962217207	7.497467757	0.6724815387
0.27	0.22	0.27	0.22	1.3461412	1.129736291	6.050435414	7.406449418	0.6766924474
0.27	0.23	0.27	0.23	1.345682273	1.180114545	6.139295978	7.345821118	0.6808894196
0.27	0.24	0.27	0.24	1.345220909	1.230373756	6.228479284	7.314240612	0.6850572279
0.27	0.25	0.27	0.25	1.344759075	1.280511731	6.317666945	7.310979998	0.6891813849
0.27	0.26	0.27	0.26	1.344298726	1.330526828	6.406542029	7.335886392	0.6932481303
0.27	0.27	0.27	0.27	1.343841787	1.380417989	6.494789404	7.389371338	0.697244412
0.27	0.28	0.27	0.28	1.343390148	1.430184767	6.582096173	7.472427928	0.7011578653
0.27	0.29	0.27	0.29	1.342945647	1.479827343	6.668152223	7.586677099	0.7049767894
0.27	0.3	0.27	0.3	1.343037348	1.515288607	6.752650875	13.00505424	0.7108229159
0.27	0.31	0.27	0.31	1.342504168	1.569446372	6.835289633	8.349121074	0.7140093377
0.27	0.32	0.27	0.32	1.34167242	1.628021252	6.915771018	8.144181677	0.7157588238
0.27	0.33	0.27	0.33	1.341273549	1.677181588	6.993803493	8.41571434	0.7190950463
0.27	0.34	0.27	0.34	1.340889962	1.726228134	7.069102449	8.740500483	0.722287346
0.27	0.35	0.27	0.35	1.340523036	1.775164783	7.141391256	9.127640401	0.7253275101
0.27	0.36	0.27	0.36	1.340174055	1.823995969	7.210402358	9.5890428	0.7282078387
0.27	0.37	0.27	0.37	1.33984421	1.872726635	7.275878404	10.14047561	0.7309211325
0.27	0.38	0.27	0.38	1.339534597	1.921362187	7.337573393	10.80314747	0.7334606838
0.27	0.39	0.27	0.39	1.339246219	1.969908461	7.395253828	11.60615654	0.7358202697
0.27	0.4	0.27	0.4	1.340297713	2.003358061	7.508494252	59.82570239	0.739786156
0.27	0.41	0.27	0.41	1.338736727	2.066758393	7.497706401	13.81518002	0.7399770598
0.27	0.42	0.27	0.42	1.338517166	2.115075479	7.54208421	15.36952557	0.7417642238
0.27	0.43	0.27	0.43	1.338321955	2.163330062	7.581660915	17.39359167	0.7433513455
0.27	0.44	0.27	0.44	1.338151656	2.211529497	7.616281971	20.12113829	0.7447346184
0.27	0.45	0.27	0.45	1.338006755	2.259681329	7.64581154	23.97314285	0.745910729
0.27	0.46	0.27	0.46	1.337887656	2.307793263	7.670133281	29.79180318	0.7468768622
0.27	0.47	0.27	0.47	1.337794686	2.355873131	7.689151036	39.54255135	0.7476307066

Table 3-Tableplot

Table that presents the change in the quadrupole strengths (KQF,KQD) and the beta functions (Bx,By)
when the phase advance is varied between 0.22 and 0.38 in both planes.
The values are used is Matlab to define the stable region of the lattice (Chapter 12)

```
@ NAME             %09s "TABLEPLOT"
@ TYPE             %04s "USER"
@ TITLE            %04s "FODO"
@ ORIGIN           %19s "MAD-X 4.01.00 Linux"
@ DATE             %08s "13/02/11"
@ TIME             %08s "21.03.53"
*               Q11               Q22                BX                BY               KQF               KQD
$               %le               %le               %le               %le               %le               %le
              0.24              0.23       9.373036094       11.07271251      0.4693609283     -0.6494576571
              0.24              0.25       9.680206207       11.06535024       0.484428063      -0.699627573
              0.24              0.27       9.981970746        11.2252205      0.4983239307     -0.7487274578
              0.24              0.29       10.27463102       11.56298933      0.5110186022     -0.7961705417
              0.24              0.31       10.55457227       12.10480989      0.5225012046     -0.8413915872
              0.24              0.33       10.81828865       12.89768695      0.5327736615     -0.8838497205
              0.24              0.35       11.06242048       14.02061353      0.5418460548     -0.9230329898
              0.24              0.37       11.28379991       15.60704495      0.5497331807     -0.9584640433
              0.26              0.23       9.441238795       11.51076374      0.5281238736     -0.6657549363
              0.26              0.25       9.732573492       11.48084899      0.5405497176     -0.7132838956
              0.26              0.27       10.02025692       11.62698219      0.5521096563     -0.7600479944
              0.26              0.29       10.30044625       11.95912768      0.5627470795      -0.805433782
              0.26              0.31       10.56939797       12.50342831      0.5724270536     -0.8488519721
              0.26              0.33       10.82349454       13.30763858      0.5811303831     -0.8897405951
              0.26              0.35       11.05928136       14.45251538      0.5888489579     -0.9275695401
              0.26              0.37       11.27351118       16.07487629      0.5955821398     -0.9618460617
              0.28              0.23       9.652340548        11.9375878      0.5851275781      -0.680480509
              0.28              0.25       9.934443525       11.88772078      0.5952735603     -0.7257301702
              0.28              0.27       10.21415161       12.02201961      0.6047803306     -0.7704414748
              0.28              0.29         10.487516       12.34995188      0.6135819865     -0.8139916762
              0.28              0.31       10.75068166       12.89778935      0.6216330262     -0.8557809278
              0.28              0.33       10.99992071       13.71413155      0.6289035219     -0.8952365477
              0.28              0.35        11.2316736       14.88156463      0.6353751312     -0.9318182218
              0.28              0.37       11.44259624       16.54031241      0.6410378605     -0.9650238868
               0.3              0.23        10.0221415       12.34835678      0.6397537566     -0.6936885124
               0.3              0.25       10.30111175       12.28084937      0.6479326988     -0.7369719104
               0.3              0.27       10.57861654       12.40499802       0.655641885     -0.7798862227
               0.3              0.29       10.85059144        12.7299161      0.6628161045     -0.8218093872
               0.3              0.31       11.11305211       13.28209701      0.6694076959     -0.8621394025
               0.3              0.33       11.36213571       14.11103872      0.6753829199     -0.9002997906
               0.3              0.35       11.59414827        15.3011743      0.6807188058     -0.9357456349
               0.3              0.37       11.80561653       16.99611106      0.6854004866     -0.9679700319
              0.32              0.23       10.58121695       12.73824328      0.6913934321     -0.7054355476
              0.32              0.25       10.86321795       12.65518773      0.6978793814     -0.7470269119
              0.32              0.27       11.14446907       12.77067764      0.7040229586     -0.7883763969
              0.32              0.29        11.4207467       13.09357324      0.7097650883     -0.8288680652
              0.32              0.31       11.68789122       13.65064704      0.7150609691     -0.8679027768
              0.32              0.33       11.94185676       14.49231286      0.7198774821     -0.9049046859
              0.32              0.35       12.17876574       15.70482364      0.7241908256     -0.9393280663
              0.32              0.37       12.39496684       17.43508215      0.7279844397     -0.9706643506
              0.34              0.23       11.38160555       13.10249244       0.739455036     -0.7157775859
              0.34              0.25       11.67350659       13.00581486      0.7444910311     -0.7559200944
              0.34              0.27       11.96523812       13.11396969      0.7492807911      -0.795916693
              0.34              0.29       12.25234275       13.43563677        0.75377402     -0.8351602112
              0.34              0.31       12.53041088       13.99789778       0.757931543     -0.8730571335
              0.34              0.33       12.79513932        14.8520685      0.7617235246     -0.9090349057
              0.34              0.35       13.04239386       16.08615299       0.765127767     -0.9425494231
              0.34              0.37       13.26827471       17.85019843      0.7681281634     -0.9730925963
              0.36              0.23       12.51021372       13.43650545      0.7833735895     -0.7247678338
              0.36              0.25       12.82047974       13.32800732      0.7871778408      -0.763679782
              0.36              0.27       13.13108081        13.4300062      0.7908085336     -0.8025183423
              0.36              0.29       13.43721351       13.75105441      0.7942250651     -0.8406860229
              0.36              0.31       13.73410672       14.31855099      0.7973951555     -0.8775961989
              0.36              0.33       14.01709003        15.1846724      0.8002936677     -0.9126810195
              0.36              0.35        14.2816659        16.4390665      0.8029014285     -0.9453994185
              0.36              0.37        14.5235843       18.23471398      0.8052041233     -0.9752451193
              0.38              0.23       14.11634793       13.73592997      0.8226204277     -0.7324552564
              0.38              0.25       14.45650917       13.61732025      0.8253912902     -0.7703350233
              0.38              0.27       14.79748613       13.71421914      0.8280434457     -0.8081961143
              0.38              0.29       15.13396054       14.03508997      0.8305458252     -0.8454505565
              0.38              0.31        15.4606315       14.60763967      0.8328733194     -0.8815188891
              0.38              0.33       15.77229585          15.48484      0.8350060273     -0.9158384999
              0.38              0.35       16.06393233       16.75784008      0.8369284743     -0.9478720317
              0.38              0.37       16.33078819       18.58228747       0.838628857     -0.9771157357
```

```
TITLE, 'FODOcell-stability';

BEAM, PARTICLE=PROTON,energy=1.238;

Nb=16;          ! Number of dipoles
ang=2*pi/Nb;    ! Bending angle

LQ1=0.25;       ! Quadrupole length (half)
LQ2=0.5;        ! Quadrupole length

KQF=0.3;        ! Quadrupole strength (focusing)
KQD=-0.3;       ! Quadrupole strength (defocusing)
Ld1=1;          ! Drift length 1
Ld2=1;          ! Drift length 2
Ld=1.4; ! Dipole length

QF: QUADRUPOLE, L=LQ1, K1 := KQF;
QD: QUADRUPOLE, L=LQ1, K1 := KQD;
DIP1: SBEND, L=Ld, ANGLE=ang;
LFODO=LQ1+Ld1+Ld+Ld2+LQ1+LQ1+Ld2+Ld+Ld1+LQ1;

FODO: SEQUENCE, L=LFODO;
  QF1:  QF,    AT=LQ1/2;
```

```
 B1:  DIP1,  AT=LQ1+Ld1+Ld/2;

 QD1:  QD,   AT=LQ1+Ld1+Ld+Ld1+LQ1/2;

 QD2:  QD,   AT=LQ1+Ld1+Ld+Ld2+LQ1+LQ1/2;

 B2:  DIP1,  AT=LQ1+Ld1+Ld+Ld2+LQ1+LQ1+Ld1+Ld/2;

 QF2:  QF,   AT=LQ1+Ld1+Ld+Ld2+LQ1+LQ1+Ld1+Ld+Ld1+LQ1/2;

ENDSEQUENCE;

USE,sequence=FODO;


create,table=tableplot,column=q11,q22,bx,by,kqf,kqd;

q11:=table(summ,q1);

q22:=table(summ,q2);

!bx:=table(summ,betx);

!by:=table(summ,bety);

q11=0.22;

q22=0.23;


 while  (q11<0.38)

{


  q11=q11+0.02;

kqf=1/(2*LQ2*LFODO)*(sin(q11)^2-
sin(q22)^2+sqrt(sin(q11)^2*(7+cos(2*q22)+sin(q11)^2)+8*sin(q22)^2+sin(q22)^4));

  kqd=-1/(2*LQ2*LFODO)*(-
sin(q11)^2+sin(q22)^2+sqrt(sin(q11)^2*(7+cos(2*q22)+sin(q11)^2)+8*sin(q22)^2+sin(q22)^
4));

  q22=0.23;

  while (q22<0.38)

  {
```

```
  !kqf=1/(2*LQ2*LFODO)*(sin(q11)^2-
sin(q22)^2+sqrt(sin(q11)^2*(7+cos(2*q22)+sin(q11)^2)+8*sin(q22)^2+sin(q22)^4));

  !kqd=-1/(2*LQ2*LFODO)*(-
sin(q11)^2+sin(q22)^2+sqrt(sin(q11)^2*(7+cos(2*q22)+sin(q11)^2)+8*sin(q22)^2+sin(q22)^
4));

 MATCH,SEQUENCE=FODO;

  GLOBAL,q1=q11,q2=q22;

  VARY,NAME=KQF,STEP=1E-6,LOWER=0;

  VARY,NAME=KQD,STEP=1E-6,UPPER=0;

  LMDIF,CALLS=500,TOLERANCE=1e-21;

 !JACOBIAN,CALLS=30,TOLERANCE=1.e-21;

 ENDMATCH;


    bx:=table(summ,betxmax);

    by:=table(summ,betymax);

    fill,table=tableplot;

    q22=q22+0.02;

    !myvar:= table(tableplot,Q11,2);

    !exec,table(tableplot,Q11,2);

            }

            }


write,table=tableplot,file=tableplot;

select,flag=twiss,column=name,s,betx,bety,alfx,alfy,dx,dpx,mux,muy;

twiss,file=fodo.dat;

plot,haxis=s,vaxis1=betx,bety,vaxis2=dx,colour=100;!,interpolate=true;

plot,haxis=s,vaxis=mux,muy,colour=100;!,interpolate=true;

*****
```